The Measurement of the Optical Absorption Cross sections of Photosystem 1 and Photosystem 2 from Whole Live Cells of *Porphyridium cruentum*, in Light State1 and Light State2.

by

Cynthia Gladys Rand, B.Sc. London, M.Eng. Yale.

A Thesis submitted to the Department of Biological Sciences in partial fulfillment of the requirements for the degree of Master of Science.

Brock University,

St. Catharines, Ontario.

LIST OF ABBREVIATIONS

ATP: adenosine triphosphate

cyt: cytochrome

CCCP: carbonylcyanide-m-chlorophenylhydrazone

DBMIB: 2,5-dibromo-3-methyl-6-isopropyl-benzoquinone

DCMU: 3-(3',4'-dichlorophenyl)-1,1-dimethylurea

EPR: electron paramagnetic resonance

ESR: electron spin resonance; EPR is the same as ESR.

F718: fluorescence at 718nm

FNR: ferredoxin/NADP+reductase

MV: methyl viologen, or paraquat

NADP+: oxidised nicotinamide adenine dinucleotide phosphate

NADPH: reduced nicotinamide adenine dinucleotide phosphate

P680: Chlorophyll*a* complex in RC2

P700: Chlorophyll*a* complex in RC1

PBS: phycobilisome

PS1, PS2: photosystem 1, photosystem 2.

RC1,RC2: reaction centre 1, reaction centre 2.

X-section: absorption X-section

TABLE OF CONTENTS

LIST OF FIGURES.

ABSTRACT.

The optical cross section of PS I in whole cells of *Porphyridium cruentum* (UTEX 161), held in either state 1 or state 2, was determined by measuring the change in absorbance at 820nm, an indication of P700+; the X-section of PS2 was determined by measuring the variable fluorescence, $(Fv-F_0)/F_0$, from PS2. Both cross-sections were determined by fitting Poisson distribution equations to the light saturation curves obtained with single turnover laser flashes which varied in intensity from zero to a level where maximum yield occurred. Flash wavelengths of 574nm, 626nm, and 668nm were used, energy absorbed by PBS, by PBS and chl*a*, and by chl*a* respectively. There were two populations of both PS1 and PS2. A fraction of PS1 is associated with PBS, and a fraction of PS2 is free from PBS. On the transition S1->S2, only with PBS-absorbed energy (574nm) did the average X-section of PS1 increase (27%), and that of PS2 decrease (40%). The fraction of PS1 associated with PBS decreased, from 0.65 to 0.35, and the X-section of this associated PS1 increased, from 135±65 $Å^2$ to 400±300$Å^2$. The cross section of PS2 associated with PBS decreased from 150±50 $Å^2$ to 85±45 $Å^2$, but the fraction of PS2 associated with PBS, approximately 0.75, did not change significantly. The increase in PS1 cross section could not be completely accounted for by postulating that several PS1 are associated with a single PBS and that in the transition to state2, fewer PS1 share the same number of PBS, resulting in a larger X-section. It is postulated that small changes occur in the attachment of PS2 to PBS causing energy to be diverted to the attached PS1. These experiments support neither the mobile-PBS model of state transitions nor that of spillover.

From cross section changes there was no evidence of energy transfer from PS2 to PS1 with 668nm light. The decrease in PS2 fluorescence which occurred at this wavelength cannot be explained by energy transfer; another explanation must be sought.

No explanation was found for an observed decrease in PS1 yield at high flash intensities.

ACKNOWLEDGEMENTS

I thank my supervisor, Doug Bruce, who encouraged me to start this project with yells which echoed down the hallway "Hey, Rand! When are you going to work for me?" I hope he doesn't regret such loud and effective encouragement.

I have been around the university for some time, before and during this project. I thank the many young people who, when I was groping my way through biology and chemistry in various undergraduate courses, overcame their reserve and tried to regard me as another student. I thank my fellow graduate students who succeeded, I hope, in regarding me both as a fellow student and as a friend. I should like to mention Jill Homer-Dixon, Jody Holmes, and Nadia Stocco, who, during their time at the lab. formed a great women's support group with their irreverent view of science, and scientists! May they succeed in their scientific careers, whatever they may be. Mike Crinson, bless his heart, was never too busy or tired to put me right on the DW2; Janet Pinder of stores always cheerfully pointed me in the right direction, and those talented guys of the electronic and machine shops would even lend me their tools. Towards the end, Patrick Chapman's presence made me feel like a senior colleague at last! I especially thank my husband, Peter, whose love I could always depend on during both my obstinate and frivolous moods. It is better to stop now and know that I have missed many, than to carry on and inadvertently miss a few.

Thank you, staff and students, you have enriched my life in more ways than you will ever know.

Finally, I have finished, but I don't believe I'm really a scientist:

We glibly talk
of nature's laws
but do things have
a natural cause?

Black earth turned into
yellow crocus
is undiluted
hocus-pocus

Piet Hein, (1973), Grooks I
Paper Jacks, General Publishing Co. Ltd., Don Mills, Ont.

INTRODUCTION.

Photosynthesis is the transformation of radiant energy to chemical energy. It is composed of two parts, one which requires light, and another in which light is not essential: the light, and dark, reactions. Reducing molecules, NADPH, and high energy molecules, ATP, are obtained during the first process; these are used during the second process for the reduction of CO_2. Both dark, and light, reactions occur in the chloroplast of eukaryotic organisms. The photosynthetic apparatus necessary for the light reactions is carried in, and on, protein-lipid membranes that are developed so as to have a large surface area, the thylakoid membrane of the chloroplast. (Lawlor,1987)

NADPH and ATP are obtained with the co-operative use of two photosystems, I and 2, the so called Z-scheme, illustrated in fig.(1). Both photosystems are held in the thylakoid membrane, each one extending across its depth. The heart of each photosystem is a reaction centre (RC), a highly specialised set of molecules so arranged that excitation at one specialised chromophore can result in stabilised charge separation. PS2 RC absorbs a photon of 680nm, whereby a specialised chlorophyll dimer, P680, is excited, loses an electron, and by a series of charge transfers two oppositely charged molecules are created, separated across the thylakoid membrane. The oxidised molecule is a strong enough oxidant to extract an electron from water; the reduced molecule is the start of an electron transport chain which includes PSI RC. This, after absorption of a photon at 700nm, which excites the specialised chlorophyll P700, produces, like PS2, charge separation across the membrane; P700+ is reduced by the last component of the electron transport chain, and an electron is transferred via several intermediaries to a stable acceptor, a ferredoxin, which can tranfer electrons to NADP+, via FNR. The transfer of an electron from PS2 to PSI results in the passage of protons from the outside of the membrane to the inside and this, together with the splitting of water molecules, ($2H_2O$---> $4H+ +4e+O_2$), creates a proton imbalance across the thylakoid membrane. The release of protons down the concentration gradient causes the production of ATP from ADP.

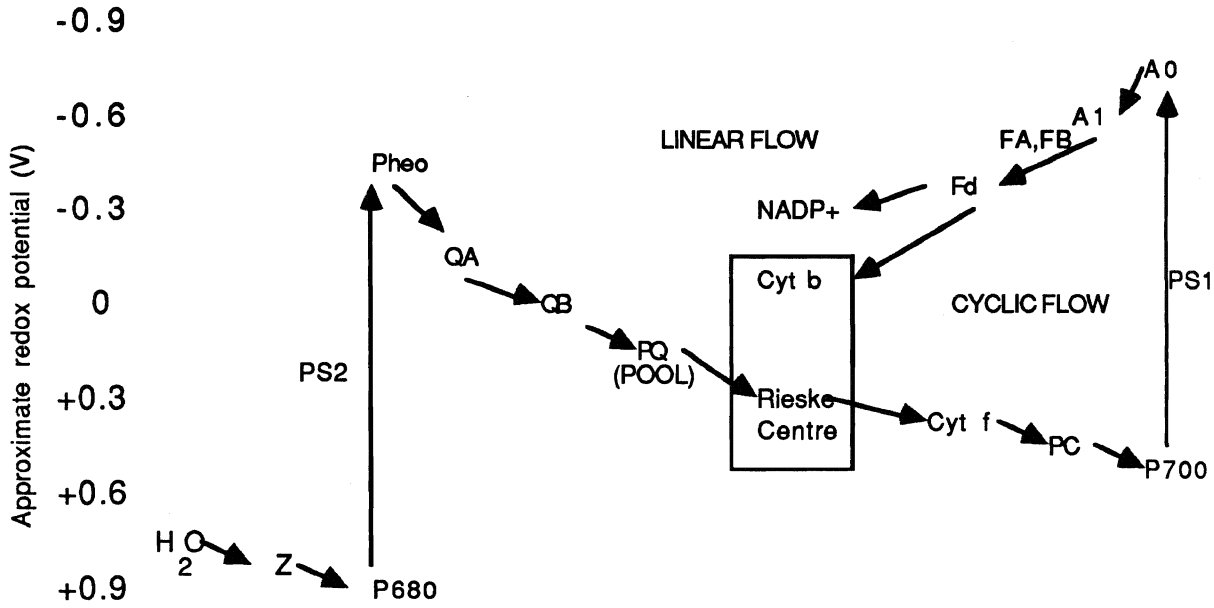

(Clayton 1980)

Fig. (1) Paths of electron transport in oxygen evolving organisms, cyclic and linear. Z is a tyrosine residue; Pheo, a pheophytin; QA, QB, PQ are plastoquinones; cyt b and Rieske centre are part of the b6/f complex; PC, plastocyanin; A0, chl<u>a</u>; A1, vitamin K1; Fd, ferredoxin. The linear flow forms the so-called 'Z' scheme.

This whole process can occur with the absorption of photons from a very narrow energy band, one covering the region 680nm-700nm. It has been pointed out by Mauzerall and Greenbaum (1989), that should a bacterium cell be completely filled with reaction centres, each with a single pigment, it would take about a month to reproduce itself. The duplication time would be dramatically reduced if attached to each RC there were additional chromophores, which could capture energy, transfer it from one to another, and eventually to the RC, of which there needs to be only one per complex. Several hundred molecules of chlorophyll<u>a</u>, the primary chromophore of photosynthetic organisms, with some secondary pigments, form antennae for both PS1 and PS2. In green plants, and green algae, chlorophyll<u>b</u>, a slight variation of chlorophyll<u>a</u> together with chlorophyll<u>a</u> are the main components of a third, mobile, antenna, LHC2, which usually transfers its captured energy

to PS2. In red algae and cyanobacteria the third antenna is the phycobilisome, PBS, comprised of biliproteins (chromophore-protein complexes), phycoerythrin, phycocyanin and allophycocyanin, so arranged that a funnelling effect is very pronounced and about 90% of the energy absorbed by the PBS is transferred to PS2 (Glazer, 1984). The PBS is water soluble and, unlike the LHC2 which is situated within the thylakoid membrane, it projects from the thylakoid membrane into the stroma. This, together with the absence of thylakoid layering into grana stacks, so typical of higher plants, are the most striking structural differences between the PBS containing organisms, and the green plants and algae (Gantt and Conti,1965; Gantt,1986).

For any one set of conditions, with constant light quantity and quality, and constant metabolic requirements, the size of the antennae and the relative number of the two photosystems may be so arranged that the light energy is used to maximum efficiency, but in order to continue with equal efficiency under changing light conditions or metabolic requirements the organism must adapt (Ley and Butler,1980; Cunningham et al,1990; Turpin and Bruce,1990). Changes which are fast and reversible may occur by temporary rearrangement of existing photosynthetic elements. Two, extreme, states, S1 and S2, are exhibited by photosynthetic organisms: state1 exists when PSI receives an excess of energy, state2 when PS2 receives an excess of energy (Bonaventura and Myers,1969; Murata,1969). Fluorescence, an alternative energy dissipation process which accompanies the photochemical reactions of the RC's, increases with the amount of energy that the photosystem, RC and antennae, receives. The fluorescence spectrum at 77^0 K, exhibits fluorescence from both PS1 and PS2, and is the main tool for distinguishing between the states; it shows a decrease from PS2 in state 2 compared to state 1, and an increase from PS1 in state 2 compared to state 1 (Ley and Butler,1980). This, together with increased electron flow between the two systems indicates that, in state 2, PS1 receives energy that, in state1 would be delivered to PS2 (Biggins,1983; Farchaus et al,1982). The ancillary antennae, LHC2 and PBS, which, in different organisms, are closely associated with PS2,

absorb energy from a part of the spectrum not available to the two photosystems alone and these normally ensure an ample energy supply to PS2.

The mechanism of state transitions in green algae and plants is thought to be well understood. In state2 the reduced plastoquinone pool activates a kinase, phosphorylation occurs on the LHC2, which is repelled from PS2 and from the stacked, grana, area in which it is concentrated, towards the unstacked, stroma, and there becomes associated with the PS1 concentrated there. Oxidation of PQ reverses the process (Staehelin and Arntzen, 1983). The process in PBS containing organisms is subject to some controversy (Review, Allen,1992). Writers disagree on the necessity of phosphorylation (Biggins et al,1984; Allen et al,1985), and on whether the energy is transferred to PS1 from the PBS or the PS2 antenna, or both. Transfer of energy from the PS2 system, comprising PBS and PS2 antenna, must result in RC2 receiving energy from an effectively smaller antenna in state 2 than in state 1, and, conversely, RC1 receiving energy from a larger effective antenna in state 2 than in state 1. The size of an antenna, defined as the number of chromophores contained in it can be inferred from the optical X-section. The optical X-section of an antenna is the area it appears to present to the incident radiation; it is measured in $Å^2$. It can also be considered as the probability that a photon will be intercepted. At wavelengths highly absorbed by the antenna, the probability of capturing a photon increases, and the X-section appears to increase although the size, the number of chromophores comprising the antenna, does not change.

The intention of this work was to measure, simultaneously, the optical X-sections for PS1 and PS2 in state1 and state2, using whole, live, cells of *Porphyridium cruentum*, a PBS-containing eukaryotic red alga. Light of 668nm, that absorbed primarily by PS1, and light of 574nm, that absorbed by PBS, and thus PS2, were used, as well as light of intermediate wavelength, 627nm. Such X-sections consist of the sum of the photosystem antenna itself plus any antennae contributing to the photosystem. Any observed differences

in cross-sections were then to be explained by energy transfer to PS1, from PBS, or from chl*a* of PS2, or both.

Such measurements should answer the following questions:

(1) Is there evidence of energy transfer from PS2 to PS1 on change of state from 1 to 2?

(2) If there is energy transfer, does it come from PBS, PS2, or both?

BACKGROUND AND LITERATURE SURVEY.

EXCITATION, WHAT, WHERE AND HOW MUCH.

The first response of a photosynthetic organism to an absorbed photon is the excitation of an electron to a higher energy. This energy is seldom used by a reaction centre directly. This section will describe excitation, how it is transferred to the reaction centres, and fluorescence, one of the ways that excitation is lost, from both PS1 and PS2.

Excitation, in a photosynthetic organism, occurs in a pigment molecule, usually chlorophyll, a molecule with an extended system of alternating double bonds, fig. (2).

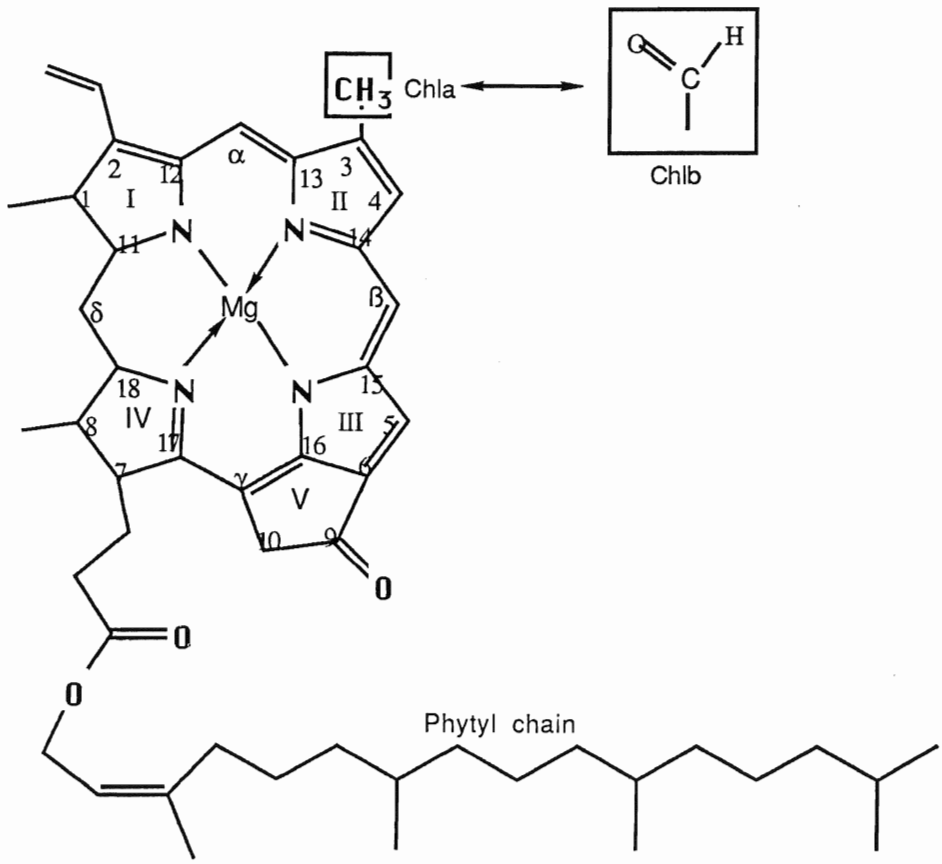

Fig(2). Structure and numbering system for chlorophyll a and b.

The energy levels of a chlorophyll molecule are usually grouped into three, a ground state and two excited levels which are within range of the energy of visible light. In addition to the valency orbitals there are vibrational and rotational energy levels, such that at room temperature the energy levels between the first and second excited levels form a continuum. The singlet states are those where the excited electron keeps its original spin, opposite to that of its former partner. When an electron is excited to another energy level, however, it is no longer constrained by the Pauli Exclusion principle and can take the same spin as that of its former partner. If the electron changes spin it is in the triplet state. (They are named thus because of the effect of an applied magnetic field on the energy levels.) A triplet state is unlikely to be formed during excitation, but is more likely to be obtained from the singlet state, as in this state it is away from the influence of its former partner and affected by the magnetic field of its new neighbours. If the molecule absorbs a photon in the blue range it is excited to the second level, but then falls through the continuum to the first excited level, a radiationless decay, releasing energy as heat. This always occurs for energy change from second to first levels and often occurs for energy loss from the first level. The photochemistry of photosynthesis is brought about by the singlet state of the first excited level but only a portion of this energy in the first singlet state gets directly to a reaction centre. Some electrons fall from this level to ground emitting a photon, fluorescence; some migrate through antennae en route to a reaction centre; others go to the triplet state. From there they may be thermally excited back to the singlet and fluoresce, delayed fluorescence; they may fall to ground, phosphorescence. (Clayton.1980)

The processes involved with absorption of energy and loss of excitation are illustrated in fig.(3).

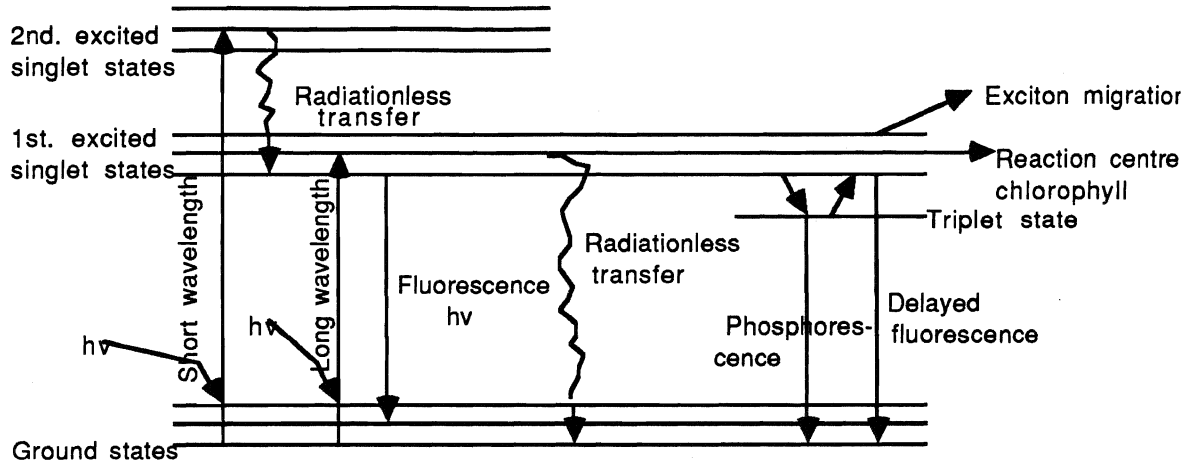

Fig.(3). Absorption of photons and transitions between ground and excited elecronic states of a molecule such as chlorophyll. (Adapted from Lawlor,1987)

Chlorophylla and chlorophyllb differ slightly in structure and absorption. Measured in organic solvents after extraction from the plant, chla absorbs most strongly at 430nm and 660nm,and chlb at 450nm and 640nm, that is, in the blue and red regions of the spectrum. The bilins of the phycobilisomes absorb in the green and orange parts of the spectrum. Absorption spectra of chlorophyll in thylakoids or of bilins in phycobilisomes show much broader peaks and even displaced peaks, due to the presence of different kinds of pigment-protein complexes, associated mainly with the antennae. These increase the absorption and by judicious arrangement ensure efficient energy transfer between antennae and between antenna and RC.

Transfer of an electron to a higher energy level means that its electron density is distributed away from its former partner, causing an electrical imbalance; the separated, but still associated, negative electron and positive hole, together constitute an exciton. When confined to a single molecule it is localised. When the exciton orginates, or arrives at, a close association (<2nm) of two or more identical or similar molecules, it may range over the collective molecular orbitals of all the molecules; the electron and hole remain

associated; it is their combination, the exciton, which can range over the collection of molecules. In this state it is delocalised. Delocalisation does not constitute transfer as such, but rather extension. Transfer between molecules or complexes separated by distances greater than 2nm occurs by inductive resonance transfer, or Forster transfer. As a classical analogy, the excited molecule acts as an oscillating dipole and induces a similar oscillating dipole in a neighbouring molecule, a coulombic interaction. In photosynthetic membranes the concentration of chorophylls falls between the delocalised situation and the inductive transfer, a region of maximum theoretical complexity. Energy transfer occurs in a "downhill" fashion, from elements which absorb at short wavelengths to those which absorb at long wavelengths. The phycobilisomes of red algae, where the pigments can be separated, provide a particularly nice example. The absorbances of the pigments are:

Phycoerythrin	570nm
Phycocyanin	630nm
Allophycocyanin	650nm
AllophycocyaninB	670nm
Chl<u>a</u>	670-680nm

Energy transfer in the orientated pigments close to the reaction centre may be by electron tunnelling , but the mechanism is not understood. Nevertheless, excitation travels from the antenna to the reaction centres as an exciton; charge separation does not occur until the reaction centre. Whatever the mechanism of energy transfer, it necessitates close association between the transferer and the transferee. (Sauer, 1986; Clayton, 1980).

<u>Fluorescence</u>, which takes about 10^{-9} s. to occur after excitation, is derived from the more persistent, first excited state, rather than from the second excited state, which decays in 10^{-13}s. Chlorophyll fluorescence is therefore always red regardless of the quality of exciting light. Once at the reaction centre there is almost no possibility of fluorescence; it has been quenched. At room temperature the fluorescence spectrum has a main broad peak at around 685nm originating from PS2 and only a minor one at 710-720nm from PS1. This is

because acceptors in PS1RC are different from those of PS2, resulting in a differently charged situation.

Both photosystems can be represented:

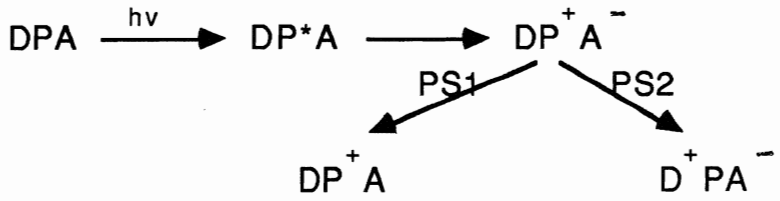

where P is the chlorophyll of the reaction centre (P680 and P700 for PS2 and PS1 respectively), D is an electron donor, A an electron acceptor, and P* the excited state of chlorophyll. DPA is the open reaction centre, the other states are closed. Butler et al. (1979) showed, however, that P+ is a quencher of fluorescence. Only in the state D+PA-, where both P and A are reduced does fluorescence emission take place. Consequently, for PS1, in both open and closed centres, the fluorescence is identical and low (Briantais et al.,1986). For PS2 when all reaction centres are open, the fluorescence is a minimum F_0; when all reaction centres are closed, it is a maximum, Fm. At liquid nitrogen temperatures, because the molecular vibrations are suppressed, fluorescence from intact chloroplasts of green plants separate into three main emission bands, F685, F695, and F735, where F685 means fluorescence at 685nm The last is indeed due to PS1; at this temperature a species in LHC1 competes with P700 for trapping; at high temperatures this energy can be transferred to P700, but at 77^0 K it cannot, and it fluoresces (Butler et al.,1979); the core components of PS1 also fluoresce, at 722nm and 690nm (Thornber, 1986). F685 was once attributed to LHC2, but it is shown by cyanobacteria and mutants with no LHC2; LHC2 fluoresces at 680nm.Hansson and Wydrznski (1990) stated that the core components of PS2 were responsible for emissions at 685nm and 695nm. F695 may arise from the PS2 reaction centre; Breton (1982) pointed out that it exhibits an unusual anisotropic property and may originate from the Pheo of the P680-Pheo pair on charge recombination

($P680^+$, $Pheo^-$---> P680, $Pheo^*$), a delayed fluorescence; there is, however, some disagreement on this explanation (Barber et al.,1989). Cyanobacteria core components fluoresce at 686nm and 696nm (Rusckowski and Zilinskas,1980; Yamagishi and Katoh, 1983).

Summarised, at 77^0 K:

F680-LHC2

F685-core antenna of PS2, PS2 reaction centre.

F690- core antenna of PS1.

F695- core antenna of PS2.

F722- core antenna of PS1.

F735- LHC1

Fluorescence emission for whole phycobilisomes at approximately 675nm at room temperature is a characteristic of most phycobilisomes (Gantt,1986). For whole cells of *Porphyridium cruentum* excited with 540nm radiation fluorescence emission at 77^0 K occurs at 580nm (phycoerythrin), 640nm (phycocyanin), 660nm (allophycocyanin), and other peaks at 685nm, 695nm, and 714nm are due to different forms of chlorophyll.

ELECTRON TRANSPORT SYSTEM.

Transfer of electrons goes from a relatively low potential molecule to a relatively high potential molecule, that is from pheophytin in PS2 to P700+ and from X in PS1 to ferredoxin and NADP+, as is illustrated in fig.(1). The system can be considered in three parts: the water splitting complex and PS2, that is from water to plastoquinone, PQ; the electron carrier train from PQ to P700+, which includes the intermediate b6/f complex and plastocyanin; and PS1 and intermediates to NADP+. Most of the work clarifying these processes has been done with higher plants and green algae, except where otherwise stated, but similarities between species, of PS2 for example, which is, in general, a highly conserved macromolecular structure (Barber et al., 1987) indicate that the information applies also to cells of red algae.

Photosystem 2 and the water splitting complex.

Physical characteristics. The only type of intramembrane protein complex that has been unambiguously identified on freeze fractured membranes is that of the PS2 complex. It takes the form of discrete particles with sizes which can vary from a minimum, 8nm, to 16nm This has been shown to be due to addition of bound chl.a/b complexes, whose synthesis can be altered by light conditions, age, and mutation. They are referred to as bound, in contrast to a mobile chl.a/b antenna, LHC2. The PS2 in the stacked, or grana, region of the thylakoid is larger, 10nm to 18nm, than that of the unstacked, or stromal, region, where the average is 10.5nm This is evidence of inhomogeneity in PS2; there are two kinds, PS2α and PS2ß, which are concentrated in the stacked and unstacked regions respectively. (Staehelin, 1986)

In red algae PS2 is randomly distributed in the thylakoid membrane, or ordered into rows; the size is 10nm and corresponds to the higher plant PS2 without the peripheral antenna; there is evidence that they may be paired when in rows (Morschel and Schatz, 1988)

The function of PS2 and the water splitting complex. The water splitting complex, or the oxygen evolving complex, lies on the lumen side of the chloroplast. With the energy from four photons two molecules of water are split into oxygen, protons which are released on the lumen side to add to the electro chemical potential, and electrons; the electrons are transferred, with protons from the stromal side, to plastoquinone.

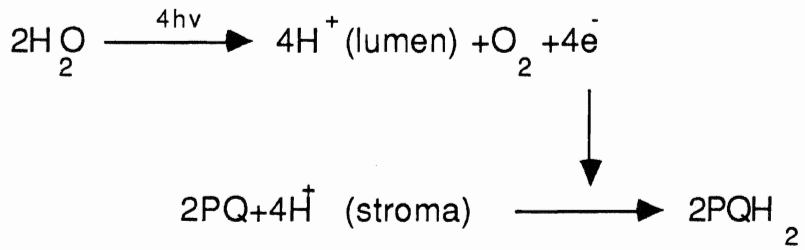

The components necessary to achieve this can be represented as:

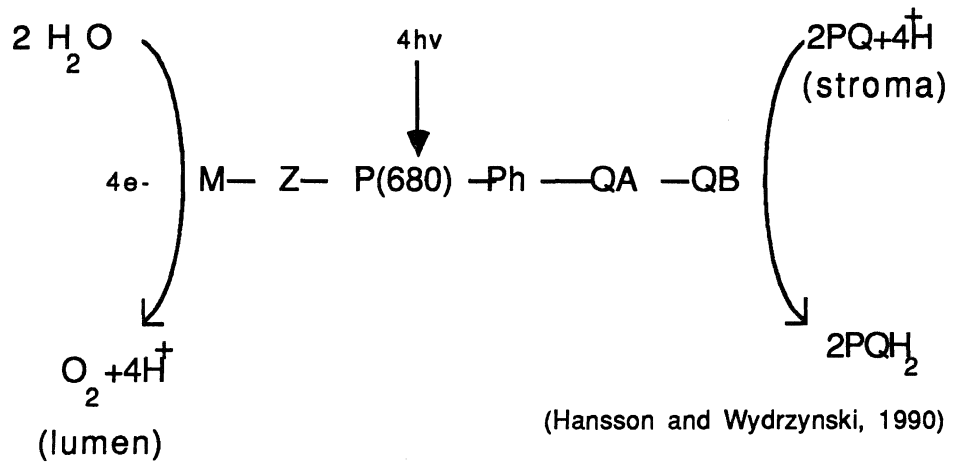

(Hansson and Wydrzynski, 1990)

where P(680) is the reaction centre chlorophyll; to the right are acceptor molecules, pheophytin, and the bound plastoquinones QA and QB; to the left is a donor molecule, Z, connecting the reaction centre with M, a component of the water splitting complex containing 4 manganese atoms. There are other components which may interact with the flow of electrons; these appear to be subsidiary to the charge separation, in that they are postulated to be not necessary but desirable. They are cyt b559, a free radical component D+ associated with the donor side, and a non-heme Fe group associated with the acceptor side.

The one electron transfers at the centre of the diagram have to be coupled with the four electron process of the water splitting unit and the two electron plastoquinone reduction.

Using a series of short saturating flashes it was found that O_2 yield per flash oscillated strongly, with period 4 (Joliot et al., 1969; Kok et al.,1970) which implies that during water oxidation four electrons are removed sequentially by one PS2; several photosystems do not combine to remove several electrons at once. Molecular oxygen is produced after the removal of the fourth electron, but the protons are released one at a time after the first and third electron removal, the other two are released together, with the

oxygen molecule. The water splitting complex is said to proceed through five states, S_0 to S_4, which depend on the special chemistry of the 4 Mn cluster as it accomodates 4 positive charges. States S2 and S3 are unstable and will revert to S1 within a few seconds in the dark. In dark adapted membranes about 75% of the PS2 is in S1 and 25% in S_0. (Ort, 1986)

QB, a plastoquinone, the same as those in the plastoquinone pool of the membrane, is the link between the single electron transfers and the doubly reduced plastoquinone, PQH_2. It is so designated because it occupies a position near to QA, a plastoquinone permanently attached to the PS2 core. Following a single RC turnover, QB receives an electron from QA. The singly charged QB becomes very securely bound to its binding site, and upon a second turnover it becomes doubly charged, is protonated with two protons from the stromal side of the membrane, and is free to leave the binding site. The site can then be occupied by a plastoquinone from a plastoquinone pool from the surrounding membrane. The reduction and protonation of QB results in the reduction of the plastoquinone pool.

Except when semi-reduced, QB can exchange rapidly with free PQ. This means that the QB site is frequently left empty and a variety of compounds can attach and inhibit. (Velthuys, 1981)Many of the herbicides act at the QB site. DCMU, a quinone-like molecule, is a competitive inhibitor of plastoquinone and is commonly used to block electron flow between PS2 and PS1.

Polypeptides of 49,45,34,33,32, and 9kD in association with bound manganese appear to form the minimum complex capable of photosynthetic oxygen evolution (Ghanotakis et al., 1987). These polypeptides, and another of 16kD, can be divided between the reaction core, the regulatory cap, and the proximal and distal antennae. The last does not apply to red algae.

The reaction core contains the 34 (D1), 32 (D2), and 9kD (cyt b559) polypeptides. On D1 and D2 are bound all the components for electron transfer from Z to QB.

Inference of positions and orientation of the PS2 reaction core components of higher plants was done by comparison with the known pigment arrangement and structure of the protein subunits of *Rhodopseudomonas viridis*, a purple bacteria, which has been crystallised and analysed by X-ray diffraction (Deisenhofer et al., 1984,1985). The two proteins D1, and D2, (D refers to 'diffuse' bands on Coomassie stained gels) have sequence homologies with the L and M polypeptides of the bacterium. The D1 and L subunits can be labelled by azidoatrazine. (Michel and Deisenhofer,1988). Atrazine, a herbicide, binds to the QB site or nearby (Lawlor 1987), so it is likely that the QB is on D1. D1 was proposed to correspond to the L unit and D2 to the M unit. If this was so then the reaction centre and its immediate donors and acceptors should reside on the D1/D2 unit. This was confirmed when a D1/D2/cyt559 complex was isolated by Nanba and Satoh (1987), and although it did not evolve oxygen, and the plastoquinones were lost, Pheo- was formed, demonstrating charge separation. D1 and D2 possess greater sequence identity than do L and M. M has an extra sequence of seven amino acids which contains glutamic acid as a fifth protein ligand to the ferrous non-heme atom. There is no such difference between D1 and D2 leading to the possibility of a fifth ligand being different to that provided by L and M, possibly a bicarbonate.(Michel and Deisenhofer, 1988)

The model of PS2 currently accepted is summarised in fig.(4) which represents PS2 of green plants. It seems very likely that this model applies also to red algae, except that the distal antenna and the LHC2 is replaced by the phycobilisome. Bricker et al (1986), for example, found that the proteins of the reaction core in cyanobacteria were similar to those of higher plants.

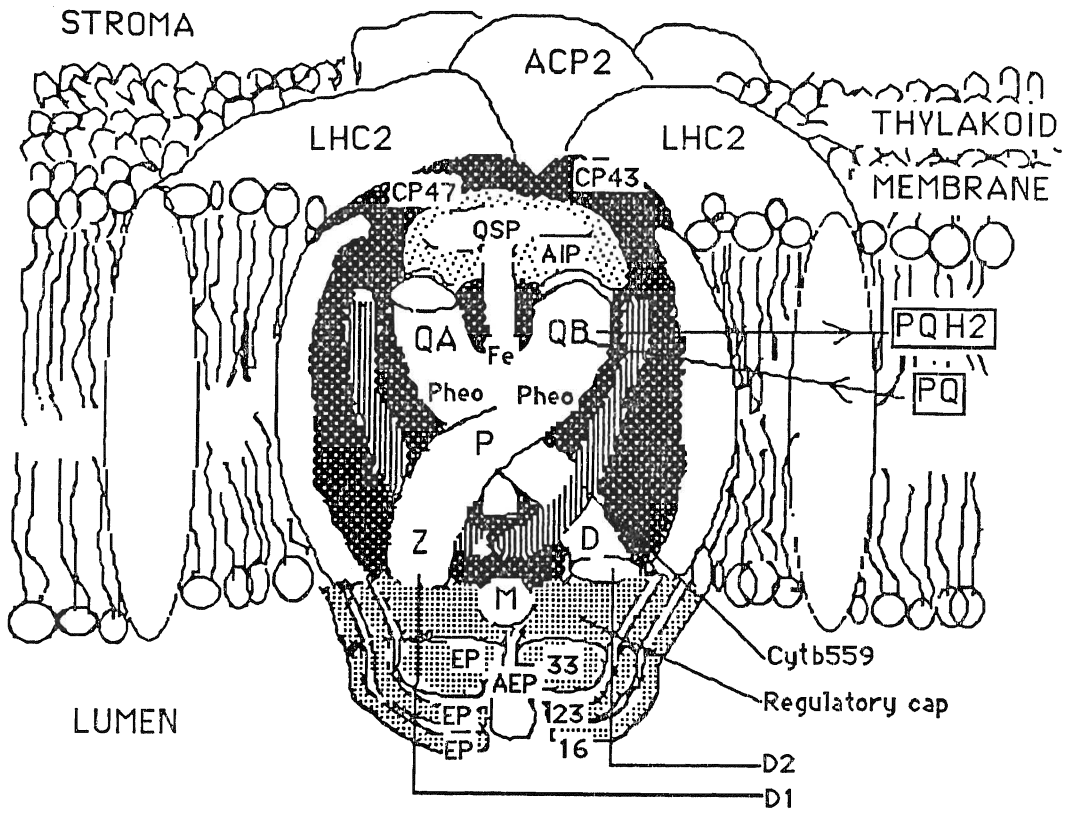

Fig.(4) A schematic representation of photosystem 2 in green plants. P is P680, the primary electron donor. Pheo is pheophytin, the primary electron acceptor, and an accesory pheophytin. QA and QB are the first and second quinone acceptors. Fe is a non-heme iron. Z is the tyrosine electron donor to P+. D is a second tyrosine. M is the manganese-containing component involved in oxygen evolution. D1 and D2 are the proteins of the reaction core. QSP is the quinone shielding protein, AIP the accessory intrinsic proteins, EP33, EP23 and EP16, extrinsic proteins of the regulatory cap, AEP accessory extrinsic proteins, CP47 and CP43 chlorophyll proteins of the proximal antenna, ACP2 accessory chlorophyll proteins of the distal antenna, and LHC2 the chla/b light harvesting complex.

(Hansson and Wydrzynski, 1990)

Heterogeneity of QA. The redox state of QA largely determines the amount of room temperature fluorescence. When reduced, fluorescence is a maximum, Fm, when oxidised, a minimum, F_0. From fluorescence measurements it has been determined that, in green plants and algae, there are two forms of PS2 (PS2α and PS2β) which differ in the total number of attached chlorophyll, 240 at PS2α,130 at PS2ß, and PS2α has increased chlb. PS2α are concentrated in the grana, PS2ß in the stroma-exposed membrane. (Melis and Homann,1976; Melis and Duysens, 1979; Thielen and Van Gorkom,1981; Anderson and Melis,1983)). The picture has been complicated by the discovery of various forms of QA: QH and QL (Horton and Croze,1979), Q1 and Q2 (Joliot and Joliot,1977). QA is usually equated with QH and Q1; QA, QL, Q2 may all be involved in both PS2α and PS2ß. Change from one to another may occur during growth or repair at which time the the 2-electron gate of QB may become inactive.

There is at present no model which accounts for all this diversity. Much of it may be due to the inhomogeneity of the thylakoid membrane of green plants and algae. PBS-containing organisms may not have such diversity; the work of Bowes et al. (1981,1983) showed that PS2 particles from the cyanobacterium Phormidium laminosum contained a single fluoresence quencher which corresponded to QH or Q1.

Sequence of events at PS2. The following timing sequence has been accepted by Govindjee (1990):

2fs

Chl antenna+hv------>Chl* antenna

n ps

Chl*antenna +P680------>P680*+Chl antenna

(energy transfer)

3 ps

P680*+pheophytin ------>P680+pheophytin-

(charge separation)

200 ps

pheophytin- +QA ------>pheophytin +QA- (electron flow)

20-300ns

P680+ +Z---------->Z+ +P680 (electron flow)

100-200μs

QA- +QB ---------->QA +QB- (electron flow)

100μs-1ms

Z+ +S(n)---------->Z +S(n+1) (electron flow)

Absorption of a second quantum leads to the reduction, again, of QA, followed by:

400-600μs

QA- +QB- ---------->QA +QB-- (electron flow)

QB-- +2H+ ------>QBH_2 (orPQH_2) (release of PQH_2)

After absorption of four quanta, O_2 is released:

1ms

S(4) +$2H_2O$ ------>O_2 +$4H^+$ +S(0) (O_2 evolution)

Cyt b559 and cyclic electron transfer around PS2. The function of cyt b559 is uncertain (Cramer et al,1986). It is closely associated with the reaction centre since it co-purifies with the reaction core minus the water splitting complex (Nanba and Satoh,1987). It seems to be associated with two polypeptides, a 39 and an 83 amino acid residue, and is probably bound by two histidines, one on each polypeptide; these two sequences form the 9kD which is normally said to contain the cytochrome (Veltuys, 1987). It can exist in the oxidised (Em=80->100mV) or reduced state (Em=370mV) but the kinetics of of its photo-oxidation under physiological conditions are slow, so it cannot be involved in the main

electron transport. The high potential form has been linked to O_2 evolution, a cycling between high and low potential forms being able to extract an electron from water (Butler,1978); the formation of the high potential form requires the integrity of the photosynthetic membrane or, at least the association of lipid (Matsuda and Butler,1983).

Cyt b559 is photo-oxidised by P680 (Knaff and Arnon,1969) and reduced by plastoquinol, so it has been proposed that cyt b559 may be involved with cyclic electron flow around PS2. Falkowski et al. (1986) showed that as a continuous background radiation was increased in intensity the ratio (fluorescence yield)/ (O_2 production), measured as a flash yield, departed from linearity in the region where O_2 production reached about 80% of maximum. This meant that there was a greater probability of QA being oxidised than S_3, indicating a cyclic flow between QA and P680. Thompson and Brudvig (1988) suggested that because the midpoint potential of P680+ was low enough to oxidise the chlorophyll connecting the proximal antenna to P680, the cyclic flow was a protective mechanism:

QH_2-->cyt b559-->Chl-->P680

Arnon and Tang (1988) suggested a cyclic transport path around PS2 that promoted translocation of protons from PQH_2 into the lumen and used some components of the b6/f complex.

The regulatory cap is composed of a set of hydrophilic proteins with masses 33, 23, and 16kD. These are often designated EP33, EP23 and EP16, where EP stands for 'extrinsic protein' (Hansson and Wydrznski, 1990), and are thought to regulate the ionic requirements, Ca++ and Cl-, for O_2 evolution. In cyanobacteria the 34kD protein required for O_2 evolution has been identified. The EP16 and EP23 are not present but there is a 13kD manganese binding protein (Bricker et al., 1986).

The Plastoquinone pool

An interesting structural component of this quinone is a side chain made up of isoprenoid units; this makes it highly hydrophobic and it is likely that the plastoquinone pool is concentrated between the two thylakoid layers.

Cytochrome b6/f complex.

The cytochrome b6/f complex oxidises plastoquinol generated by PS2 and reduces plastocyanine, or, in cyanobacteria, cytc; both are oxidised by PS1. Its more descriptive name is plastoquinol:plastocyanine oxidoreductase. Not only are electrons transferred parallel to the membrane in the direction from PS2 to PS1 but across the membrane; a transmembrane electric field demonstrates its presence by causing a change in absorbance at 515nm which occurs not only with linear electron transport, but also when the electrons are transferred via the cyclic path in PS1, indicating that the b6/f complex is implicated in the cyclic path. The complex can use the reducing power of either PS1 or PS2.

It is an intrinsic membrane protein, containing a c-type cytochrome (cyt f), a Rieske 2Fe-2S centre, and two b-type cytochromes attached to a 35kD, 20kD and 27kD polypeptide respectively; during purification these were accompanied by a 17kD polypeptide of unknown origin; a plastoquinone also tended to co-purify. (Hurt and Hauska, 1981, 1982, 1983)

The electron transfer through the complex occurs in a complicated series of reactions which is not entirely understood, and is accompanied by proton translocation. This function together with its composition demonstrates its analogy to the b/c1 complex of mitochondria and photosynthetic bacteria. Although it is usually accepted that the passage of each electron results in the translocation of two protons, the experimental determination of the ratio H+/2e- varies considerably. Rich (1984) obtained with a vesicle b6/f preparation an initial ratio of 4, which rapidly dropped to 2; a b6//f PS1 incorporation gave cyclic electron transfer but had rather poor pumping ability. Cramer et al (1987) stated that the experimental ratio could vary from 2 to 0.7.

Efforts to establish a model that will account for the properties of the b/f complex with the known structure are continuing today, but none is completely satisfactory; most are based on b6/f being a monomer. Ort in his review of 1986 stated that there were several indications that b6/f may be other than a monomer. Freeze fracture analysis with

b6/f in reconstituted lipisomes showed a size which implied a dimeric state. DMBIB, an inhibitor of linear electron transport at the R Fe-S site on the b6/f complex combined 1:2 with the complex, implying that a dimeric b6/f may operate in the linear path. Cramer et al (1987) suggested that dimers could oxidise quinol immediately without using the cytb as reductant. The monomeric form, obtained from the dimeric by some conformational change would be used during cyclic transfer. The possibility of two forms with two mechanisms may be pursued further; Chain and Malkin (1991) in their purification have found both forms present. State1 to state2 transitions have been shown to involve cyclic flow around PS1 and the b6/f complex. (see state transition section later).

Photosystem 1

The reaction core, unlike that of PS2, does not have a bacterial counterpart, although it shows parallels to the poorly-known green sulfur bacterium, *Chlorobium*. Information of its structure has been obtained from well defined subchloroplast preparations which yield good optical and ESR data, although as Golbeck and Bryant (1991) point out, the interpretation of this data is not without difficulty. As with PS2, excitation is channelled to a primary donor, which for PS1 is designated P700; it becomes excited and loses an electron to a series of acceptors, resulting in charge separation across the membrane.

The sequence of electron carriers is:

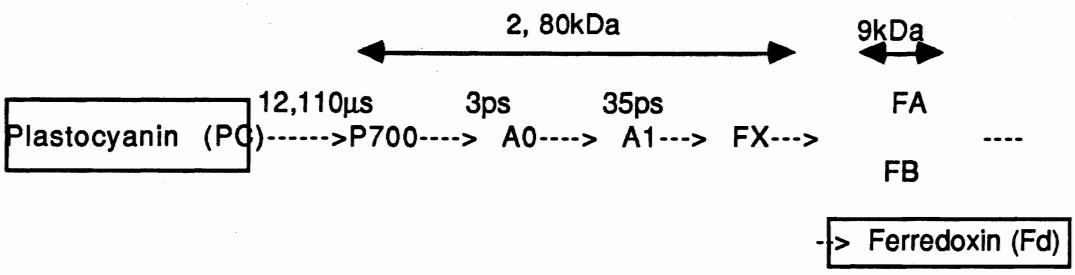

(Andreasson and Vanngard,1988)

One approach to determining the identity of the acceptors has been to reduce these successively to study their spectoscopic properties. PS1 is characterised by the low redox potentials of its bound acceptors; A0,for example is approximately -1.2V, which, again, makes experimental conditions difficult when it is desirable to keep these acceptors reduced. (Lagoutte and Mathis, 1989)

P700. Like P680, P700 has an absorbance spectrum very similar to that of Chla , absorbing strongly at 700nm; there seems to be no conclusion, as yet, on whether P700 is a monomer or dimer.

The primary acceptor A0 has been identified by flash absorption spectroscopy with picosecond or nanosecond resolution (Nuijs et al.1986; Shuvalov et al. 1986) as Chla.

A1 is a transient intermediate operating between A0 and FX. It has been suggested that A1 is a quinone on the basis of ESR experiments, and because of the exclusive location of vitamin K1, phylloquinone, in PS1 it appears possible that A1 may be equated with that. Biggins and Mathis (1988) found two vitamin K1molecules for each PS1. One was more easily extracted than the other. The absence of the more easily extracted vitamin K1 did not interfer with the function of PS1, so it is presumably not involved in primary electron transfer. Extraction of the second vitamin K1 inactivated the photosystem, and recombination occurred between P700+ and A0- , consistent with interruption of electron flow beyond A0. Replacement of vitamin K1 restored function of the photosystem. The functon of the second vitamin K1 is unknown. The situation is not quite as simple as the preceeding makes it appear, as further experiments have tended to make the situation more complex (Lagoutte and Mathis, 1989)

FX, FB and FA are mainly identified by the EPR spectra of their reduced forms. EPR signals indicated that FX was an Fe-S centre in close association with P700. A back reaction attributed to $FX^{-}P700^{+}$ was obtained from particles which did not contain FA/FB (Golbeck and Cornelius, 1986) and a core protein of P700-FX, without FA/FB, has been isolated (Golbeck et al, 1988). FA and FB give typical spectra of Fe-S centres, and are both (4Fe-

4S). There are about 12 each of non-heme Fe and S. FA and FB each contribute 4Fe and 4S leaving 4Fe and 4S for FX. (Lagoutte and Mathis,1989). FX has been considered as a pair of (2Fe-2S) clusters (Golbeck et al.,1987), but Petrouleas et al.(1989) showed with Mossbauer spectroscopy that the most likely structure was that of a (4Fe-4S) cluster. Two paths of electron transfer have been postulated: a linear path FX-FB-FA, or a branched scheme with FX delivering electrons either to FA or FB. Genetic work which changed FB to the inactive (3Fe-4S) showed that FA could still be reduced, indicating that FB was not an obligatory intermediate in the path of electrons to FA (Zhao et al.,1992).

Protein partners. There are two main P700 apoproteins, of molecular weight 65kD according to Lagoutte and Mathis (1989), and 80kDa according to Andreasson and Vanngard (1988). It is now generally accepted that these two proteins are of molecular weight 83.2kDa and 82.4kDa which provide cysteine ligands for FX and accommodate A0 and A1. They are accompanied in higher plants by ten other, smaller, proteins; the genes have been identified and designated psaA-psaH; a small cysteine-rich polypeptide of about 9kD binds FA and FB, the FA/B protein. PsaH, producing what is thought to be a linker protein between PS1 and LHC1, does not appear to be present in PBS-containing organisms. Peripheral proteins are probably involved in the interactions with ferredoxin and plastocyanin. (Golbeck and Bryant, 1991).

A proposed model is shown in fig.(5).

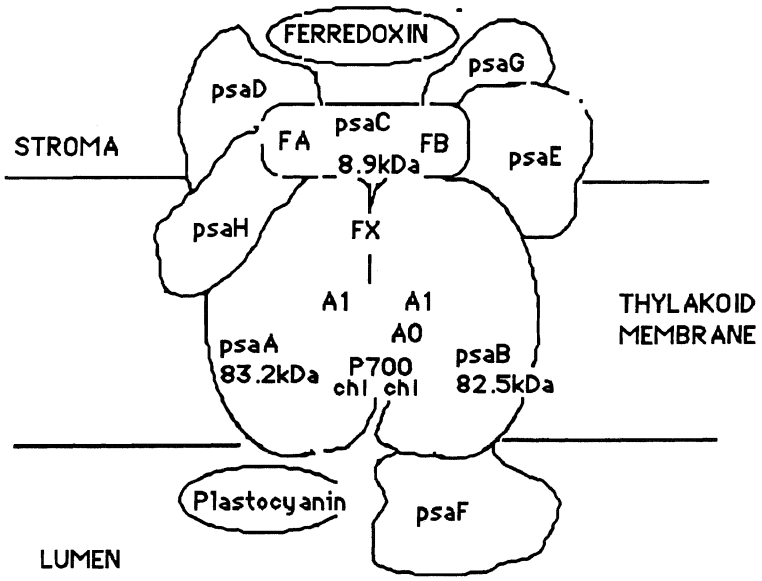

Fig.(5) Diagram of a proposed model of the PS1 complex. The exact locations of the smaller proteins are not certain, but the situations towards the stromal or lumenal sides of the membrane are known. The two large proteins scan the membrane and are closely associated with other, smaller proteins, psaJ, psaK, and psaI, which are not shown. P700 is shown here as a chlorophyll dimer, A0 is a chlorophyll, the two A1 molecules, vitamin K1, are assumed to be symmetrically distributed, FX is bonded to cysteine residues of both psaA and psaB, and FA and FB are similarly bonded to the psaC protein. The chlorophyll molecules of the PS1 antenna of red algae are associated with the psaA and the psaB molecules. (Golbeck and Bryant, 1991)

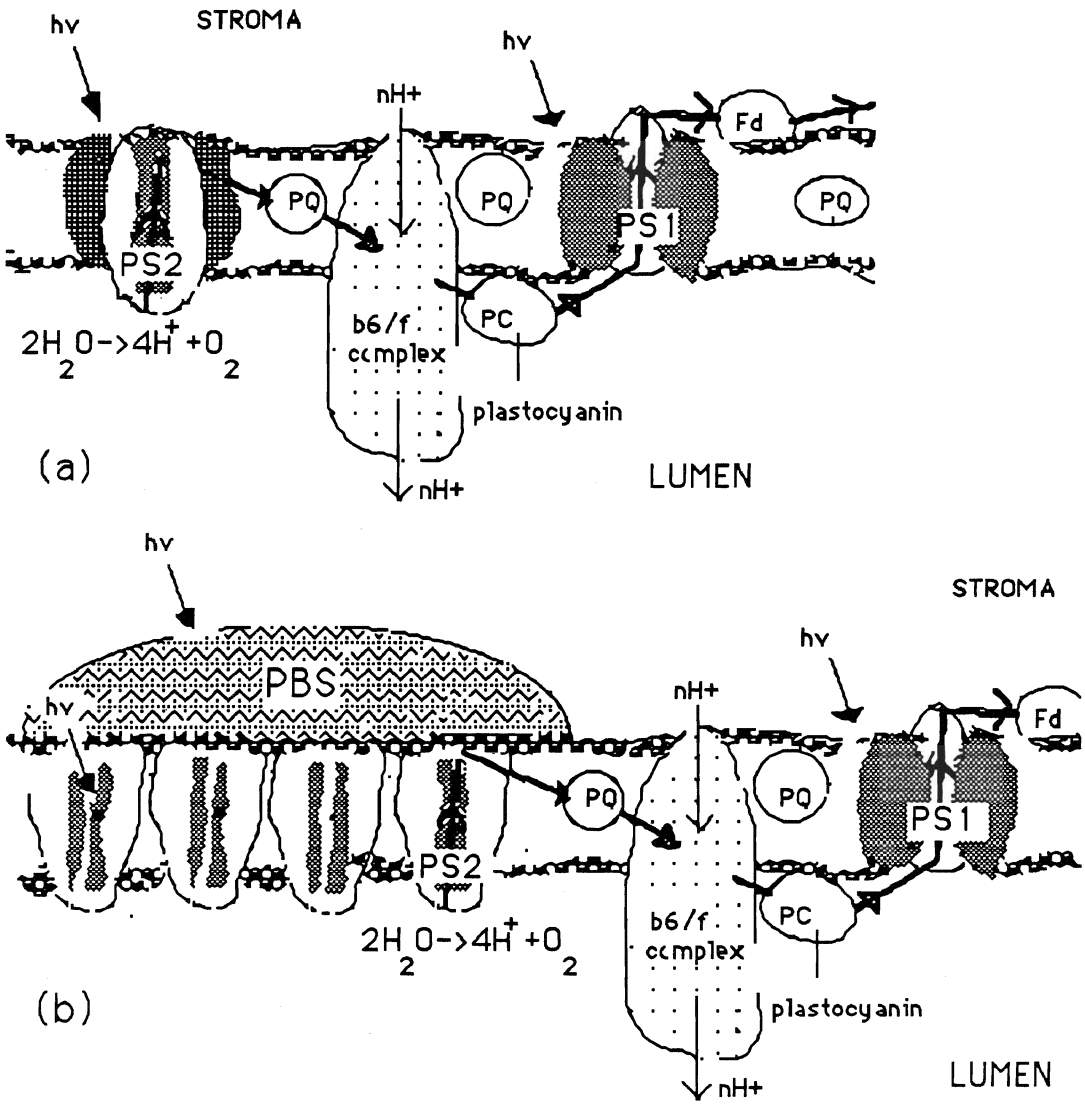

(adapted from Staehelin,1986)

Fig. (6). Diagram illustrating antennae and electron flow in the thylakoid membrane of (a) green plants and (b) *Porphyridium cruentum*. The shaded areas represent chlorophyll. The outer antenna of PS2 in (a) has been replaced in (b) by the phycobilisome.

ANTENNNAE

PS1 Higher plants have both a proximal, and a distal antenna. The proximal is composed of Chla associated with the two large apoproteins of 80kDa which appear to contain all the chla of this antenna. One group of experimenters, including Wollman (1986), determined that each protein had 20 Chla attached. Vierling and Alberte(1983) reported that there were four copies of a large protein. Thornber (1986) states that it is generally agreed that there are more than 40 Chla molecules associated with the PS1 inner core. Golbeck and Bryant (1991) state that there are 100-130chla per P700; for cyanobacteria specifically, the range is the same (Mauzerall and Greenbaum,1989). The distal antenna, called LHC1 in analogy to the LHC2 of PS2, is a chlorophyll a/b complex (a/b=3.5-3.7) and was not thought to occur in PBS-containing organisms. B. Gantt (private communication) has recently found evidence in red algae of an antenna analogous to LHC1. It is assumed here, however, that the PS1 Porphyridium cruentum has 100-130 chla.

PS2 has a proximal, and, in green plants and algae, a distal antenna. The latter is replaced by the phycobilisome in cyanobacteria and red algae.

The proximal antenna consists, in the main, of two pigment-protein complexes, CP47 and CP43, the numbers being about equal to the protein mass. Each contains 11-12 histidine residues, probably used in chlorophyll binding, in contrast to the other antennae where chlorophyll is not covalently bound. Each protein binds 20-25 chla and about 5 ß-carotene. At 77^0 K, CP43 fluoresces at 685nm and CP47 at 695nm CP43 absorbs at 669nm and 682nm The absorbance of CP47 is more complex, with bands at 660,668, 677, and 690nm The last is probably associated with a single chlorophyll molecule oriented with its Qy transition moment parallel to the membrane normal, which may be responsible for the 695nm fluorescence, and it is interesting in that CP47 contains an energy trap deeper than P680. Both CP47 and CP43 are always present in O_2 evolving particles, so they are closely coupled to the reaction core. They may be involved in electron transport: the ability to

reduce QA is lost when both are removed; QA can be reduced if CP47 only is present. (Hansson and Wydrzynski, 1990).

In cyanobacteria proteins of approximately 47kD and 40-45 kd have been found which fluoresce as those of higher plants. The 47kd fluoresces at 696nm and the 40kD at 686nm (Rusckowski and Zilinskas, 1980; Yamagishi and Katoh, 1983). With the same chlorophyll content per protein as that of higher plants the cyanobacteria PS2 antenna would contain 40->50 chl*a* molecules, about one third the size of the PS1 antenna.

The distal antenna consists of at least two parts, LHC2 and ACP2. LHC2 is a chl a/b complex involved in membrane stacking and the transfer of energy from PS2 to PS1 (see the state transition section). Its size and composition can vary with age and growth conditions. It normally has a chl a/b ratio of ~1.2 and contains xanthophyll as the major carotenoid. The ACP, accessory chl. proteins, have several components which are separable from LHC2 and have a slightly higher chla/b ratio of 2-3. They may be more closely associated with the proximal antenna and may form a linker between it and LHC2. They may also participate in the dissipation of excess energy as a protection against photo-inhibition (Bassi et al.,1987). In higher plants the total distal antenna contains about 200chl(a+b) molecules per PS2 unit (Hansson and Wydrznski, 1990)

Analysis of fluorescence induction curves has shown the existence of two sizes of PS2 antennae in green plants and algae, PS2α and PS2β, due to addition of chl*b*-containing segments to the distal antenna. In cyanobacteria the shape of the induction curve could be explained by aggregation of PS2, and it was not necessary to postulate two discrete sizes (Bowes and Horton, 1982).

In conclusion, PBS replaces LHC2 in the PBS-containing organisms. The chl*a* of PS2 is that of the proximal antenna, which contains 40-50 chl*a* molecules, about one third the size of PS1. There is no evidence of PS2 antenna heterogeneity in PBS-containing organisms.

PHYCOBILISOMES are the distal antennae of cyanobacteria and red algae, including *Porphyridium cruentum*. They are the counterpart of LHC2 of green plants.

The ultrastructure of *Porphyridium cruentum.*

Porphyridium cruentum is a unicellular eukaryote of class Rhodophyceae and division Rhodophyta. It is spherical with an eccentric ellipsoidal nucleus, and a large, red, lobed chloroplast, which occupies most of the cell.The cell also contains mitochondria, endoplasmic reticulum, and golgi bodies. Starch granules are randomly distributed throughout the cytoplasm. Cytoplasmic vacuoles are located among the cytoplasmic organelles and starch grains. A double membrane surrounds the chloroplast. The thylakoids are folded to form pairs of parallel planes with a spacing of about 50nm (Gantt and Conti,1965). Attached to the stromal surface are numerous, apparently circular, phycobilisomes. Their position is illustrated below.

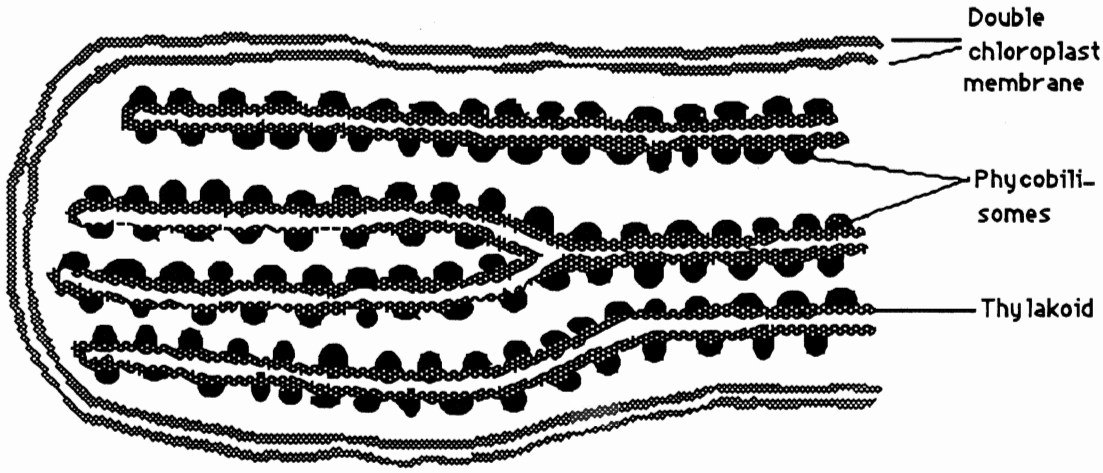

Fig.(7). The organisation of the thylakoid membrane in the Rhodophyceae algae, to which *Porphyridium cruentum* belongs.

Composition. Phycobilisomes are protein and pigments.Phycobiliprotein accounts for 85% of the stainable polypeptides; uncoloured linker polypeptides form the remaining 15%.(Gantt 1986). Phycobiliprotein consists of bilin pigments covalently bonded to protein. There is some variation, but there are three main groups, phycoerythrin with absorption maxima at 490-570nm, phycocyanin with absorption at 620nm and allophycocyanin which absorbs at 650nm. All of the biliproteins are oligomers of αß monomers where α and ß are dissimilar polypeptide chains of approximately 160-180 residues. The bilin pigments are open chain tetrapyrroles and are covalently bound to the protein. Phycoerythrobilin, the chromophore of phycoerythrin is illustrated in fig.(8) as a free unit and as it is covalently bonded in the α subunit of *Porphyridium cruentum*. Its similarity to chlorophyll is readily apparent. Spectral variation among the phycobiliproteins is due to aggregation of the biliprotein and the conformational state of the apoprotein. (Glazer 1984)

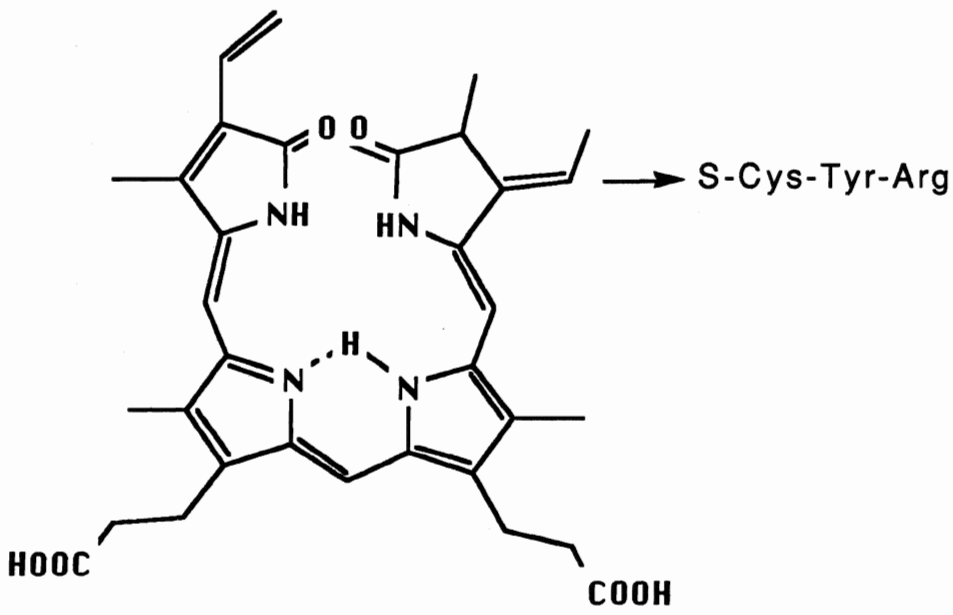

Fig.(8) Chemical structure of phycocyanobilin, showing point of bonding to protein. (Glazer, 1984)

Morphology and structure. Phycobilisomes often form highly regular arrays on the thylakoid surface. The shape of the phycobilisome varies with the organism; the size and number can depend on the organism and on the intensity of illumination during growth. Many cyanobacteria and red algae have hemidiscoidal (fanlike) phycobilisomes; those of Porphyrium cruentum are hemispherical-prolate, 48nmx32nmx32nm (Gantt 1981)

The arrangement of the phycobiliprotein within the phycobilisome has been determined from spectral analysis of intact and selectively dissociated phycobilisomes, and electron microscope examination. *Porphyridium cruentum* was the first one determined in this manner (Gantt et al 1976), and is illustrated in fig.(9). Its core structure is assumed to be similar to that of the hemidiscoidal structure common in both red algae and cyanobacteria, illustrated alongside, whose central structure in the electron microscope is not obscured by surrounding rods. The core consists of allophycocyanin cylinders parallel to the thylakoid surface. Projecting radially are rods composed of coaxial discs, containing phycocyanin next to the core and phycoerythrin on the periphery. Each disc has dimensions of 3nmx10nm and is thought to be a trimer of $\alpha\beta$, with a molecular weight of 100kD-130kD. Change can occur in the length and composition of the rods in some organisms, an example of long term adaptation to lighting conditions. In green light, absorbed mainly by phycoerythrin, its synthesis increases and phycocyanin synthesis is suppressed. The size of the phycobilisome may change with change in size of the linker proteins.(Anderson et al (1983), Bryant (1981), Bryant and Cohen-Bazire (1981), Ohki et al (1985))

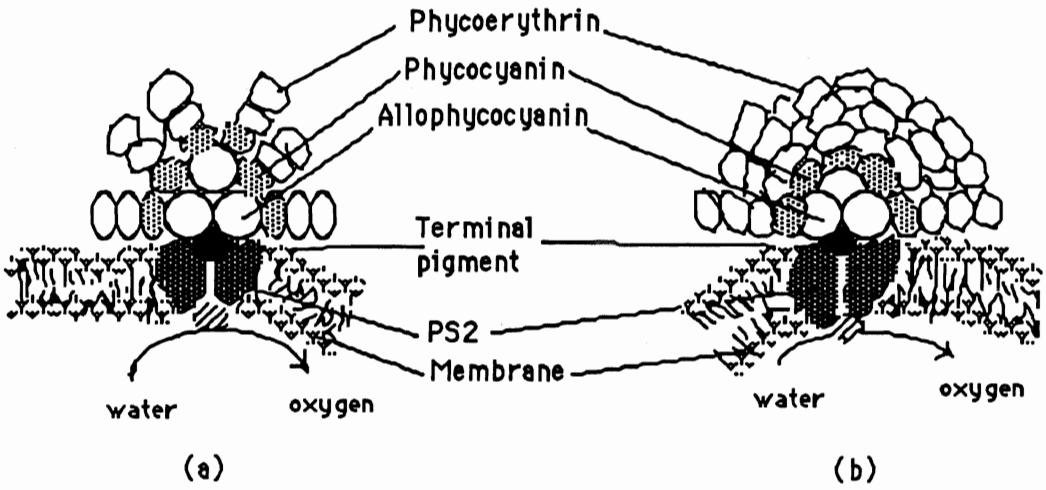

Adapted from Gantt (1986)

Fig.(9). Schematic arrangement of phycobiliproteins typical of (a), a hemidiscoidal phycobilisome and (b), a cut-away view of the phycobilisome of *Porphyridium cruentum*.

Contact with PS2. For cyanobacteria "...PS2...receives most, if not all, of the energy harvested by the phycobilisomes" (Glazer1984)

Ley and Butler (1977) used the extent of 77^0K fluorescence at 695nm and at 718nm as an indication of the activity of PS2 and PS1 respectively. They showed that 95% of the energy absorbed by PBS is transferred to the RC of PS2. Energy transfer of this magnitude implies close physical association.

In *Porphyridium cruentum* a 95kD polypeptide was found to be common to an allophycocyanin-associated polypeptide and to a chl*a*-associated polypeptide, strongly indicating that it must connect the PBS to PS2.(Redlinger and Gantt,1982). A similar protein, common to allophycocyanin and thylakoid membranes, was found in Nostoc sp., a cyanobacterium, indicating in this case a connection to the membrane.(Rusckowski and Zilinskas (1982), Zilinskas (1982)). This kind of approach culminated in the isolation of O_2 evolving PS2-PBS particles from *Porphyridium cruentum* . (Clement-Metral and Gantt (1983), Chereskin et al (1985))

Examination of surfaces made apparent by freeze fracture electron microscopy demonstrated not only a connection between PS2 and PBS, but also a very ordered association. Examination of the cyanobacterium, *Mastigocladus laminosum*, showed that the phycobilisomes were directly related to particles which appeared on the endoplasmic fractured surface (EF), a surface exposed when the bilayer of the thylakoid membrane fractures on freezing.

The EF particles were identified as PS2 complexes by comparing the *in vivo* distribution of the particles with that obtained from PS2 particles reconstituted into lipisomes. EF particles occurred singly as 10nmx10nm or as rows of doublets 10nmx20nm, joined along their lengthwise edge. The doublet separation was 10nm and the row separation 45nm,The hemidiscoidal phycobilisome of this cyanobacterium could be fitted to these particles, one to each doublet, stacked one against the other along the rows. Each phycobilisome is then in close contact with two PS2 particles and with neighbouring phycobilisomes. It was suggested that the hemispherical phycobilisome of *Porphyridium cruentum* could be linked to two or three row doublets and hence to four or six PS2 particles (Morschel and Muhlethaler (1983),Morschel and Schatz (1987)). In contrast, the two unit EF particles found by Giddings et al(1983), in very similar work with *Cyanophora paradoxa*, were interpreted as being single PS2 complexes, with two sections, but with a single RC. The essential difference in these two groups of work is not only in the number of PS2 attached to PBS but also in the interpretation of the single 10nmx10nm EF particle. In *Masigocladus* it was considered a PS2 particle with attachment to PBS. In *Cyanophora* it was not identified with certainty, and attachment to PBS was uncertain. It was pointed out by Staehelin (1986) that such regular phycobilisome organisation may be less common than is generally supposed. The extent to which EF particles and phycobilisomes are formed into rows seems to be related to the light conditions during growth. Low light leads to greater phycobilisome density and row formation.

Kursar and Alberte (1983) determined the relative concentration of various

photosynthetic components in *Anacystis nidulans* (cyanobacteria) and *Neoagardhiella bailyei* (red alga). The mass of the phycobilisomes from the former was 40% of that from the latter; the ratio PS2/PSB was 1.7 and 4.1 respectively. The number of PS2 connected to each PBS may therefore depend on the size of PBS.

Contact with PS1 ....." In the cyanobacterium *Anacystis nidulans,* 40% of the quanta absorbed by phycocyanin were contributed to PS1, and 60% to PS2..."(Gantt 1981)

Wang et al (1977), by careful choosing of the wavelength of the incident radiation causing O_2 production, were able to differentiate between the contributions of PS1 and PS2 to the action spectrum. The individual action spectra so obtained, from *Anacystis nidulans,* showed that about half of the energy absorbed by PBS was transferred to PS2, the other half to PS1.

Energy transfer from PBS to PS1, according to Ley and Butler (1977), occurs via PS2, as a spillover. This model depended on their assumption that 77 K fluorescence at 718nm (F718) was due to fluorescence from PS1Chl*a*. Wang et al (1980) argued that F718 was due 80% to PS2 and 20% to PS1. If this is the case there is no need for the spillover model PBS-->PS2-->PS1 to account for F718 when PBS is excited, and the path PBS-->PS1 is possible, that is, there may be a direct connection between the phycobilisome and PS1.

If such a direct association exists electron microscope work might demonstrate it. Giddings et al (1983) comment that the precise location of of the PS1 complex was not known, and the probability of PS1-PBS transfer could not be determined.

An indication that PBS may be physically associated with PS1 came with the detection of allophycocyanin in PS1 preparation from the cyanobacterium *Chlorogloea fritschii* (Pullin et al, 1979).

Gantt (1986) suggested several possible arrangements of the photosystems around the base of the phycobilisome, all of which included the close association of PS1 with the phycobilisome, but not its attachment to it.

Mullineaux (1992) determined the PS1 X-section of the cyanobacterium, *Synechococcus 6301* in S2, with flash light of 680nm, and 630nm, and found that the latter X-section was only slightly smaller than the former. If the X-section was due to PS1Chla alone, then at 680nm it should be much larger than that at 630nm, in proportion to PS1 absorbance. Mullineaux argued that the small difference in X-section was due to a direct contribution of PBS energy at 630nm to PS1.

STATE TRANSITIONS. Photosynthetic organisms adapt to different growth conditions with altered pigments and PS1/PS2 ratios; these are long term changes (Ley and Butler,1980; Cunningham et al, 1990). A quicker, and reversible, response, takes only minutes, and occurs during temporary changes in light conditions. This is the light state transition and is a method whereby the organism can transfer energy from one overstimulated photosystem to the other. It was discovered independently in a green alga, Chlorella pyrenoidosa, by Bonaventura and Myers (1969), and in the red alga, *Porphyridium cruentum*, by Murata (1969). State 1 occurs when PS I receives an excess of energy, and state 2 when PS II receives an excess of energy. The main criterion for distinguishing between the two is a difference in fluorescence spectra exhibited by the organisms in the two states. As the state changes from 1 to 2, there is a decrease in fluorescence from PS2, and at 77^0 K an increase in fluorescence from PS1 (Ley and Butler, 1980). There is a corresponding increase in the rate of PS1 charge separation in state 2 and increase in PS2 activity in state 1 (Bonaventura and Myers,1969; Biggins, 1983; Farchaus et al.,1982). It appeared that the data could be interpreted in two ways, the rate of energy transfer from PS2 to PS1 increases in state 2, found by Ley and Butler (1980) in *Porphyridium cruentum*, or the amount of energy transferred is increased, found by Bonaventura and Myers (1969) in Chlorella pyrenoidosa. In fact, the two are equivalent; it will be shown in the next section that the rate of a property change dependent on the photochemical reaction depends on the X-section of the photosystem producing the

photochemical reaction, that is, on the amount of energy transferred to the photosystem.

The following model for transfer of energy from PS2 to PS1 in green plants and algae is generally accepted. In state 2, as a result of phosphorylation and mutual repulsion between phosphorylated units, triggered by reduction of PQ, the mobile portion of LHCII moves from its position in the grana, associated with PS II, to the unstacked portion of the thylakoids where the PS1 is concentrated and there can transfer its energy to PS I; oxidation of PQ starts the reversal of the process (Staehelin and Arntzen, 1983). In this model, with energy absorbed by LHC2, the absorbance X-section of PS2 decreases and that of PS1 increases as S1->S2; the amount of transferred energy changes.

A model of state transition in PBS-containing organisms is still in dispute. Experimentally, PBS-containing organisms are particularly suitable for investigating state transitions. In the red alga *Porphyridium cruentum*, the phycoerythrin of the PBS absorbs maximally at 560nm; in cyanobacteria the phycocyanin of the PBS absorbs maximally at 590nm, both are regions of low Chl*a* absorbance; Chl*a* absorbs maximally in the red and blue, and is mainly associated with PS1; hence, if the PBS is mainly connected to PS2 the two photosystems of the cyanobacteria and red algae can be separately excited. Examination of the effect of PBS-absorbed and Chl*a*- absorbed light on fluorescence emission which is, almost totally, the property of PS2 and its closely associated antennae, is a powerful tool to determine the mode of energy transfer from the PBS/PS2 system to PS1.

If, in analogy to higher plants, the S1->S2 transition involves release of PBS from PS2 and transfer of PBS excitation to PS1, the fate of some of the PBS-absorbed energy must differ in state1 and state2 whereas the fate of Chl*a* -absorbed energy would be the same in state1 and state2. Ley and Butler (1980), from 77^0 K fluorescence, determined that any redirection of excitation energy must occur at the Chl*a* level as did Dominy and Williams (1987) who showed that at room temperature the fluorescence difference spectra between state1 and state2 was the same for radiation absorbed by PBS and that absorbed by Chl*a*. From analyses of time resolved fluorescence spectra with picosecond time resolution Bruce

et al.(1985) showed that, for cells frozen in state1 and state2 at 77 ^{0}K, the decay kinetics of the PBS pigments were the same in state1 or state2; PS2-chl was uncoupled from energy transfer to PS1 and the decay lifetime of PS2 fluorescence was longer in state1 than in state2. This would indicate a 'spillover' mechanism whereby energy is transferred from PBS->PS2-chl ->PS1-chl. In a later experiment Bruce et al. (1986) showed that the PS2 decay of fluorescence in state2 was related to a slow rise component in the PS1 emission. In this model the PBS remains attached to PS2 and in transition to state1 the combination associates more closely with PS1. This model depends on PBS-PS2 movement, not uncoupling of PBS from PS2. Bruce et al.(1989) appeared to confirm this by showing that state transitions, exhibiting typical state1- state2 fluorescence spectra, could be performed by a PBS-less mutant of cyanobacteria.

In contrast, another body of work indicates that the main event in energy transfer is the uncoupling of PS2 from PBS. In analogy to green plants, Allen et al. (1985) proposed that in S2, the PBS is detached from PS2 and becomes attached to PS1. This would cause a decrease in PS2 X-section and an increase in that of PS1. By measuring fluorescence induction transients Mullineaux and Allen (1988) determined that with PBS-absorbed light there was a reduction in PS2 X-section during the transition to S2. With chl*a*-absorbed light there was increased energy transfer away from PS2 in S2, probably due to spillover from PS2 to PS1. They suggested that the mobile PBS could accompany a modified form of spillover: as the PBS is detached from PS2Chl to move to PS1, the detached PS2Chl can associate with another PS1. Although they wrote that they were able to distinguish between a change in absorption X-section and spillover it should be pointed out that the two are intertwined. The X-section of a RC is determined by the absorbance of the antenna contributing to that RC. If spillover entails the transfer of energy normally received by RC2 being received instead by RC1, then the X-section of PS1 has increased and the X-section of PS2 has decreased. Mullineaux and Holzwarth (1990) used fluorescence induction from non-frozen cells treated with DCMU, as an indication of the number of PS2 RC's closed by

incident light absorbed by PBS or by chla, and found that, in S2, the number of RC2 closed by phycocyanin absorbed light was less than that closed by chla absorbed light; they concluded that in S2 a fraction of PS2 must be decoupled fron PBS. Mullineaux et al (1990) used picosecond resolution of fluorescence decay spectra, from cells at 35^0C, which were analysed by global data analysis. This analysis interpreted the fluorescence decays in terms of amplitudes, and lifetimes. The relative amounts of energy going to PS2 in S1and S2 can be obtained by comparison of amplitudes, and is an indication of the X-section; lifetimes are an indication of energy dispersal from PS2. The authors found that, in S2, for both 620nm and 670nm light, less energy went to PS2, and there was more emission from the PBS terminal emitter. It was proposed that PS2 became uncoupled from PBS and the possibility of spillover from coupled PBS-PS2 was discounted as there was no change in lifetime of PS2 fluorescence with change of state. There was no change in lifetime of the fluorescence from the terminal emitter, and the authors entertained the possibility of PBS transfer to PS1. The fact that in S2 less energy derived from chla absorbed radiation gets to PS2 was not adequately accounted for.

Room temperature fluorescence is a property primarily of PS2 and is not very useful for measuring the affect of a state transition on PS1. Measurement of PS1 X-section, as it varied with the wavelength of incident light was done by Mullineaux (1992). Absorbance changes at 700nm were used to measure the X-section; the X-section of PS1 showed a peak at PBS absorbed light; transition from state2 to state1 resulted in a decrease in X-section with PBS-absorbed light. His conclusions were, not only does a mobile PBS go from PS2 to PS1 in the transition of state1 to state2, but there is, in state1, already a proportion of PS1 connected to PBS's.(Connection of PS1 with PBS has already been discussed in the section " Phycobilisomes")

The state transition appears to be controlled by the redox condition of an element in the electron flow chain, in that there are very low quantum requirements for either transition, a short exposure time is sufficient for maximum response and the system can

sum small impulses over a time of minutes (Ried and Reinhardt, 1980). Biggins and Bruce (1985) extended this experiment using single turnover flashes of light and found that the transition to state1 required a minimum of 15 turnovers of RC1 at an optimal frequency of 2.5HZ, a frequency which was consistent with the turnover time of in-vivo cyclic electron transfer of P. cruentum. S2 ->S1 is inhibited by DBMIB, which acts at a site just beyond PQ in the electron flow from PS2 to PS1, and so prevents PQ oxidation (Biggins,1983); it is also inhibited by MV which preferentially accepts electrons from PS1 and prevents cyclic electron flow (Satoh and Fork, 1983). Ionophores such as CCCP, which negate the potential gradient across the membrane prevent the S2->S1 transition (Biggins et al 1984b). Transition to state1 therefore requires cyclic electron transport through the b6/f complex, coupled proton transport, and PQ oxidation. According to Mullineaux and Allen (1986) PQ is reduced during respiration in cyanobacteria and induces S2.

Dependence on a redox component made it appear that the trigger of state transitions could be similar to that of higher plants, and a search was made for light induced phosphorylated proteins. Although many such proteins were found (Biggins et al.,1984a; Kirschner and Senger,1986), Biggins et al. could find no differences in P. cruentum, between the phosphorylated proteins of state1 and state2. On the contrary, Allen and colleagues (Allen et al.,1985; Sanders et al.,1986) found that two proteins in particular, 18.5kDa and 15kDa, were labelled in cells grown with ^{32}P- P_i in a light dependent fashion, with light conditions that caused S1, S2 fluorescence patterns. Labelled ATP also caused light dependent phosphorylation of a 15kDa in thylakoid membranes. They concluded that phosphorylation of a PBS 18.5kDa, and of a 15kDa thylakoid protein were responsible for S2. Despite a repeat of the experiments of Allen et al. with the same cyanobacterium, Biggins and Bruce (1989) could not confirm that specific phosphorylated proteins were caused by the same light conditions as the transitions, or that phosphorylated proteins caused the fluoresence spectra typical of state transitions. Allen, in his review (1992), states that work subsequent to 1985 suggests that modification of the 18kDa protein is not

activated in the same way as the 15kDa protein and may not be necessary for the state transition. If this is so, then the state transitions observed in a PBS-less mutant (Bruce et al. 1989) are not inconsistent with a phosphorylation procedure. Harrison et al (1991) showed that a 15kDa protein was phosphorylated under PQ reducing conditions known to give rise to S2 and was not phosphorylated under PQ oxidising conditions. There is still, however, the fundamental inconsistency on the observation of the light dependent phosphorylated proteins ; Allen (1992) says that the reason for this inconsistency is not clear.

That a state transition is accompanied by some conformational change was postulated by Murata (1969). Biggins (1983), Bruce et al. (1985) and Bruce and Biggins (1985) fixed cells in state1 and state2, chemically with glutaraldehyde and found, that although the cells were photosynthetically competent, they could not undergo a transition to the other state. This group has proposed that local charge effects caused by cyclic electron transfer can cause enough perturbation to cause the closer approach of PS2-chl, either in distance or orientation, to PS1-chl (Biggins et al.1984; Biggins and Bruce, 1989).

Fuelled by the different results obtained regarding phosphorylated proteins, there are two very different mechanisms proposed for the state transition in PBS-containing organisms: the mobile antenna model and the spillover model. The reality may be one of either or a combination of the two. The three possibilities are illustrated in fig.(10) in the next section.

OPTICAL CROSS-SECTION (X-section)

The concept that many pigment molecules might contribute to a single photochemical centre originated with the experiments of Emerson and Arnold (1932), who found that, in chlorella, about 2500 chlorophyll molecules contributed to the production of each O_2 molecule caused by a saturating flash of light. How these chlorophyll are distributed between the two cooperating photosystems now known to exist, cannot be simply determined. The size of a photosynthetic unit is defined as the number of light absorbing pigment molecules

contributing to a reaction centre. The optical X-section, σ, is the area provided by the antenna pigments for photon capture; it can be considered as the probability that a photon will be captured from light with unit intensity; it is a function of wavelength; it is not equal to the physical dimensions of the pigments. For an isotropic system randomly oriented to the incident light the X-section is related to the absorbance.

σ (in $Å^2$)= decadic molar extinction coefficient ($M^{-1}cm^{-1}$)x 3.82 x 10^{-5} (Greenbaum and Mauzerall, 1991).

It is obvious that the thylakoid membrane does not provide an isotropic system and the X-section determination is not simple. Simplistically, the size could be obtained by the experimental separation of PS1 and PS2, together with their intact connected antenna, and the ratio of the number of pigments for each system to the number of RC's determined.

In the intact thylakoid it is usually necessary to consider the following parameters:

N(1), N(2), is the # pigment molecules associated with PS1, PS2, the photosystem size.

n(1), n(2), is the # RC1, RC2

$\sigma(1)$, $\sigma(2)$, is the optical X-section of PS1, PS2

$\sigma(1)=N(1).\sigma(pig1)$ where $\sigma(pig)$ is the X-section of a single pigment or, more accurately, $\sigma(1)=\Sigma\ N(1).\sigma(pig)$, if different pigments are present.

$\phi(1)$, $\phi(2)$, is the quantum efficiency, the fraction of the photons absorbed which arrive at RC1, RC2

I is the incident intensity, the number of photons per unit area per second.

If the yield Y1, Y2, of a property of PS1, PS2 can be measured then:

$d(Y1)/dt=\int n(1).N(1).\sigma(pig1).\phi(1)I\ d\lambda$ where the integration is done over the total range of λ, the wavelength, and there is a similar equation for PS2. (Greenbaum and Mauzerall,1991). In effect the antenna size is proportional to the rate of the reaction measured.

Simplifications can be made, such as the elimination of the summation of pigments

as above; $\phi(1)$ is often equated to $\phi(2)$, and sometimes both are taken as unity. The determination of n(1) is most usually done using absorption at 700nm which decreases as P700+ is formed, assuming a value for the extinction coefficient. There is a variety of ways of determining n(2), absorption of QA- at 325nm, the division of the rate of O_2 formation by four, EPR detection of Z+, atrazine binding to QB position, and estimation of the area above the fluorescence induction curve with DCMU which is related to the number of QA. (Greenbaum and Mauzerall,1991). In all of these methods the ratio of the total number of pigments to n(1) or n(2) can be found but unless the distribution of energy to PS1 and PS2 is known the size of PS1 and PS2 cannot be determined.

The energy distribution can be found. Butler (1978) used the excitation spectra of fluorescence at 77 K, emission at 730nm, to which PS1 contributes and a model of energy distribution. Wang and Myers (1976) used an O_2 evolution method based on the difference in absorption of PS1 and PS2 in the far red, the Emerson drop. Experiments at liquid nitrogen temperatures can always be criticised because of the non physiological conditions, and there is some disagreement on the origin of fluorescence at 720-730nm (see the section on PBS connection); the differential absorption of PS1 and PS2 is difficult to interpret.

In contrast, a light saturation curve obtained using monochromatic, single-turnover flashes of light can supply, directly, the optical X-section. The light saturation curve, of yield versus flash energy will, for a homogeneous photosystem, follow the equation, which is derived in the appendix, $Y=Y_0(1-\exp(-\sigma E))$, where Y_0 is the maximum yield and it is assumed that one or more hits to a photosystem produce the same effect. The Poisson distribution can be used because the photosystems provide a very large number of targets each of area much smaller than the illumination area. This approach, pioneered by Mauzerall and his associates, takes advantage of the shape of the whole saturation curve and not of the saturation yield alone, which was, in fact, done by Emerson and Arnold and, in a repeat of their experiment, by Myers and Graham (1971). The essential requirement of this contemporary approach is use of monochromatic light pulses of duration shorter than

the fastest turnover time in the photosynthetic apparatus. (The need for this short duration is illustrated in the appendix). In this laboratory, using this approach, it is possible to measure the X-section of both PS1 and PS2 at room temperature, under the same physiological conditions without the use of poisons or artificial electron acceptors or donors.

Measurement of PS1 X-section. A direct approach involves observation of the oxidation of P700 made apparent by an absorbance increase at 820nm. An absorbance increase is also caused by the oxidation of P680 but this is reduced in ns. whereas the increase caused by P700 decays in a polyphasic manner with half times of 17μs..210μs., and over 1ms. (Van Best and Mathis 1978). It is possible therefore to monitor the oxidation of P700 without interference from P680. Harbinson and Woodward (1987) concluded that the light induced absorbance changes at 820nm from leaves were due to the oxidation and reduction of P700.

Measurement of PS2 X-section. When a saturating actinic flash was followed by a less intense pulse Mauzeraull (1976) found that a maximum fluorescence yield was obtained from the second pulse when this occurred about 30μs after the first. He showed that the yield closely followed a cumulative one hit Poissonian distribution, when it was plotted against the average number of hits of PS2 caused by an actinic pulse of variable intensity, and claimed that the data would have fitted the distribution directly if the photosynthetic unit (of chlorella) were composed of one trap per antenna of uniform X-section (Mauzeraull, 1978). This method, the so called pump-probe method, can therefore be used to determine the X-section of PS2. From information already given on PS2 ('sequence of events at PS2') the state of the hit RC2 30μs after the actinic pulse is:

$$Z+ \quad P680 \quad QA- ,$$

i.e. both P680 and QA are reduced, a state of maximum fluorescence.

Ley and Mauzerall (1986) showed that the PS2 X-sections of Chlorella measured with O_2 formation and fluorescence yield were identical. Greenbaum and Mauzerall (1991) used O_2 flash yields for PS2 and a post-illumination respiratory oscillation for PS1, to

determine both PS1 and PS2 X-sections for Chlorella (a green alga)

Previous measurement of X-sections in state1, state2, using saturation curves.

PS1 Telfer et al. (1984) found that the rate of P700+ formation as measured by ΔA820nm increased when the amount of unstacking in pea thylakoids was increased, when QA was previously reduced, and when LHC2 was phosphorylated, that is, under all conditions required for state 2 in higher plants. They concluded that the increased efficiency of PS1 was due to an increase in the absorption X-section of PS1, but did not analyse the saturation curve using a Poisson equation fit. Tsinoremas et al (1989) followed the oxidation of P700 in cyanobacteria with the change in absorbance at 820nm and found that with a single laser intensity the amount of $P700^+$ formed in S2 was greater than that in S1 for both chla absorbed radiation (337nm) and PBS absorbed radiation (532nm) As one measurement followed immediately upon the other the difference was not due to an increase in the number of PS1, and must be due to a larger amount of energy passed to PS1 in S2. The authors were able to conclude that for PBS absorbed light the X-section of PS1 was greater in S2 than in S1, but did not come to the same conclusion with chla absorbed light as "at 337nm chla absorbs as well as phycocyanin". This work supports the model of a decoupled PBS. An extension of this work was done by Mullineaux (1992) who used blue (chla absorbed and perhaps more selectively absorbed than the 337nm, near UV, light of the previous experiment) and yellow (phycobilin absorbed) flashes and varied the intensity to obtain PS1 X-sections for both wavelengths. He concluded that in S2 PBS made a major contribution to the energy used by PS1 and its X-section increased relative to that of S1. The PS1 X-section for chla absorbed light was apparently unchanged.

PS2 Ley (1984) determined the effective PS2 X-section for O_2 production with *Porphyridium cruentum* and found that, with PBS absorbed light, the X-section in S1 was 50% larger than in S2. Post et al (1991) grew *Synechocystis 27170* (a cyanobacterium) in green, orange and red lights to cause changes in relative amounts of pigments and measured the PS2 X-sections, using both O_2 production and fluorescence from the pump-

probe method. The cells could be continuously illuminated with a background light of 435nm (PS1 absorbed) or 620nm (PS2 absorbed) during the actinic flashes of white light. They found, from O_2 production, that the PS2 X-section increased in 435nm light compared to that of cells adapted to the dark (S2), but the X-section further increased in 620nm light and this increase was larger the greater the intensity of 620nm light. In relative units the results for green light grown cells, were 0.105 (S2,dark), 0.177 (S1), and 0.313 (S2, high intensity). This increase with intensity did not occur for Ley (1984) with *Porphyridium cruentum*. The increase in X-section with intensity of background light was explained by the authors as due to increased energy transfer from PS2 to PS1 (a greater degree of S2?), so that when the flash hit there were more open PS2 traps and larger yields. Because of the different continuous background illumination, the condition of PS2, both in regard to the number of reaction centres closed, and the possible connectivity between centres, may have been different in S1 and S2, and comparison of the X-sections in the different states may not be legitimate.

PS1 and PS2. Although the X-sections of both PS1 and PS2 of a green alga (Chlorella) were determined by Greenbaum and Mauzerall (1991), they did not extend the work to cover state transitions. It is only in this laboratory that the simultaneous measurement of the X-section of both PS1 and PS2 in S1 and S2 has been done, just recently with cyanobacteria (unpublished results). The experiments of this thesis extend this work to a eukaryotic PBS-containing organism, *Porphyridium cruentum*.

The three models of the state transition and the paths of PBS-absorbed energy and chl*a* absorbed energy are illustrated in fig.(10)

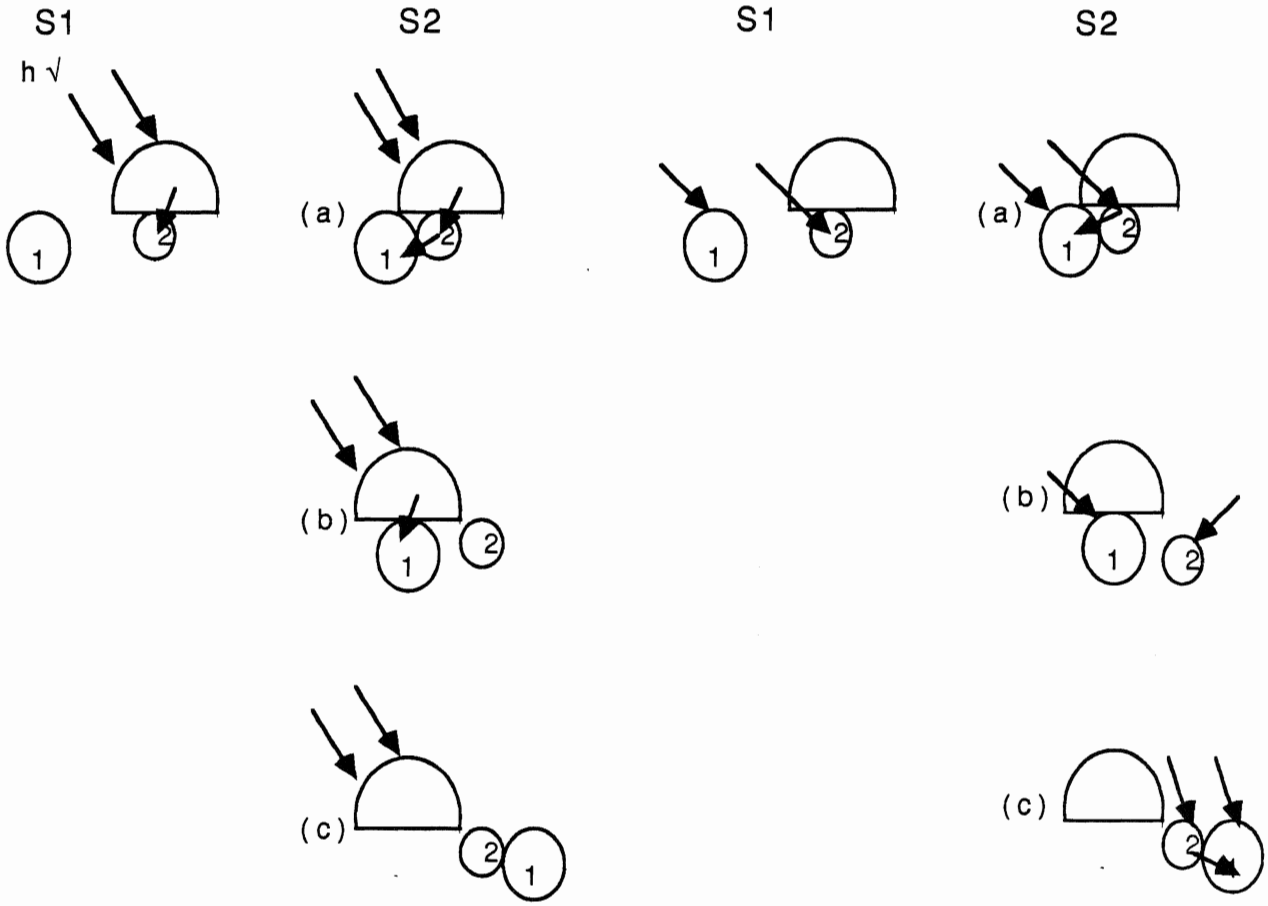

Fig.(10). The three models of the state transition in PBS-containing organisms. The dome is the PBS and (1) and (2) are PS1 and PS2 respectively. On the left is shown the path of energy absorbed by the PBS; on the right is the path of energy absorbed by chl*a*. (a) is the spillover model, (b) the mobile PBS model and (c) the combination spillover-mobile PBS model. State1 is the same for all models.

The expected effect on the X-sections of PS1 and PS2, with the different models, on the transition from S1 to S2:

PBS absorbed light	(a) PS1 increases PS2 decreases	chla absorbed light	(a) PS1 increases PS2 decreases	spillover
	(b) PS1 increases PS2 decreases		(b) PS1 unchanged PS2 unchanged	mobile PBS
	(c) PS1 unchanged PS2 decreases		(c) PS1 increases PS2 decreases	combin--ation

It appears possible to discriminate between the three models by measuring the changes in PS1 X-section with the use of both PBS- and chl*a*- absorbed light. Measurement of the PS2 X-section would act as confirmation of the choice.

MATERIALS AND METHODS.

Porphyridium cruentum (utex 161) was grown in Jones medium (Jones et al, 1963) at 18^0 C under white light of 6 W/m^2 with supplementary CO_2. The cells were used during the late exponential stage; the concentration was adjusted so that for measurements of PS1 the absorbance at 678nm was about 0.8; for measurements of PS2 the concentration was halved. The absorbance was measured on a DW2 spectrophotometer. 77^0K fluorescence emission spectra were obtained with apparatus described by Brimble and Bruce (1989). Measurements were made to obtain F695/F715 and F660/F715.

The apparatus is shown in fig.(11). The laser pulse, width 2nm and duration 250ns., was supplied by a PhaseR flashlamp pumped dye laser. DCM was used to produce 668nm and 627nm light (the former is that absorbed mainly by chl*a*), and Rhodamine 570 was used for 574nm light (absorbed mainly by PBS). A portion of the pulse was reflected onto a Molectron light pulse meter (referred to later as the pyrometer) before entering the cuvette from below via a fibre optic cable. PS1 yield was determined from the change in absorbance at 820nm. The slit aperture of the 820nm laser diode was placed horizontally, so that, in effect, the cells contributing to the signal occupied a narrow horizontal plane, uniformly illuminated by the incident pulse. M and N were two matched photodiodes; the potential difference between them was transferred to an Hitachi digital storage oscilloscope by a multistage very low noise amplifier (Brock University electronics shop). Conditions were such that light incident at M and at N were equal. Fluorescence from the sample caused by the pulse was received at M, and, via a curved mirror, at N; an adjustable slide at the side of the cuvette could be used to minimise the fluorescence difference. This is illustrated in fig.(12) Ancillary periodic green or blue light was incident on the other side of the cuvette or on the upper surface; the timing of the pulse ensured that all RC's were open at the time of the pulse; the dark time was not sufficient to change the state of the cells. This periodicity is demonstrated in fig.(13).

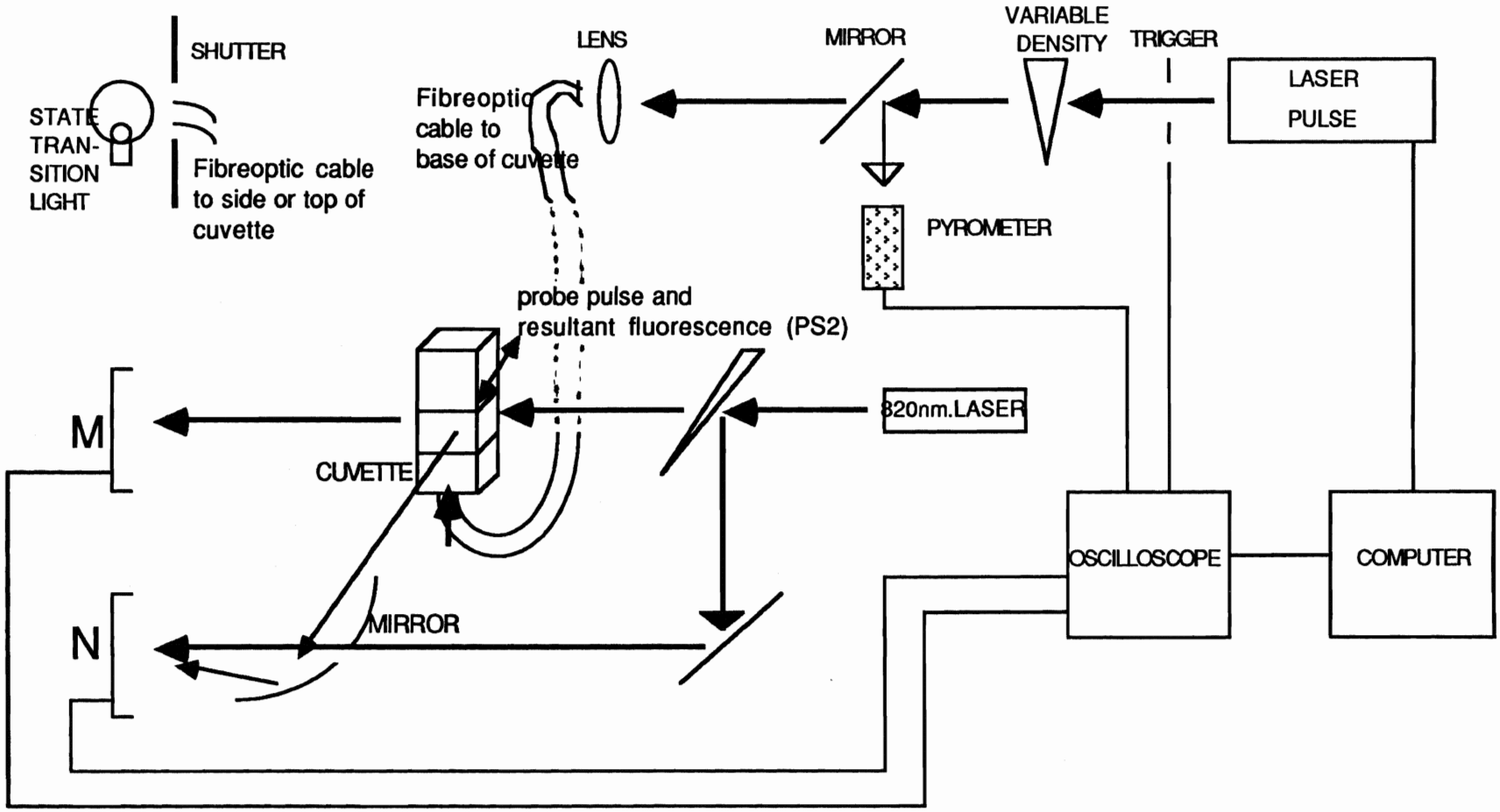

Fig.(*11*). Apparatus for PS1 and PS2 saturation curves.

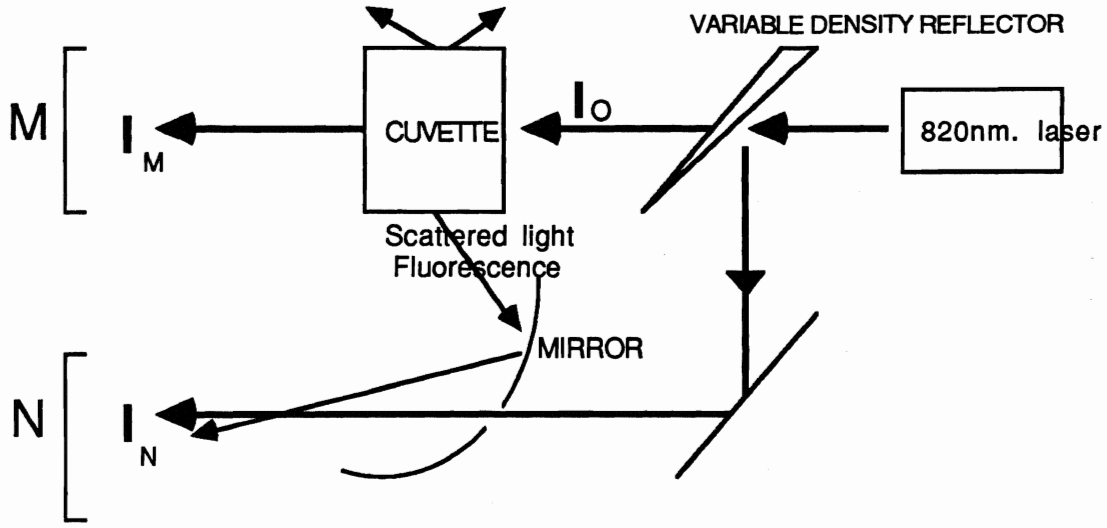

Fig.(12). The addition of scattered and fluorescent light from the cuvette to the diode, N, so that the measured voltage difference between M and N is that due to the change in absorbance at 820nm, ∂A(820), only.

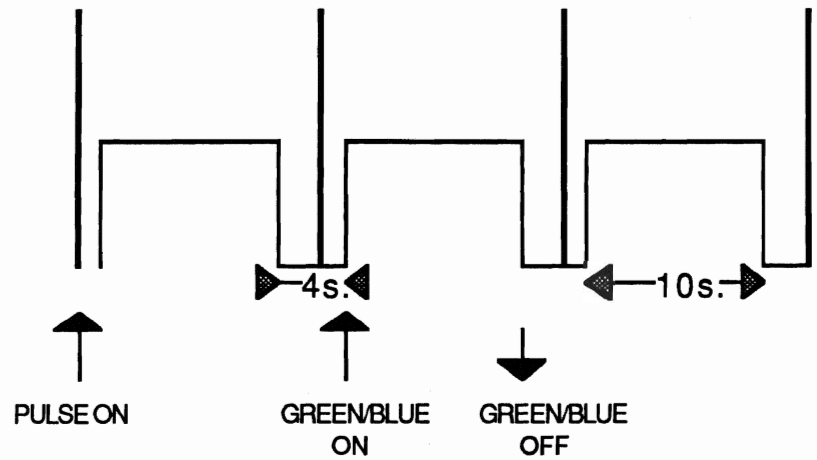

Fig.(13). Pattern of light at cuvette to produce state1 and state2

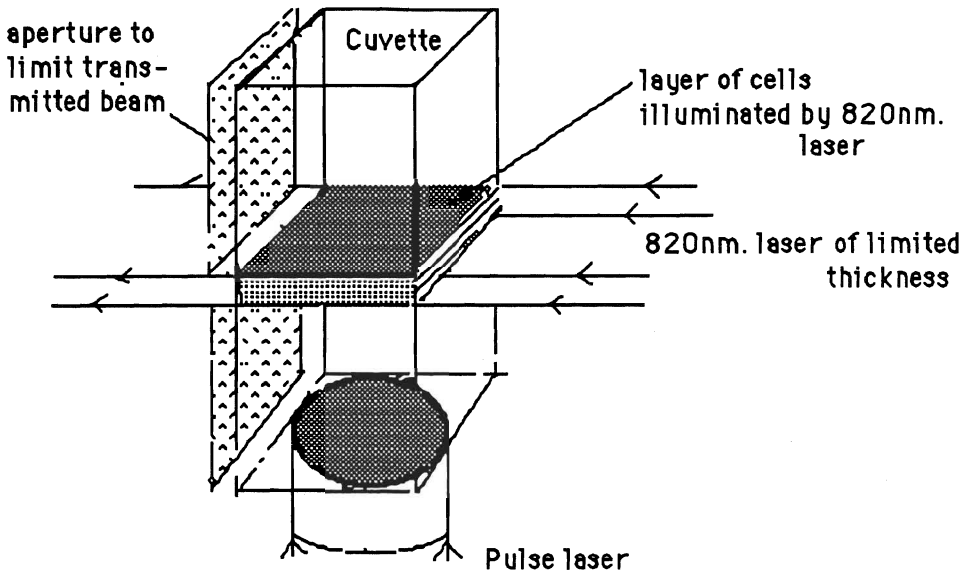

Fig. (14). The 820nm transmitted light received by diodes is limited to narrow layer over which the laser pulse is homogeneous.

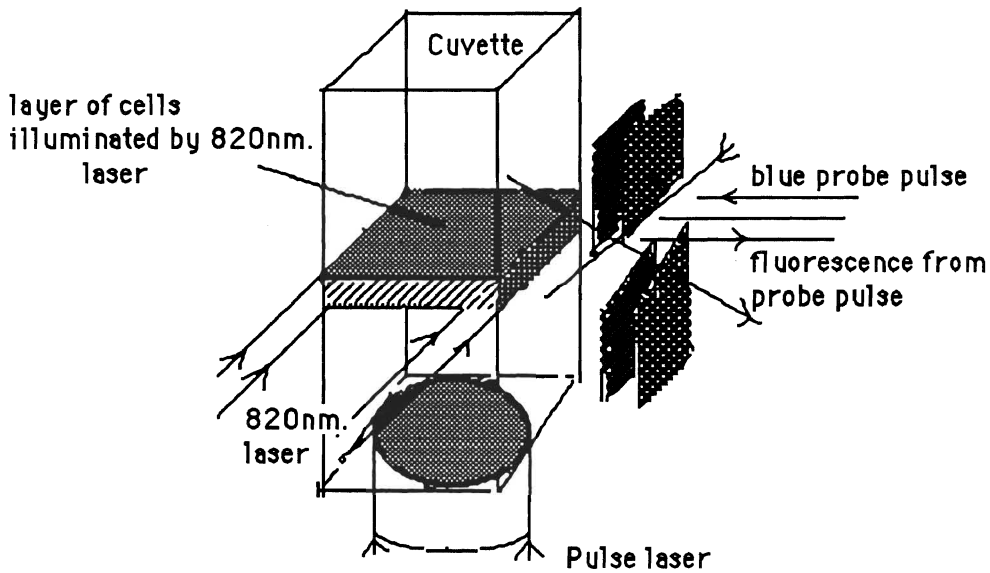

Fig. (15) Apertures which limit the probe pulse and the resultant fluorescence still allow irradiation of and collection from a larger depth of sample than is illuminated by the 820nm plane. This view is caused by rotation of cuvette 90^0 from the last figure.

The cells were always subjected to at least 5min. of periodic green or blue before the start of the experiment. 75μL aliquots were removed from the cuvette several times during the experiment and frozen in liquid N_2 at the time when the pulse would normally occur; the 77^0K fluorescence emission spectra verified the states. At each pulse intensity, 20 absorbance changes and 20 intensity reflections were synchronously averaged.

The flash induced 820nm absorbance increase, and subsequent recovery, is illustrated in fig.(16). This kind of curve was obtained in the early experiments, p231, p245, and p251. The section ot the curve from a point 4μs after impact of the pulse to the end, about 100μs later, was fitted to the equation, y=a*exp(-kt)+c, where a and c are constants related to the amplitude of the absorbance change and k is a measure of the rate of recovery; the fitting was done with the program Spectrocalc. The P700+ saturation curves were obtained by plotting the 820nm signal, (a+c), in volts, against the pulse intensity, E, as measured by the pyrometer in mV.

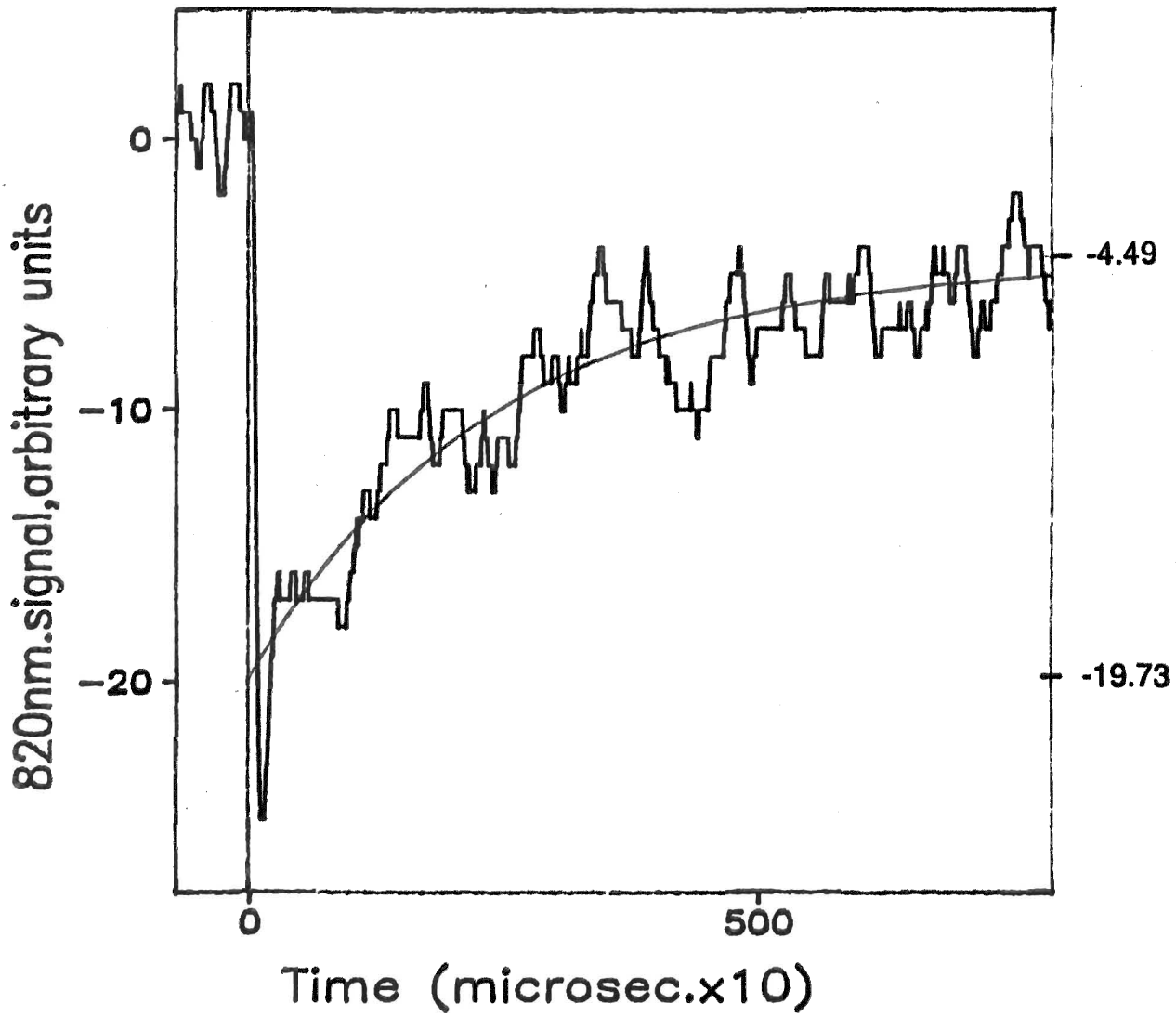

Fig.(1b). Measurement of the 820nm. signal for the PS1 saturation curve (p231, 574nm. pulse), with laser pulse of low intensity (E=5.23mV.). The sample was in S1. The equation fitted by 'Spectrocalc' had the form, y = a exp (-kt) + c, a = -15.24, k = 0.0042, c = -4.49. The 820nm signal, |a+c|, was 19.7 units, 0.40V.

The apparatus was modified for the measurement of the PS2 X-section. A pulse of blue light (the probe pulse), obtained from an Xenon flash with filter, was applied at the side of the cuvette 30μs after the laser pulse; both the probe pulse and the PS2 fluorescence resulting from it was conveyed via a bifurcated optic cable at the side of the cuvette, replacing the S1, S2, light which was applied at the top of the cuvette. The fluorescence, amplified by a photomultiplier tube, was measured as a voltage at a Tetronix TDS540 digitising oscilloscope which could also handle the 820nm signal, and the reflected pulse intensity. The probe pulse needed for the fluorescence interfered with the 820nm absorbance recovery curve and the previous method of measuring the 820nm signal could not be used; the 820nm signal was measured directly as a maximum amplitude. Averages of 10 or 20 were used. PS2 saturation curves were plotted as fluorescence, (Fv-F0)/F0, where Fv is the fluorescence measured with the probe pulse following the laser pulse, and F0 the fluorescence measured with the probe pulse alone. F0 was obtained as an average by plotting Fv versus the measured laser intensity using points at low intensity, and extrapolating a curve of best fit to zero intensity.

In experiments to obtain the PS1 saturation curves with 574nm energy there were differences experimentally between p231, p292, and p303. In experiment p231 the same sample was used for both S1 and S2 . In p292, the sample was changed between S1 and S2. In p303 the sample was changed continually during both saturation curves by exchanging 300μL with fresh culture at regular intervals. In both p292 and p303 the PS2 and the PS1saturation curves were measured under identical conditions; the fluorescence was limited by a single 4mm wide horizontal slit on the cuvette, at the same level as the 820nm laser plane. In p306, only the fluorescence was measured, from a diluted sample; the sample was changed continually as above; the fluorescence was limited by a double aperture formed by two coplanar slits. The double apertures had to be of sufficient width to allow a reasonable fluorescence signal, and may have been of sufficient width to allow illumination of the probe to levels in the cuvette outside the 820nm layer, and collection of the fluorescence from a

similar volume. This is illustrated in fig.(15). For all experiments, the cells were stirred between each series of flashes, by pipetting and expelling small portions of the sample.

The saturation curves, both PS1 and PS2, were fitted, using the program Multifit, with the Poisson single shot equation of Mauzerall (1982), Y=B(1-exp(-AE)), where Y is the 820nm signal or the fluorescence, B the maximum signal, and A a constant related to the absorption X-section of the photosystem. In the fitting of PS1 the points at highest intensities which fall significantly below a maximum obtained at lower intensities were ignored. For some curves a double exponential equation: Y=B(1-exp(-AE)) +D(1-exp(-CE)) was found to fit the saturation curves better than the single component equation.The fits with both types of equations are shown in figures, (36) to (50); all fits were those with a minimum residual sum of squares, rΣsq.; other solutions, which might still be appropriate, had therefore been disregarded. To obtain an average X-section for the double component curves, with an appropriate error, the maximum yield was set to unity, hence **B**+**D**=1, and **B**,**D** became the fraction of the photosystems with X-sections A and C respectively; these are now called the big and the small X-sections. **B**, the fraction of the small X-section was varied and values of A,C, were calculated to give a minimum rΣsq for each **B** value. The average X-section, A**B**+C(1-**B**), was plotted against rΣsq, and the acceptable values of the average X-section were those which lay between the overall minimum rΣsq and 10% more. This is illustrated in fig. (17). A single best value of **B** occurred at the overall minimum of rΣsq. A more detailed analysis was also done with experiment p303 which is described later.

For tranformation of E, the intensity at the pyrometer (in mV) into the number of photons per $Å^2$ hitting the sample, the fibre-optic cable was removed from the base of the cuvette and placed with its end parallel to the receiving surface of the pyrometer, at a distance from it equal to the distance of the fibre-optic cable from the base of the cuvette. The intensity measurement at this position, was I_0, the intensity of the pulse at the cuvette base, and the ratio I_0/E, could be determined for each experiment. The use of this to obtain a X-section in $Å^2$ is illustrated in the appendix.

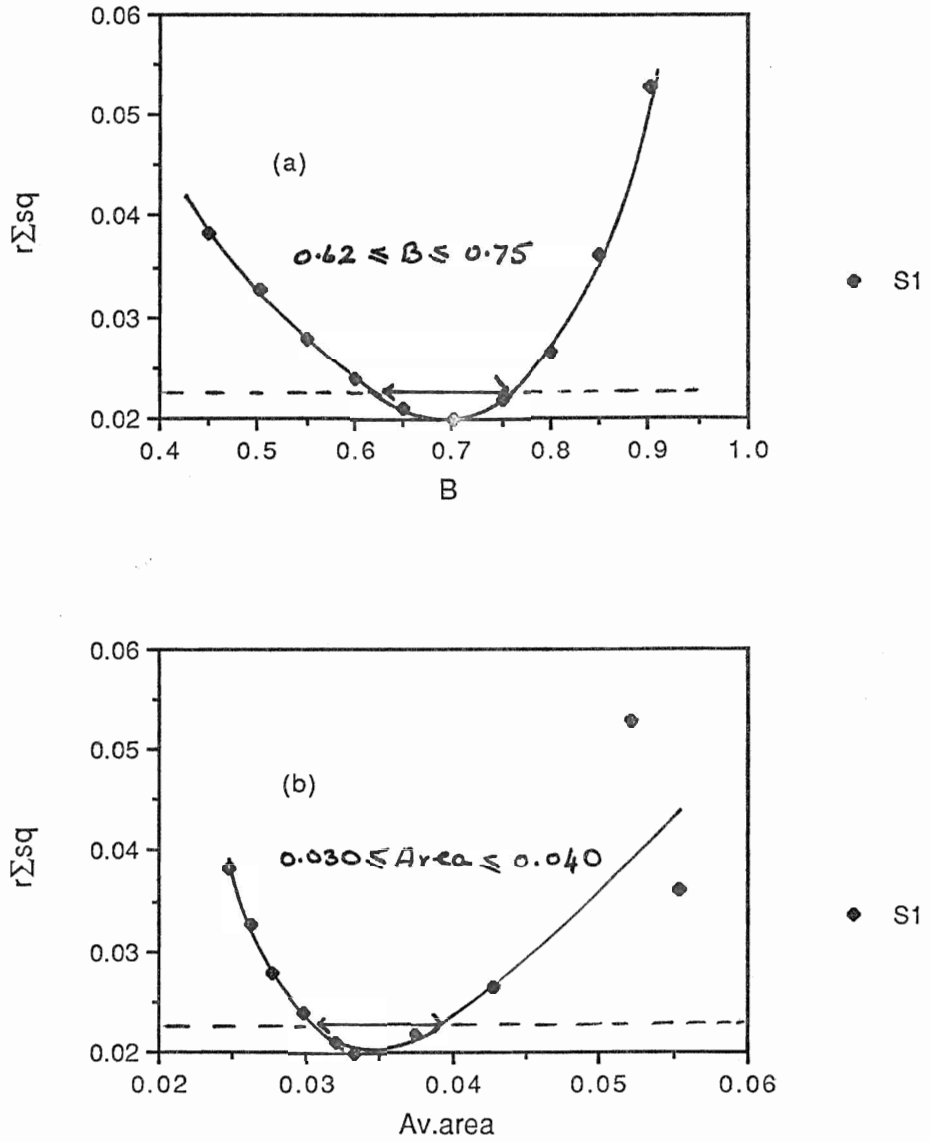

Fig.(17)..Method of determining the fraction, B, of the small component in a two component system, and the average Xsection. B, and the average area, were taken to be those values which fell between min(rΣsq)±10%. The data were from p292, PS2, S1.

RESULTS

ABSORBANCE of a typical whole-cell sample is shown in fig.(18). There are three prominent peaks, two due to chl*a* in the blue and red regions and another, in the green region, due to the phycoerythrin of the PBS. None of these peaks significantly overlaps another, demonstrating that the laser pulse of 668nm is absorbed mainly by the ch*a* of the photosystems, in particular the larger PS1, and the laser pulse of 574nm is absorbed mainly by the PBS, which transfers most of its energy to PS2.

77^{0}K FLUORESCENCE SPECTRA A typical example is shown in fig.(19). All the samples have an increased PS2 fluorescence, 685nm and 695nm, in S1 compared to S2. This is typical of the state transition phenomenon: in S2 PS2 donates some of its energy to PS1, in consequence there is less excitation in the PS2 antenna and as the fluorescence varies with the amount of excitation present, there is less fluorescence. The two small peaks at 640nm and 660nm are due to PBS, a cut-off filter prevents the registration of any shorter wavelength emission. The PBS peaks are usually regarded as constant in S1 and S2 (Ley and Butler, 1980); normalisation was done using the 660nm peak. The emission peak at 715nm, due to PS1, is small and is overlapped by the PS2 emission peaks. Comparison of the fluorescence spectra was done by normalisation on the PBS peaks. All samples underwent a state transition under the conditions of the experiment. In all experiments the ratio F660/F715, was greater in S2 than in S1. The spectrum for p292 showed that the ratio of PS2 fluorescence to PS1 fluorescence, F695/F715, was lower for both S1 and S2 (1.92, 1.52 respectively) than in all the other samples whose average was 2.44 and 2.06 respectively, see table (1). The state of the photosynthetic components of the sample in this experiment was obviously not the same as the others.

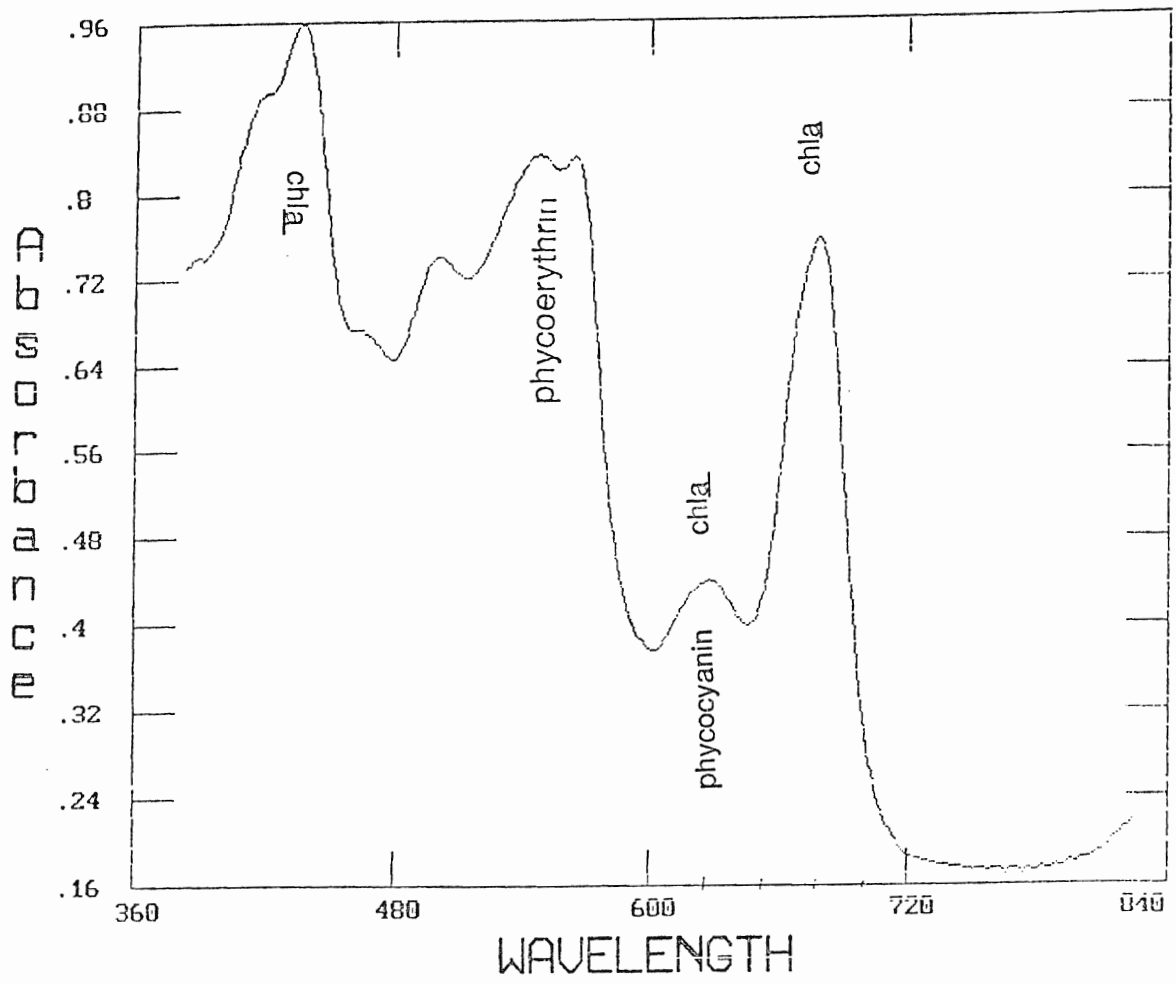

Fig.(18). Absorbance of sample p231. A(678) is 0.76. Regions of maximum absorbance of component pigments are shown: chla, phycocyanin, phycoerythrin.

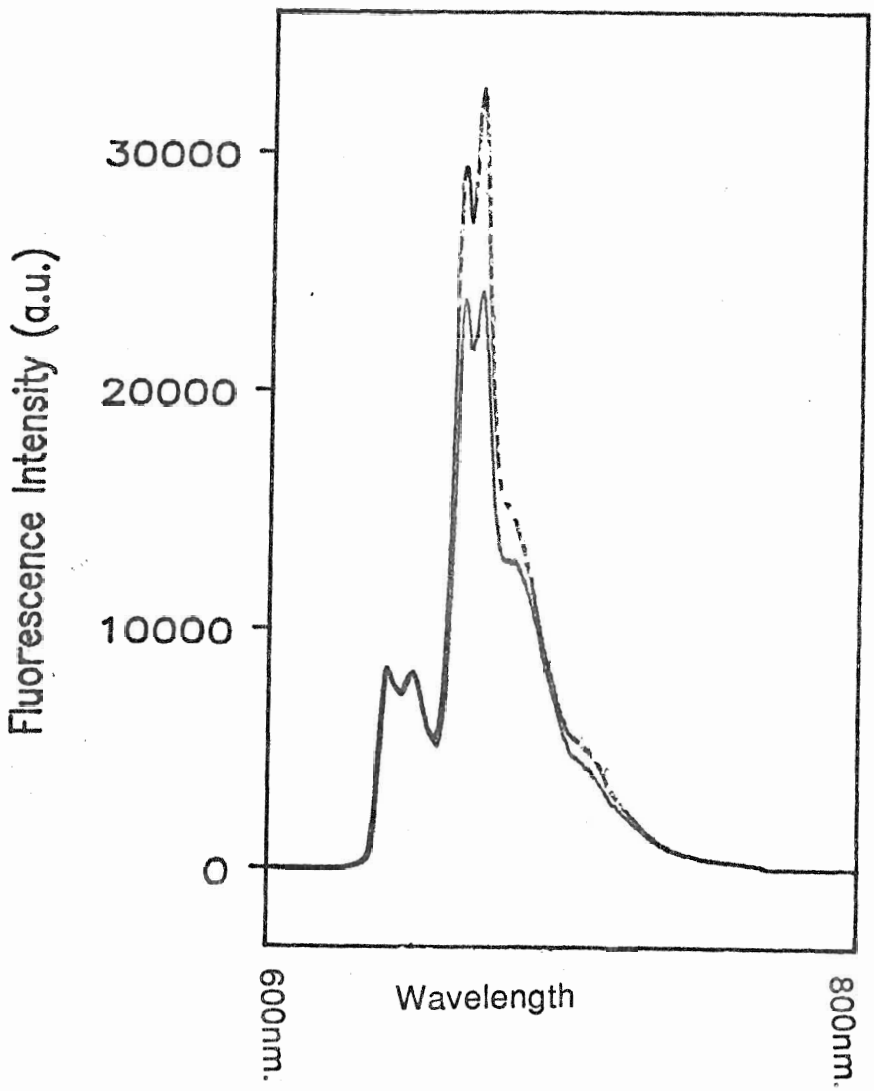

Fig.(19). Example of 77^0K fluorescence from sample of cells taken during experiment at a time when the laser pulse would normally fire. The solid curve is state2 and the broken curve state1. The curves were normalised on the PBS peaks. The cells were excited with 560nm light. Emission peaks occur at 640nm and 660nm (PBS), 685nm and 695nm (PS2), and 715nm (PS1). (Gantt et al. 1976)

Table (1). List of experiments with wavelength of exciting light, absorbance at 678nm, ratio of fluorescence (77^0K) at 695nm and at 660nm to that at 715nm in state1 and state2, and growth time (since innoculation) of sample.

Exp.	wave-length	A(678)	F695/715		F660/F715		Growth time	Order of curves
			S1	S2	S1	S2		
p231	574nm	0.76	2.30	2.03	-	-	7 days	S2,S1
p245	627nm	0.83	2.31	1.93	-	-	6 days	S1,S2
p251	668nm	0.83	2.29	1.92	0.55	0.62	7 days	S2,S1
p241	668nm	0.76	2.39	2.02	0.46	0.55	7 days	S1,S2
p263	668nm	0.78	2.48	2.16	0.60	0.65	3 days	S2,S1
p268	627nm	0.78	2.48	2.13	0.57	0.66	4 days	S2,S1
p271	668nm	0.81	2.54	2.11	0.53	0.58	5 days	S2,S1
p279	668nm	0.32	2.53	2.12	0.66	0.78	5 days	S1,S2
p285	668nm	0.33	2.36	1.98	0.57	0.65	7 days	S2,S1
p292	574nm	0.82	1.92	1.52	0.49	0.57	5 days	S1,S2
p303	574nm	0.75	2.44	2.20	0.61	0.63	6 days	S2,S1
p306	574nm	0.39	2.68	2.06	0.58	0.66	4 days	S1,S2

SATURATION CURVES. PS1 were obtained at three wavelengths, 574nm, 627nm, and 668nm, in both S1 and S2. All demonstrated a minimum yield, near zero, with the lowest intensity laser pulse, rising to a maximum at stronger intensities; when the yield was plotted (measured in V) against the log. of the pulse intensity (measured in mV) the shape was that of an S typical of the single hit Poisson distribution. Some noticeably deviated from this, p303 with 574nm in both S1 and S2, p268 with 627nm in S1 (where it was suspected that cell aggregation had occurred in the sample during the S1 experiment), and p263 with 668nm in S2. The saturation curves of S1 and S2 usually had very close maximum yields and so were directly comparable for visual comparison. When there was a difference in maxima, normalisation was done to ensure that comparison was done under the best conditions. These curves are shown in fig.(20) to fig.(28).

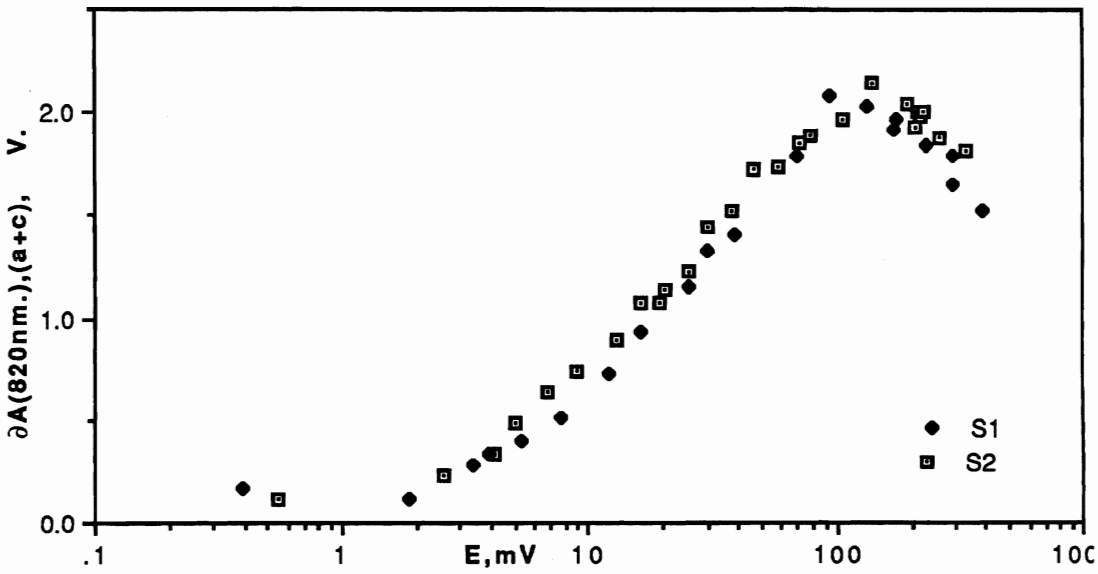

Fig.(20). PS1 saturation curves, S1 and S2, with 574nm radiation, experiment p231, measured as a change in absorbance at 820nm (in volts) against the intensity of the laser pulse measured at the pyrometer (in mvolts). The extent of the absorbance change (a+c) was measured by curve fitting to the P700+ recovery curve from a point 4μs from the start, as described in materials and method. Both S1 and S2 have approximately the same maximum yield and are not normalised.

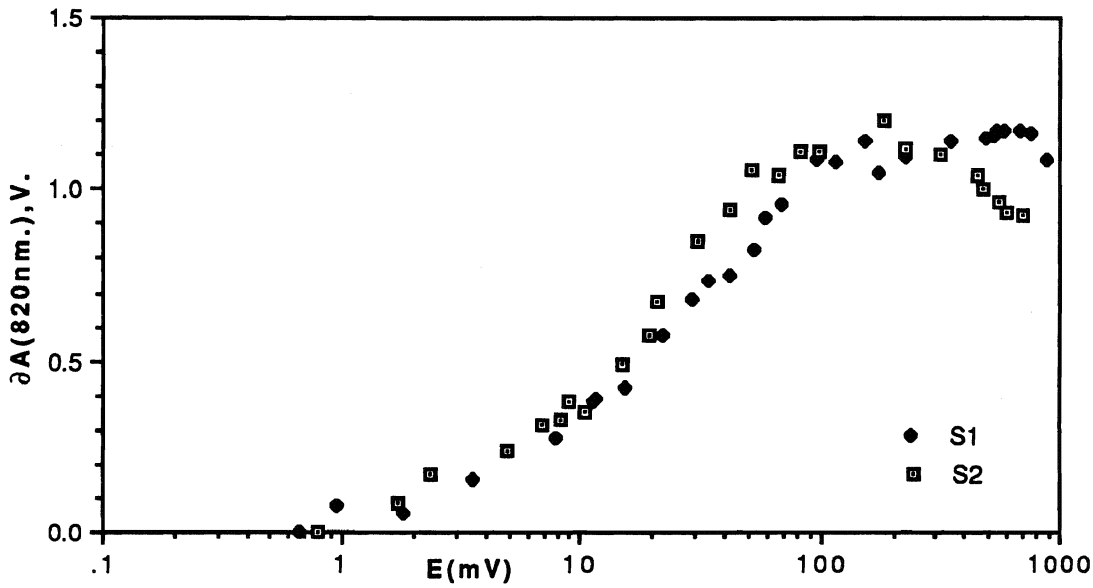

Fig.(21) PS1 saturation curves, S1 and S2, with 574nm radiation, experiment p292, measured as a change in absorbance at 820nm (in volts) against the intensity of the laser pulse measured at the pyrometer (in mvolts). The change in absorbance was measured directly. Both S1 and S2 have approximately the same maximum yield and are not normalised.

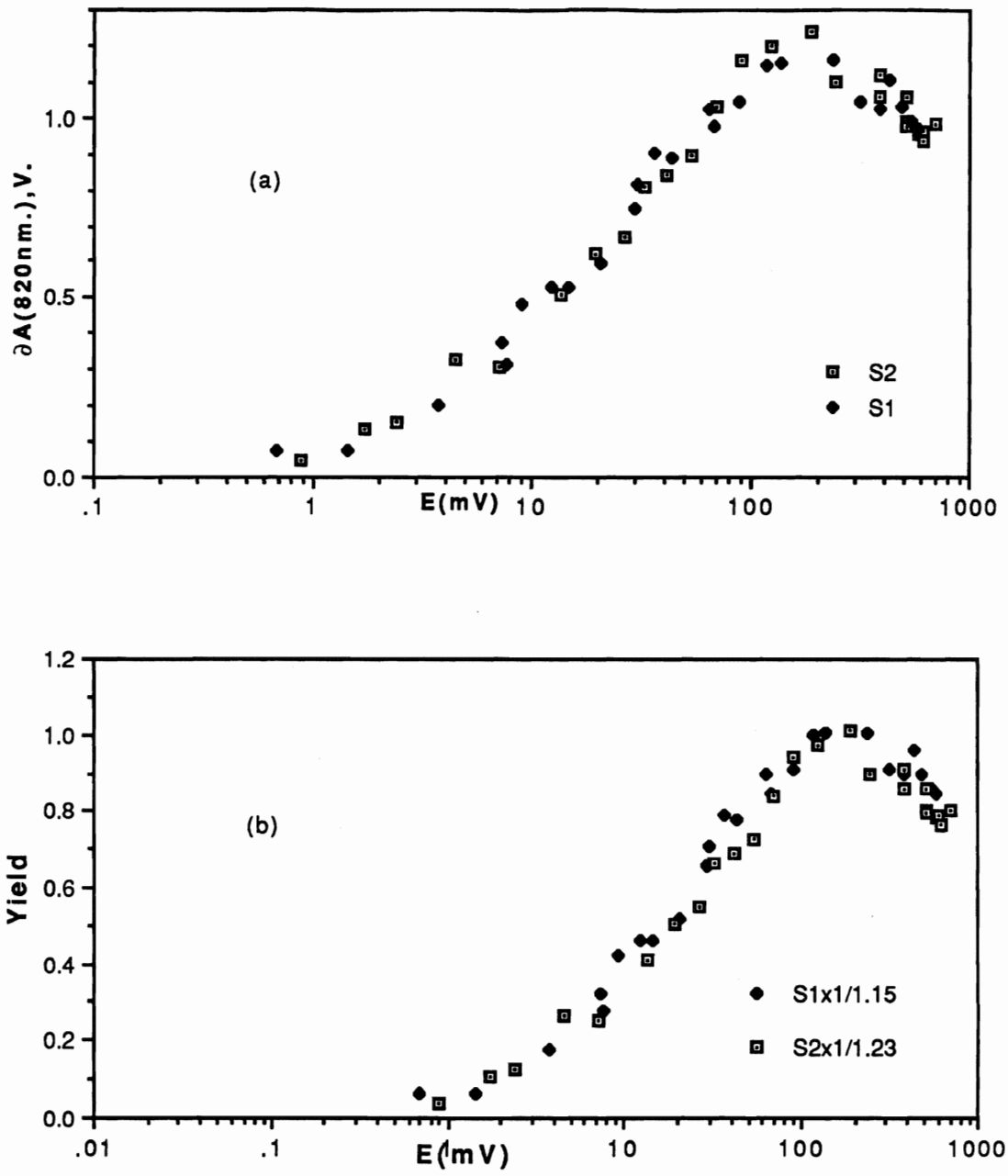

Fig.(22). PS1 saturation curves, S1 and S2, with 574nm radiation, experiment p303, measured as a change in absorbance at 820nm (in volts) against the intensity of the laser pulse measured at the pyrometer (in mvolts).The extent of the change in absorbance was measured directly. The maximum yield in S2 is greater than that in S1. Normalisation is done in (b).

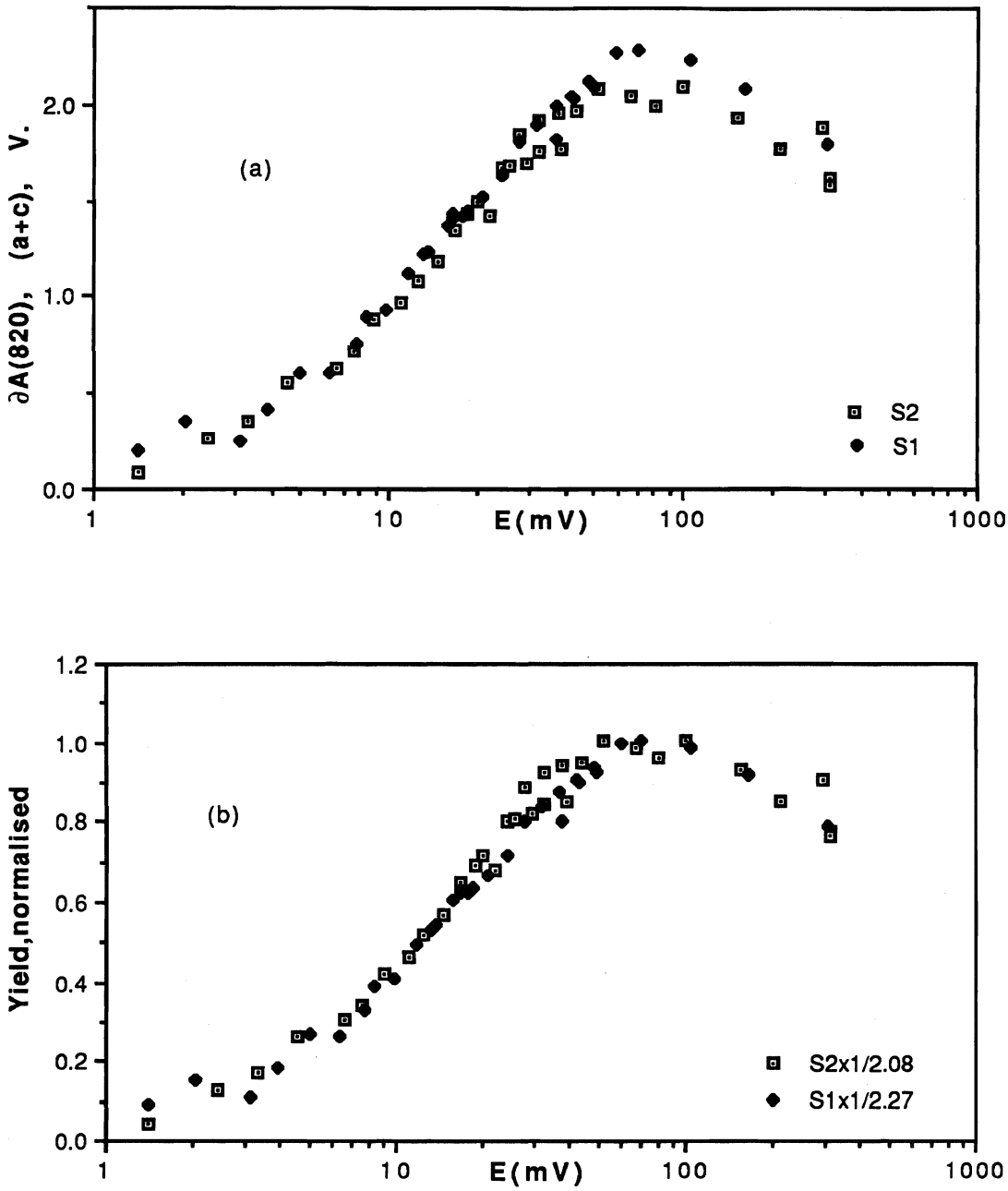

Fig.(23). PS1 saturation curves, S1 and S2, with 627nm excitation, experiment p245, measured as a change in absorbance at 820nm (volts) against the intensity of the laser pulse at the pyrometer. The extent of the absorbance change (a+c) was measured by curve fitting to the P700+ recovery curve from a point 4μs from the start, as described in the materials and method. The maximum yield in S1 is greater than that in S2. Normalisation is done in (b).

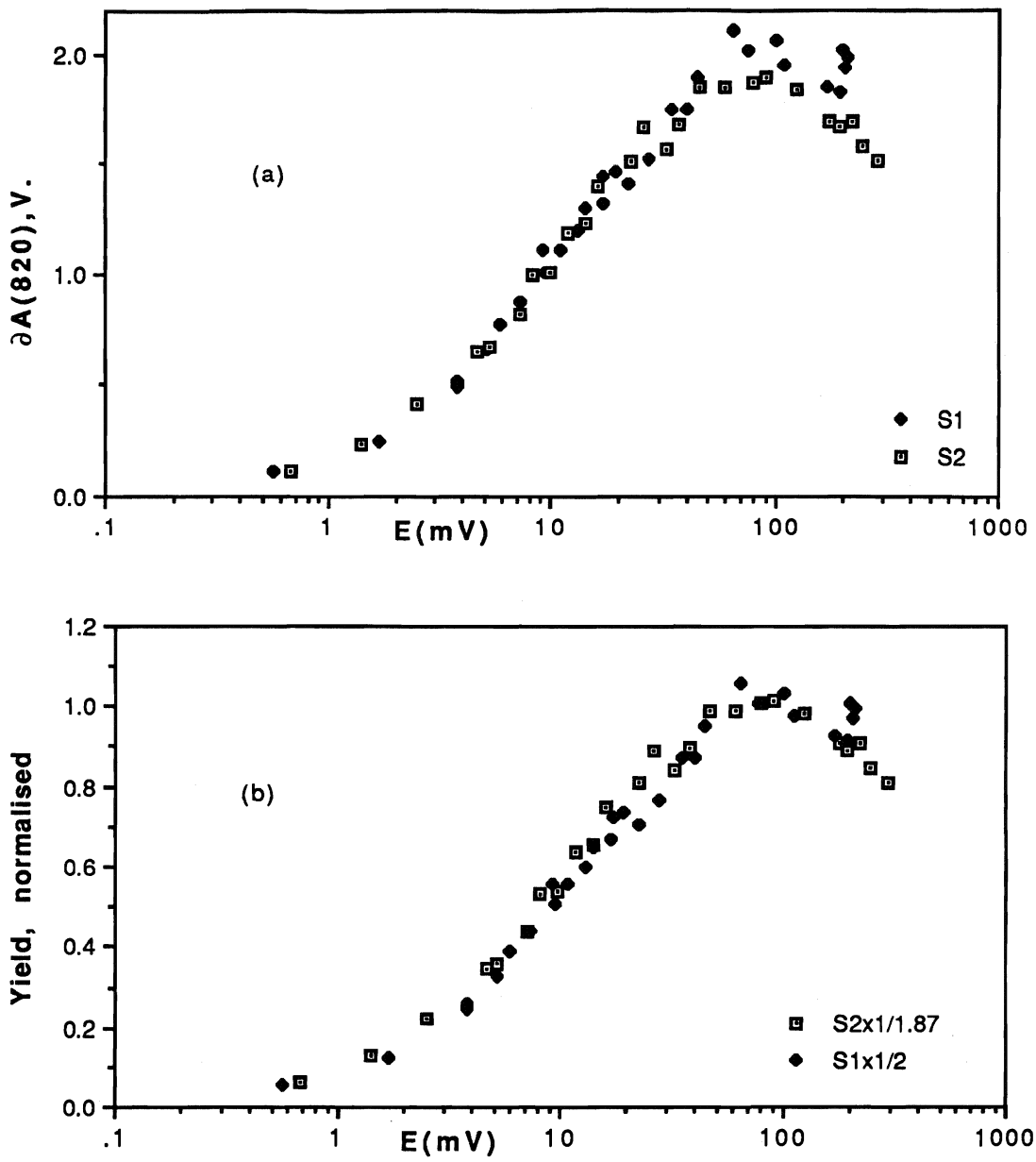

Fig.(24) PS1 saturation curves, S1 and S2, with 627nm radiation, experiment p268, measured as a change in absorbance at 820nm (volts) against the intensity of the laser pulse at the pyrometer (mV). The extent of the absorbance change was measured directly. The maximum yield in S1 is greater than that in S2. Normalisation is done in(b).

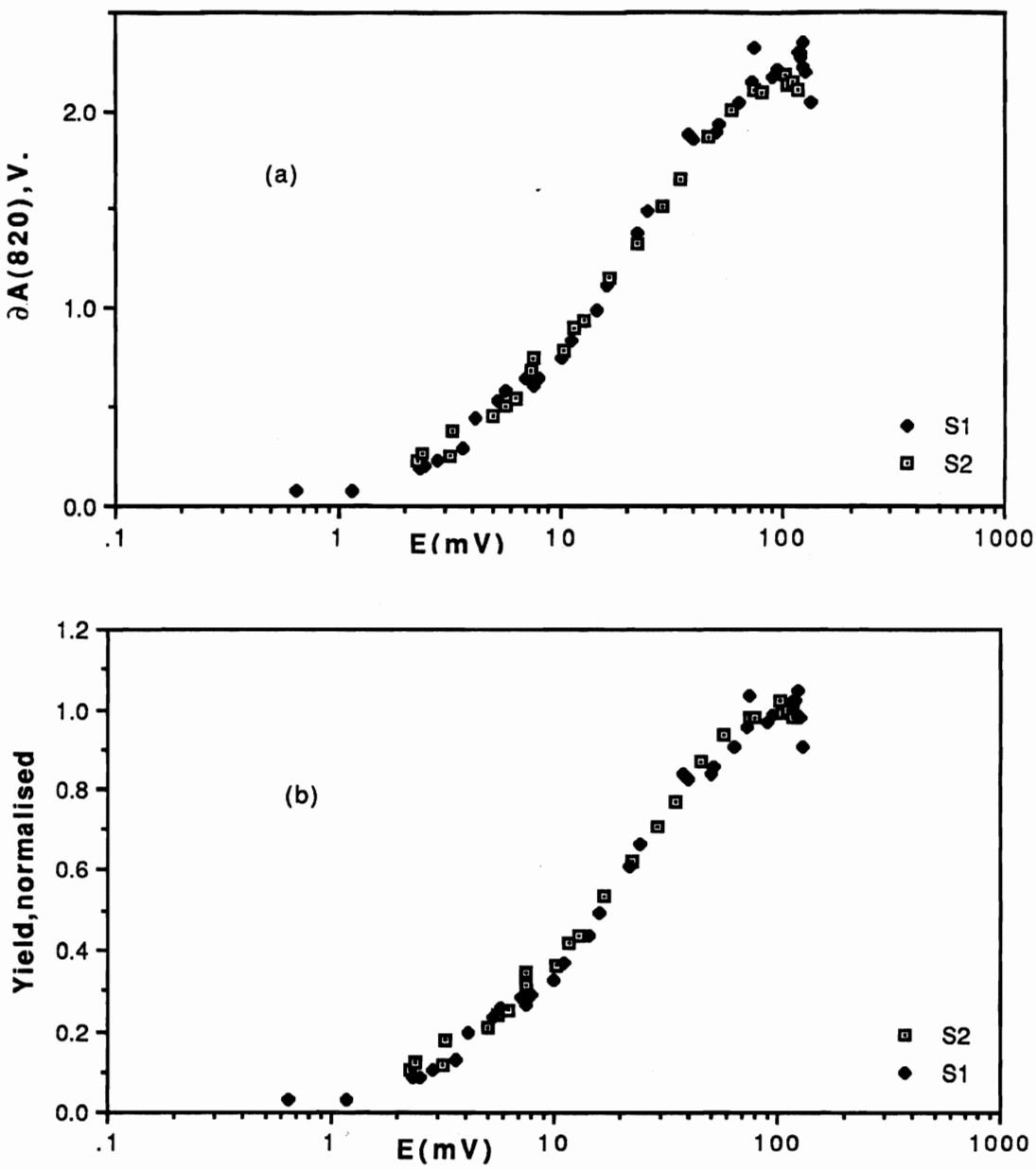

Fig.(25). PS1 saturation curves, S1 and S2, with 668nm excitation, p241, measured as a change in absorbance at 820nm (in volts) against the intensity of the laser pulse at the pyrometer (in volts). The extent of the absorbance was measured directly. The maximum yield in S1 was greater than that in S2. Normalisation is done in (b).

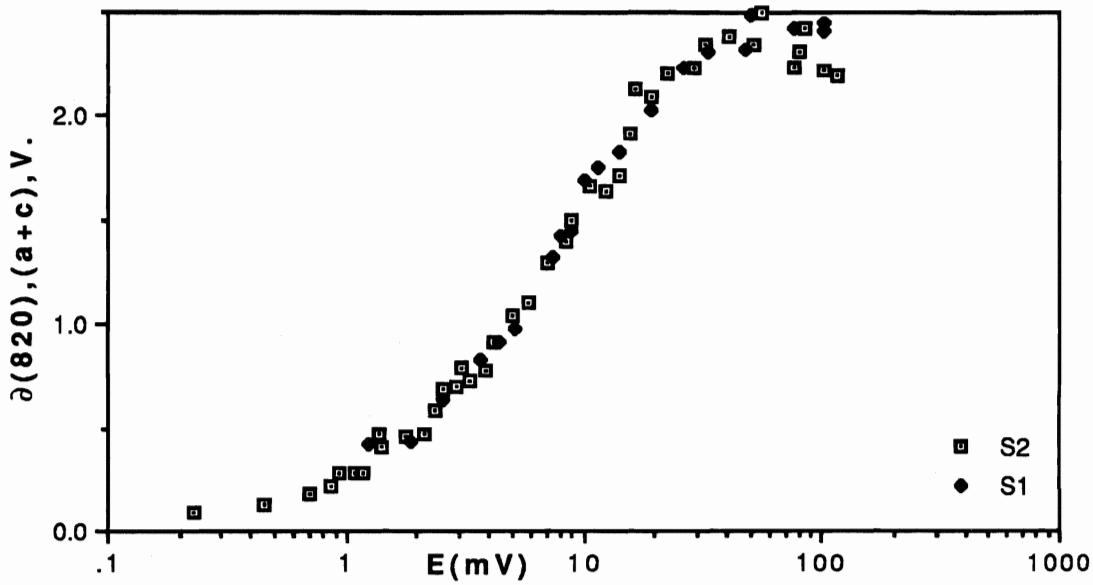

Fig.(26) PS1 saturation curves, S1 and S2, with 668nm excitation, experiment p251, measured as a change in absorbance at 820nm(in volts) against the intensity of the laser pulse at the pyrometer (in mvolts). The extent of the absorbance change was measured by curve fitting to the P700+ recovery curve from a point 4μs from the start, as described in materials and method. Both S1 and S2 have the same maximum yield and are not normalised.

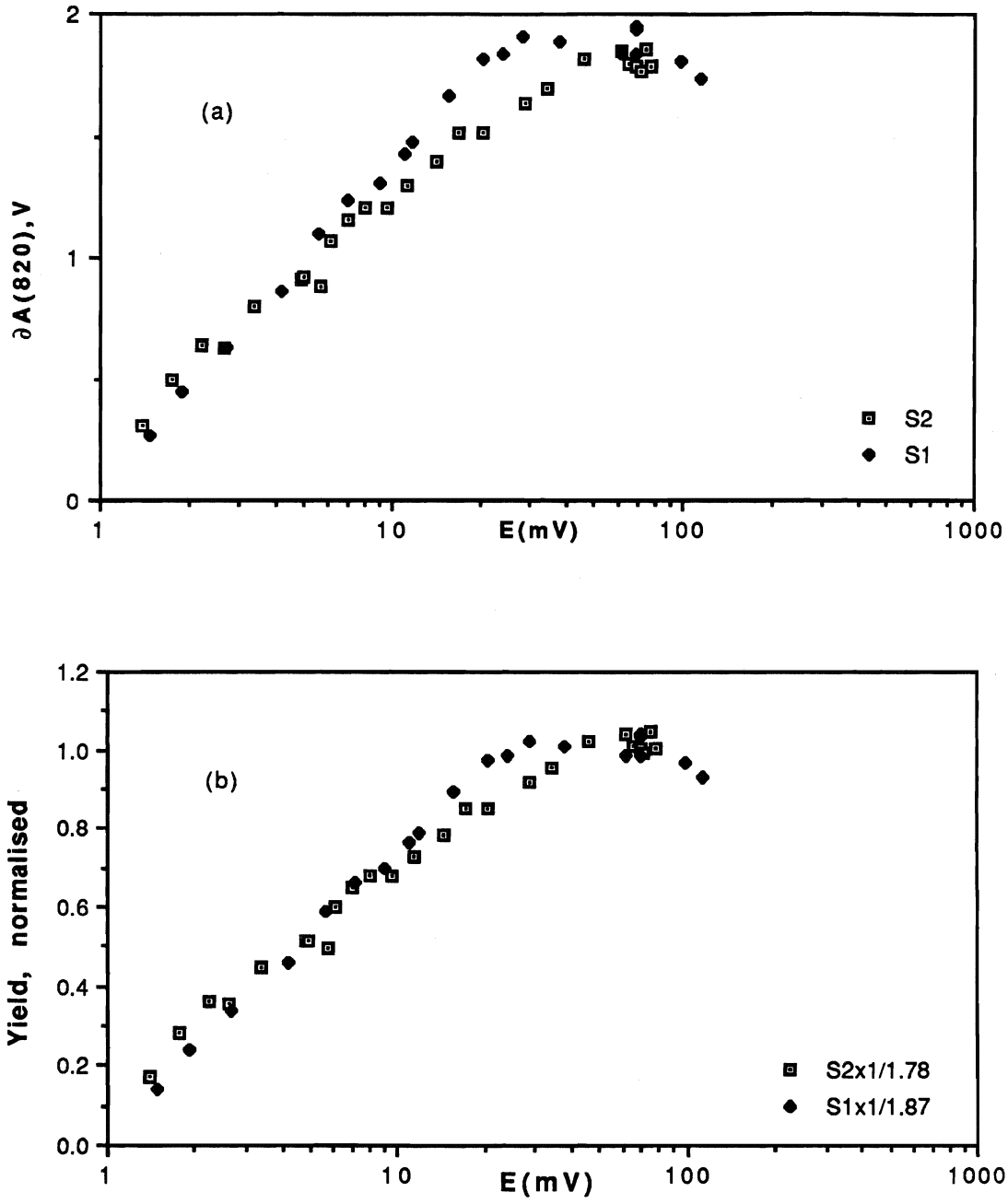

Fig.(27) PS1 saturation curves,S1 and S2, with 668nm excitation, experiment p263, measured as a change in absorbance at 820nm (volts) against the intensity of the laser pulse at the pyrometer (mV). The extent of the absorbance change was measured directly. The maximum yield in S1 was greater than that in S2. Normalisation is done in(b).

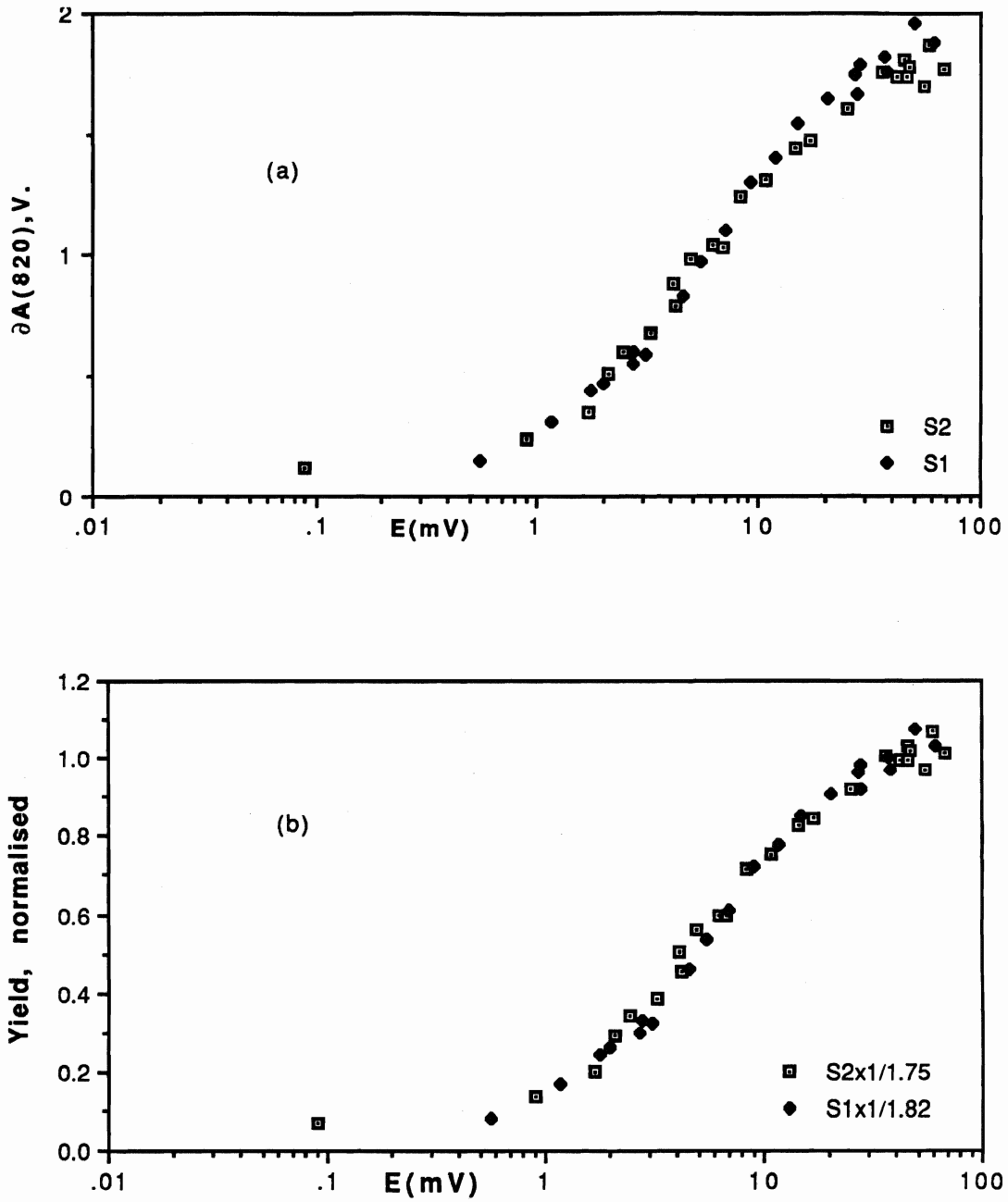

Fig.(28) PS1 saturation curves, S1 and S2, with 668nm excitation, experiment p271, measured as a change in absorbance at 820nm (in volts) against the intensity of the laser pulse measured at the pyrometer (in volts). The extent of the change in absorbance was measured directly.The maximum yield in S1 is greater than that in S2. Normalisation is done in (b).

A decrease in yield at high intensities appears in PS1 saturation curves in both S1 and S2, at all wavelengths. The decline in yield appears as the pulse intensity is increased above the point where saturation is reached and increases with increase in pulse intensity. This is shown, for example, in fig. (20) and fig.(22). It was observed during the determination of a PS1 saturation curve that as the intensity of the pulse was increased, the sharp negative minimum, caused by the increase in 820nm absorbance, such as shown in fig.(16), became rounded. It was suspected, that at high intensities, another 820nm absorbance effect was produced, opposite to that caused by P700+. The latter effect can be eliminated by illuminating the sample with light during the passage of the pulse so that the P700 is already oxidised and the pulse can cause no further increase in 820nm absorbance. The form of this high intensity effect obtained on its own was of a wide positive peak, which lasted approximately 40μs from start to finish, in contrast to the 2μs that it takes for the 820nm negative absorbance peak to form. At the higher intensities the modified absorbance-recovery curve was recorded; the absorbance-recovery curves obtained in the presence of saturating light, both with and without the 820nm light were recorded. In this way, by comparison of the curves, the P700+ effect could be corrected for the high intensity effect and any unexpected fluorescence. Two saturation curves, p211 and p221, obtained at 627nm and 668nm, demonstrate that, with a correction at high intensities, they tend to level off at a maximum. These saturation curves are shown in fig.(29) and (30).

Possible causes of the decrease in yield are discussed in appendix 2.

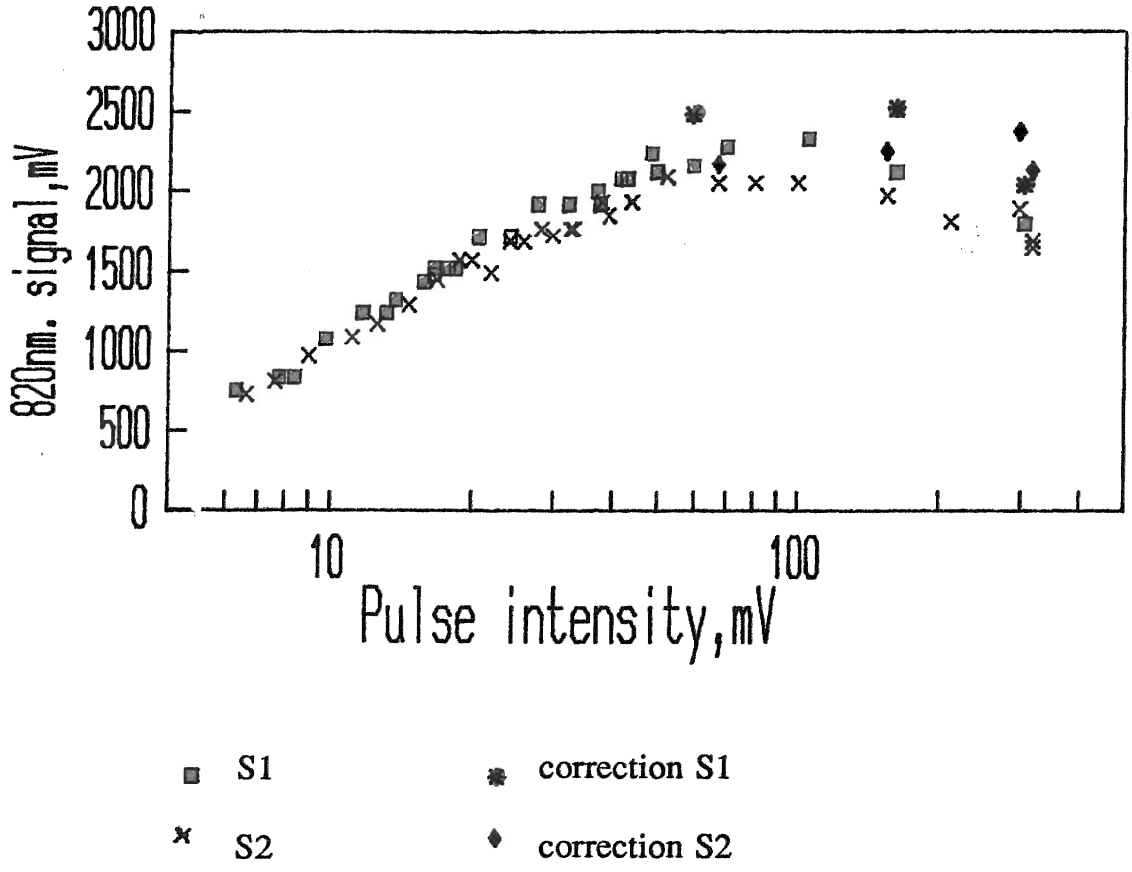

Fig.(29). PS1 saturation curve, with high intensity corrections, for state1 (S1) and state 2 (S2), with 627nm. radiation, p211.

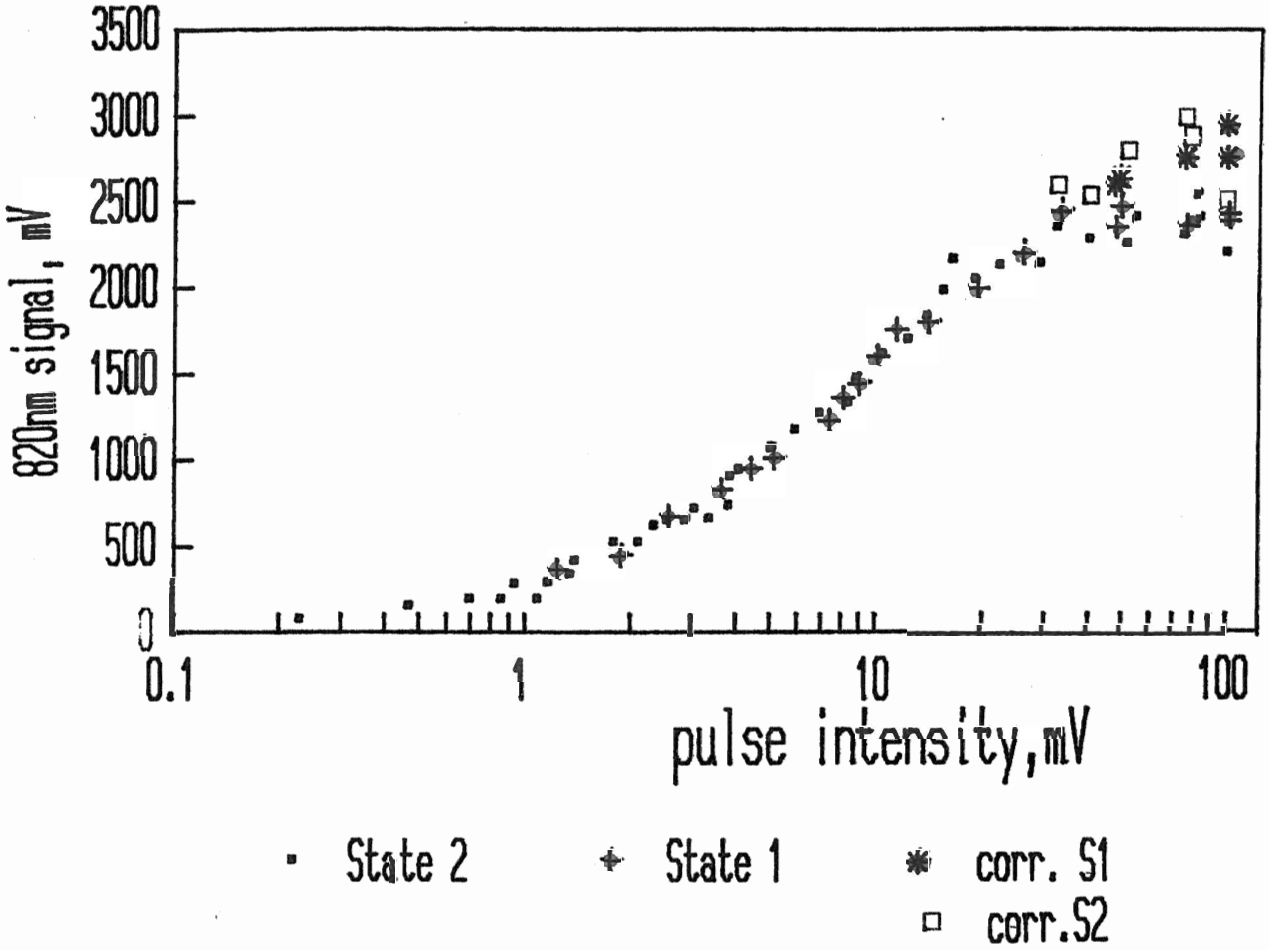

Fig.(30). PS1 saturation curve, with high intensity corrections, for state1 (S1) and state 2 (S2), with 668nm. radiation, p221.

SATURATION CURVES PS2 were obtained for three wavelengths, 574nm, 627nm, and 668nm in both S1 and S2, and are shown in fig.(31) to fig. (35). All demonstrated a minimum yield, near zero, with the lowest intensity laser pulse, rising to a maximum at stronger intensities; when the fluorescence, (Fv-F0)/F0, was plotted against the log. of the pulse intensity (measured in mV) most of the plotted curves deviated from the S shape of the single hit Poisson distribution, tending to have a more stretched-out character. The maximum yield in S1 was approximately twice that in S2, and for visual comparison, normalisation had to be done. In the experiment with 627nm energy, p268, it was suspected that aggregation of the sample had occurred during the S1 experiment.

The scatter in these curves is especially apparent in the normalised S2 curves, for example p285 fig.(35). The double aperture of p306 did not significantly reduce the scatter, fig.(47).

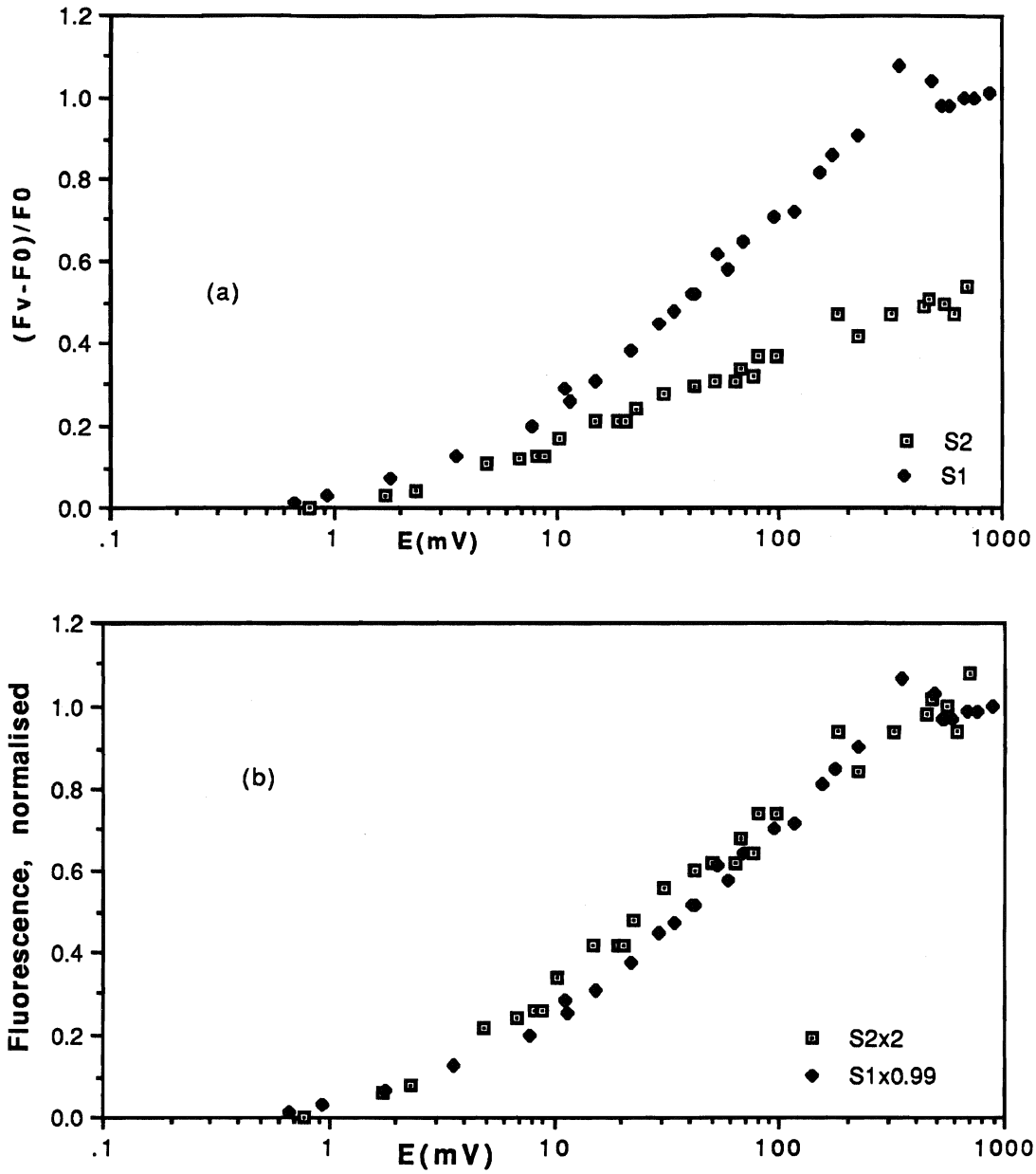

Fig.(31). PS2 saturation curves, S1 and S2, with 574nm pulse, measured as fluoresence yield against the intensity of the laser pulse measured at the pyrometer, experiment p292.

(a) Fluorescence yield as measured.

(b) Fluorescence yield for both S1 and S2 normalised to unity.

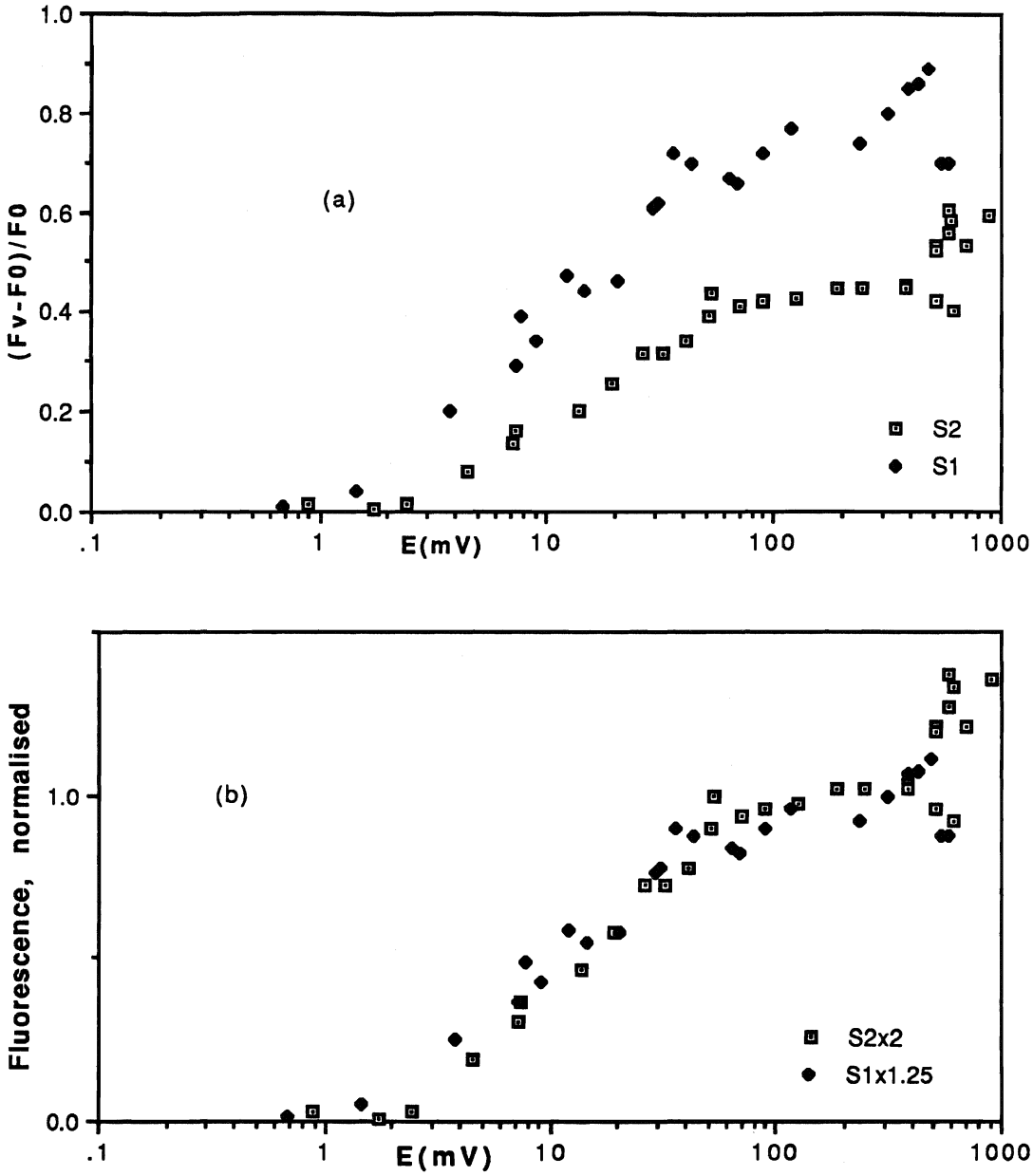

Fig.(32).PS2 saturation curves with 574nm pulse, S1 and S2, measured as fluoresence yield against the intensity of the laser pulse measured at the pyrometer, experiment p303.

(a) Fluorescence yield as measured.

(b) Fluorescence yield for both S1 and S2 normalised to unity.

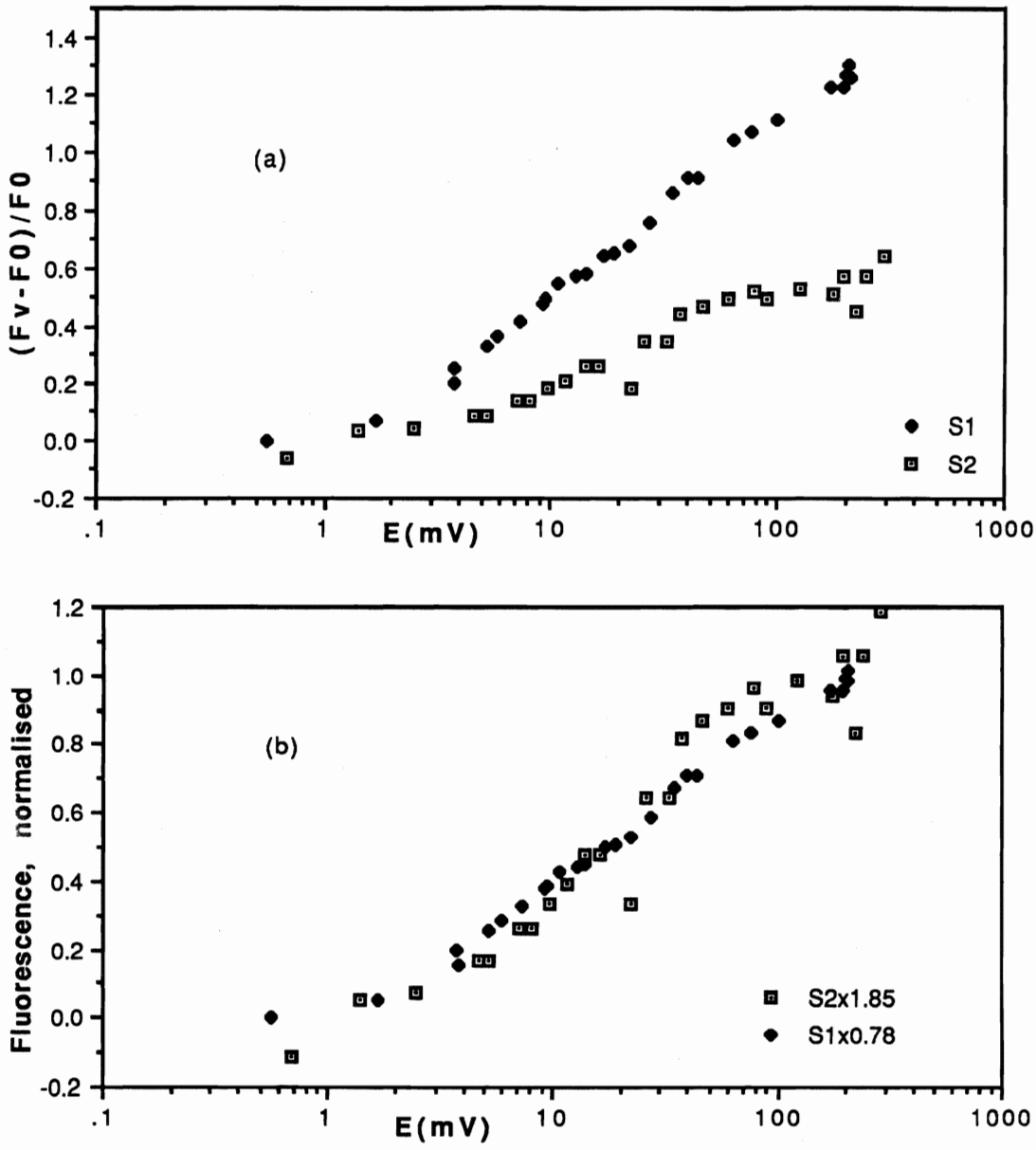

Fig.(33). PS2 saturation curves, S1 and S2, with 627nm pulse, measured as fluoresence yield against the intensity of the laser pulse measured at the pyrometer, experiment p268.

(a) Fluorescence yield as measured.

(b) Fluorescence yield for both S1 and S2 normalised to unity.

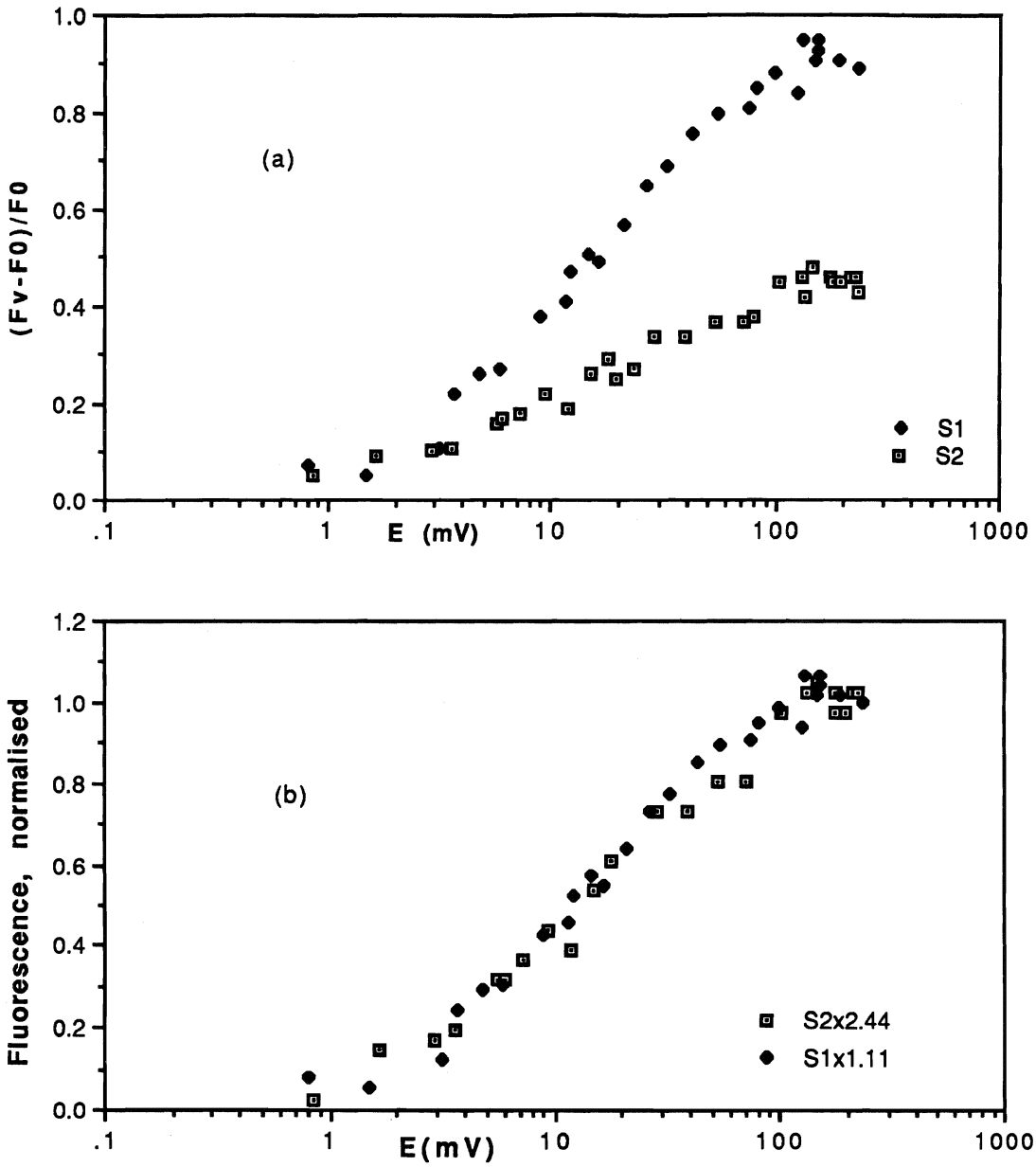

Fig.(34). PS2 saturation curves, S1 and S2, with 668nm pulse, measured as fluoresence yield against the intensity of the laser pulse measured at the pyrometer, experiment p279.

(a) Fluorescence yield as measured.

(b) Fluorescence yield for both S1 and S2 normalised to unity.

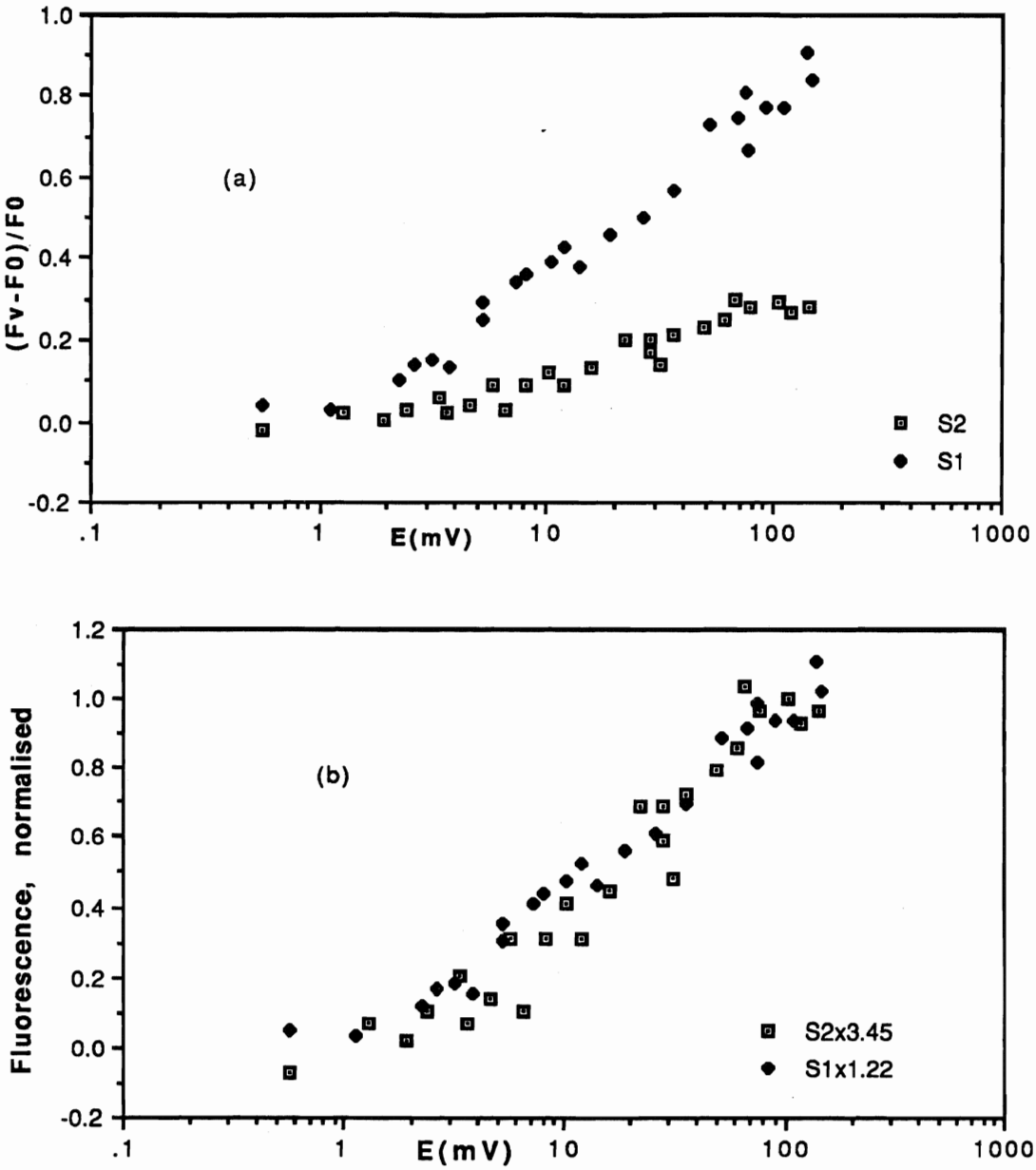

Fig.(35). PS2 saturation curves, S1 and S2, with 668nm pulse, measured as fluoresence yield against the intensity of the laser pulse measured at the pyrometer, experiment p285.

(a) Fluorescence yield as measured.

(b) Fluorescence yield for both S1 and S2 normalised to unity.

FITTING OF PS1 AND PS2 SATURATION CURVES TO POISSON EQUATIONS.

Maximum information from the saturation curves, both qualitative and quantitative, can only be obtained by interpreting all the curves, including those which deviate from the single-hit Poisson equation. This equation applies to a single population of photosystems with the same X-section ; deviations from the equation can be obtained by postulating a population with two-components of different X-section.

A single component Poisson equation is of the form, Yield=B(1-exp(-AE)); a double component equation is of the form, Yield=B(1-exp(-AE))+D(1-exp(-CE)). For these experiments E is the energy in mV delivered to the measuring pyrometer and is related to the intensity delivered to the plane illuminated by the 820nm laser (the relationship between them is described in the appendix. The yield is the change in absorbance at 820nm, ∂(820nm), measured in V, or the fluorescence, (Fv-F0)/F0, where Fv is the fluorescence caused by the probe pulse after the laser pulse, and F0 that obtained from the probe pulse alone, with no laser pulse. The double component fits shown in the following figs. (36) to (50) were obtained from 'Multifit', which adjusted A,B,C,D, to yield an answer with a minimum rΣsq.

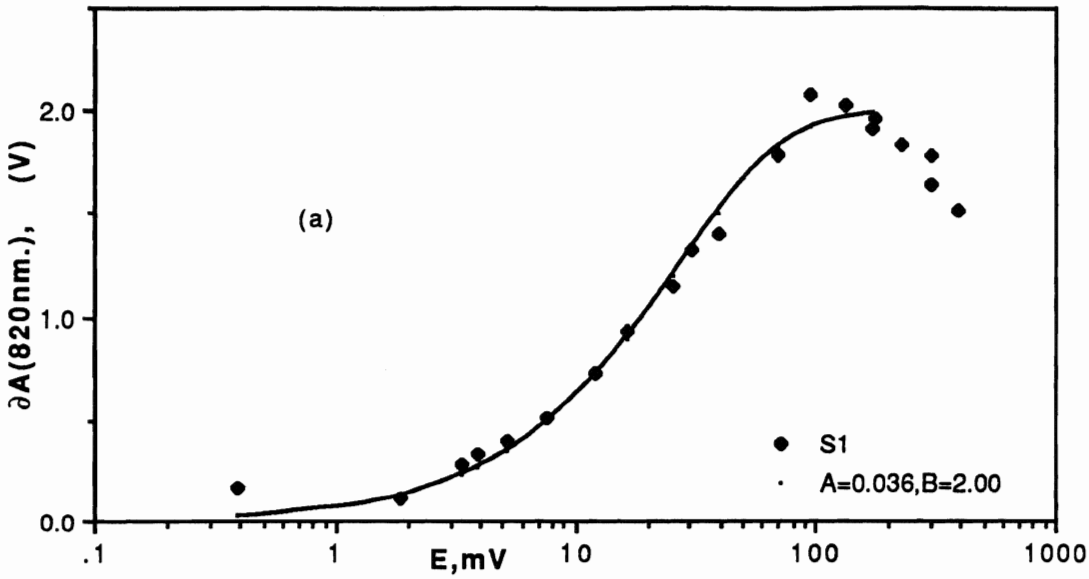
∂A(820nm.), (V)
2.0
1.0
0.0
(a)
S1
A=0.036,B=2.00
.1
1
E,mV
10
100
1000

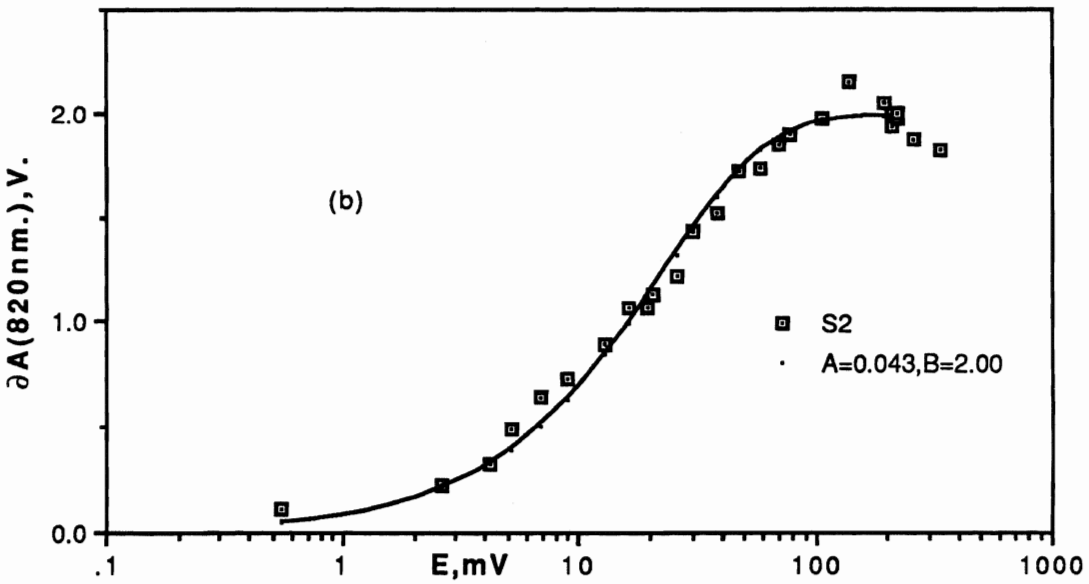
∂A(820nm.),V.
2.0
1.0
0.0
(b)
S2
A=0.043,B=2.00
.1
1
E,mV
10
100
1000

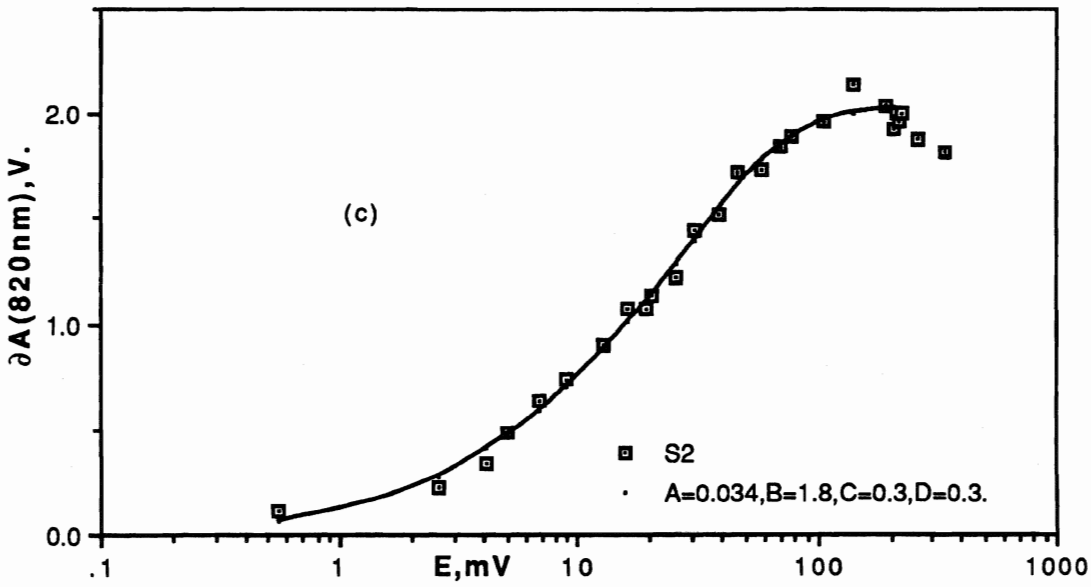

Fig.(36). The fit of PS1 saturation curves in state1 and state2 to Poisson equations. (574nm, p231)

(a) State1. A single component curve, A=0.036±0.002, B=2.00±0.04, rΣsq=0.0785.

(b) State2. A single component curve, A=0.043±0.002, B=2.00±0.03, rΣsq=0.1149.

(c) State2. A double component curve, A=0.034±0.004, B=1.8±0.1, C=0.3±0.2, D=0.3±0.1,rΣsq=0.0609.

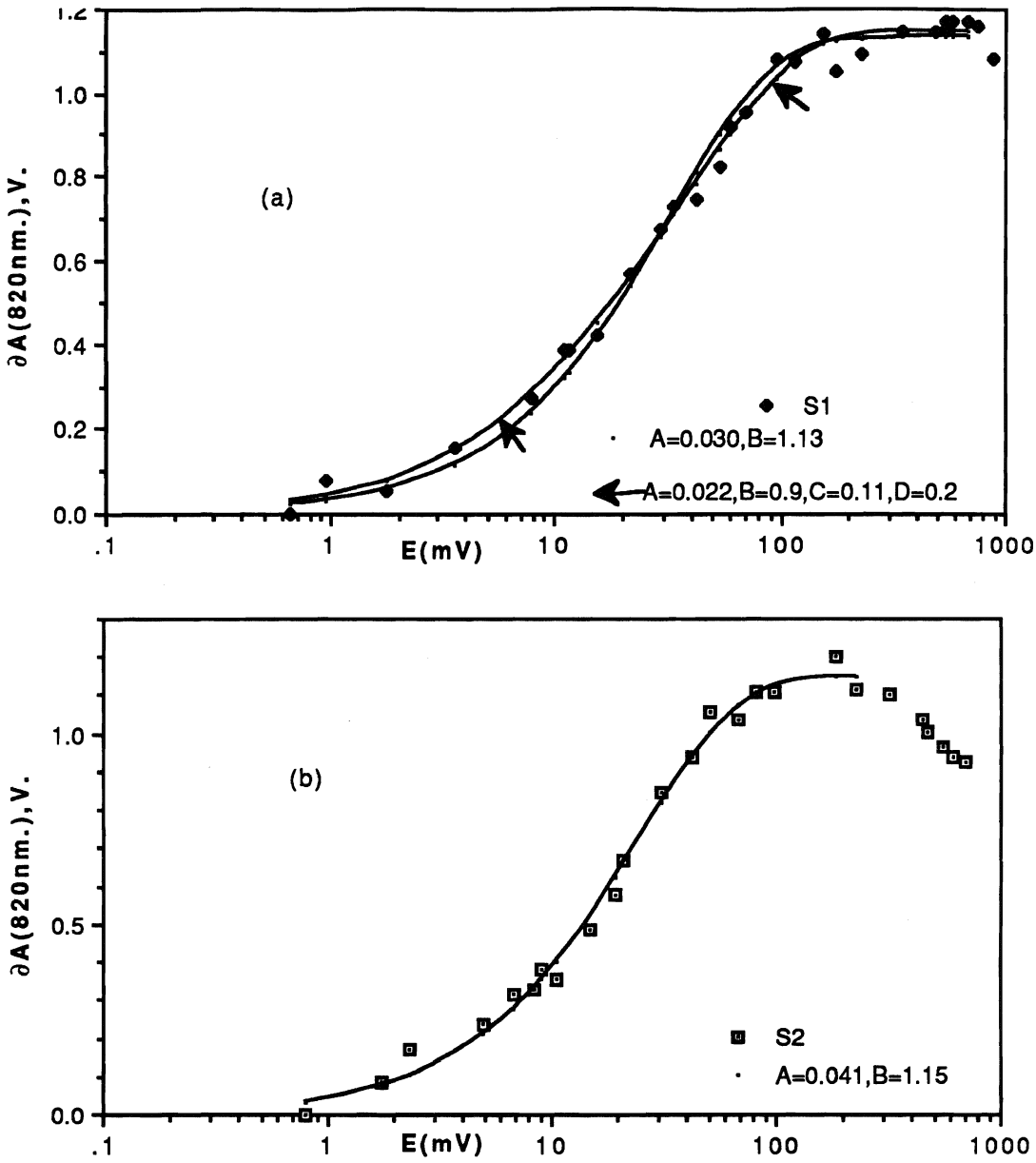

Fig.(37) The fit of PS1 saturation curves in state1 and state2 to Poisson equations. (574nm p292)

(a) State1. A single component curve: A=0.030±0.001,B=1.13±0.01, rΣsq.=0.038.

A double component: A=0.022±0.003, B=0.9±0.1, C=0.11±0.06, D=0.2±0.1, rΣsq=0.0210. The double component is indicated with arrows.

(b) State2. A single component curve: A=0.041±0.002, B=1.15±0.02, rΣsq.=0.0236.

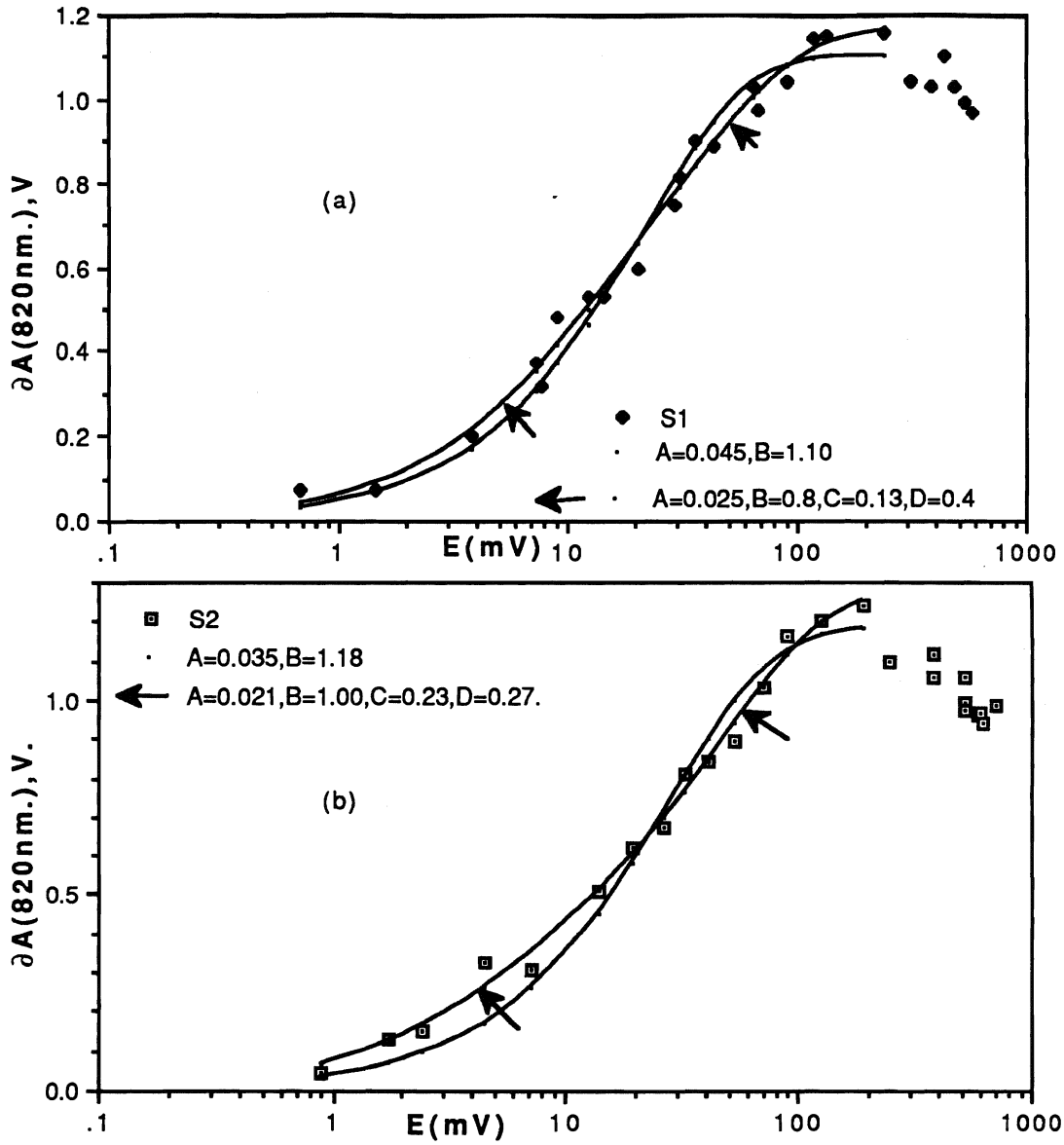

Fig.(38). The fit of PS1 saturation curves in state1 and state2 to Poisson equations. (574nm p303).

(a) State1. A single component: A=0.045±0.003, B=1.10±0.03, rΣsq.=0.05.

A double component: A=0.025±0.008, B=0.8±0.2, C=0.13±0.06, D=0.4±0.2, rΣsq.=0.0246.

(b) State2. A single component: A=0.035±0.003, B=1.18±0.04, rΣsq.=0.0622.

A double component: A=0.021±0.003, B=1.00±0.06, C=0.2±0.1, D=0.27±0.08, rΣsq.=0.0145.

The double component curves are indicated by arrows.

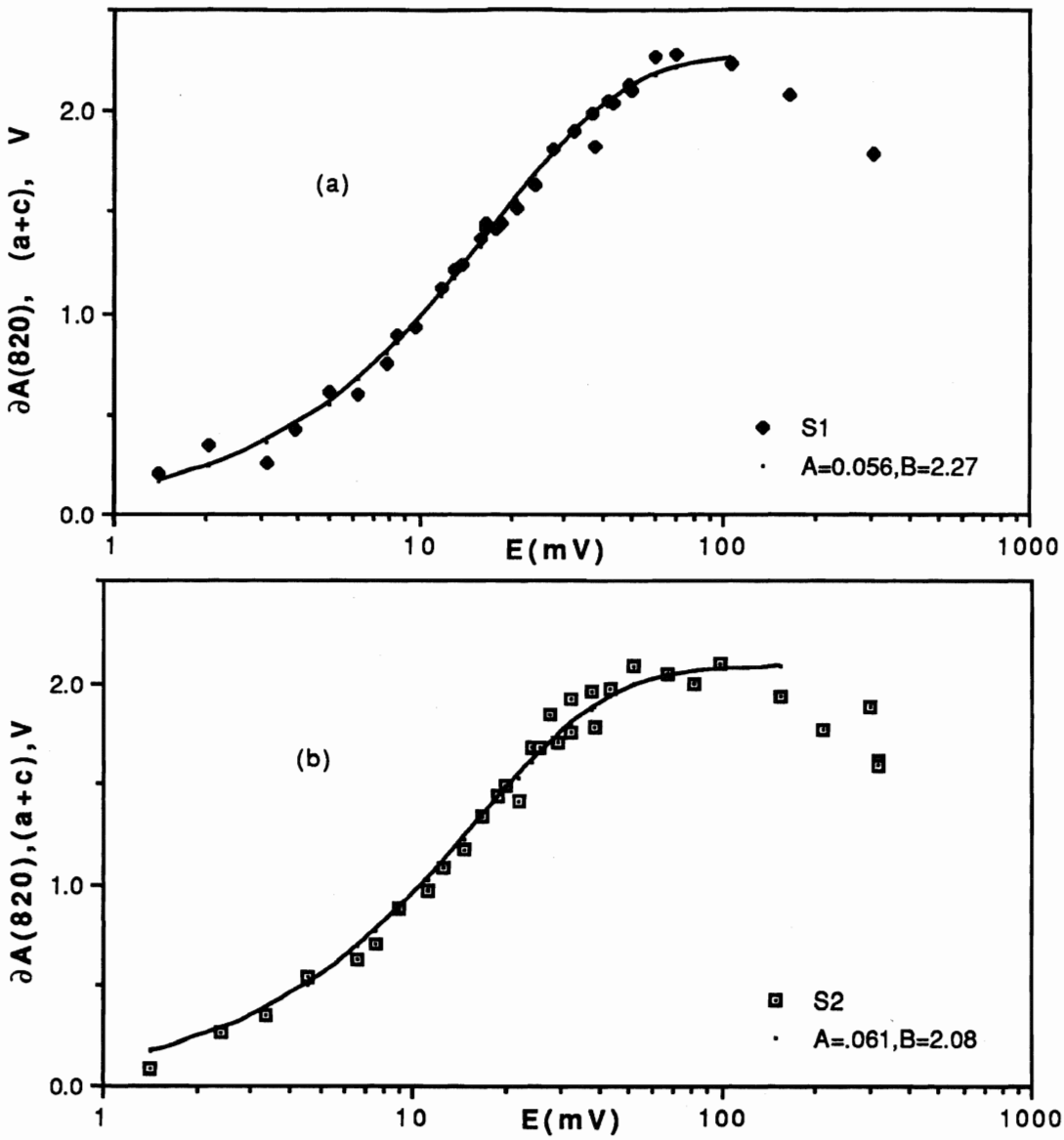

Fig.(39) The fit of PS1 saturation curves in state1 and state2 to Poisson equations. (627nm,p245)

(a) State1. A single component curve: A=0.056±0.002, B=2.27±0.03, rΣsq=0.0918.

(b) State2. A single component curve: A=0.061±0.003, B=2.08±0.03, rΣsq=0.1388.

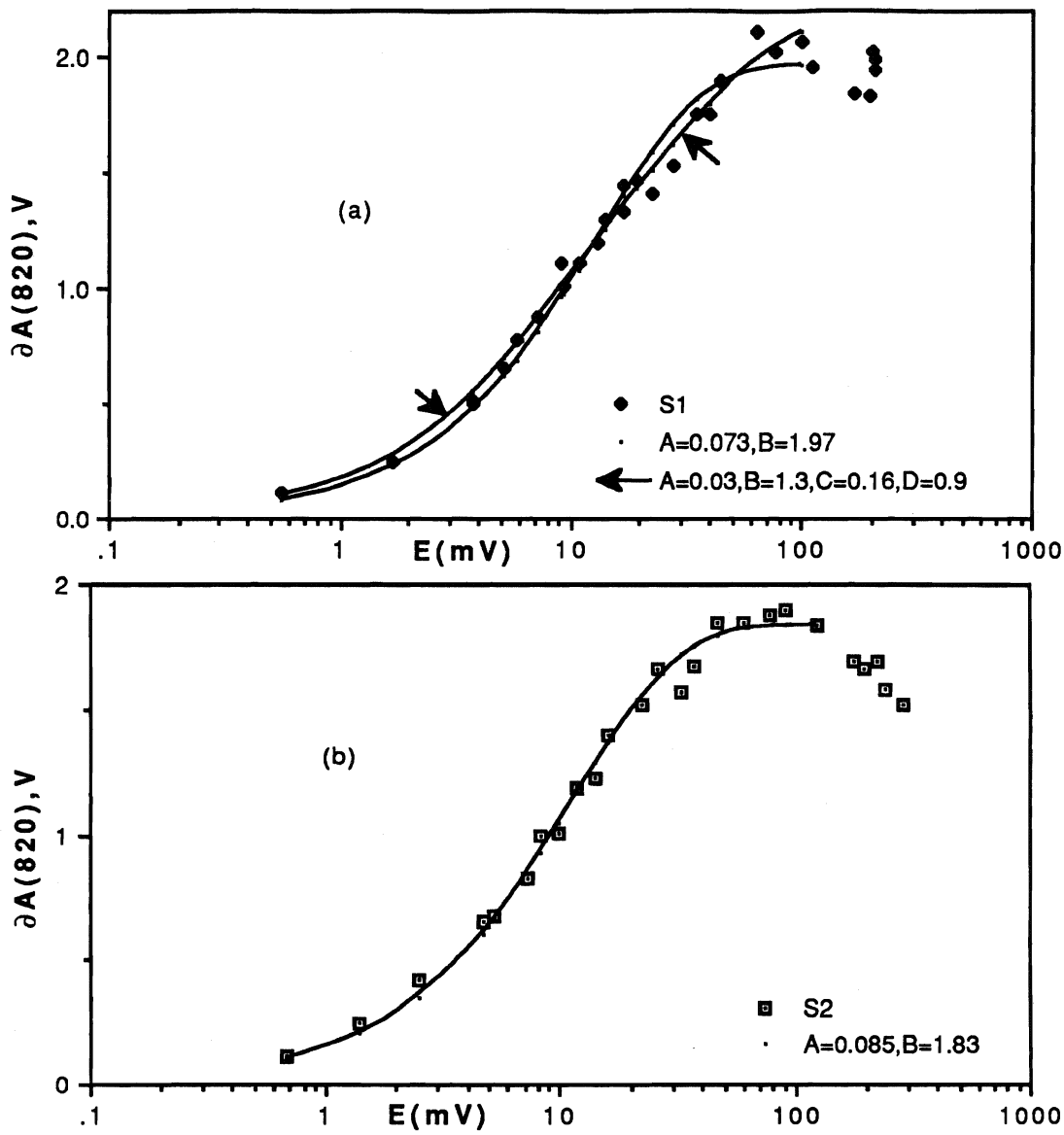

Fig.(40) The fit of PS1 saturation curves in state1 and state2 to Poisson equations. (627nm p268)

(a) State1. A single component curve: A=0.073±0.004, B=1.97±0.04, rΣsq=0.1668.

A double component curve: A=0.03±0.01, B=1.3±0.3, C=0.16±0.05, D=0.9±0.3, rΣsq=0.0677. The double component curve is indicated by arrows.

(b) State2. A single component curve: A=0.085±0.004, B=1.83±0.02, rΣsq=0.0643.

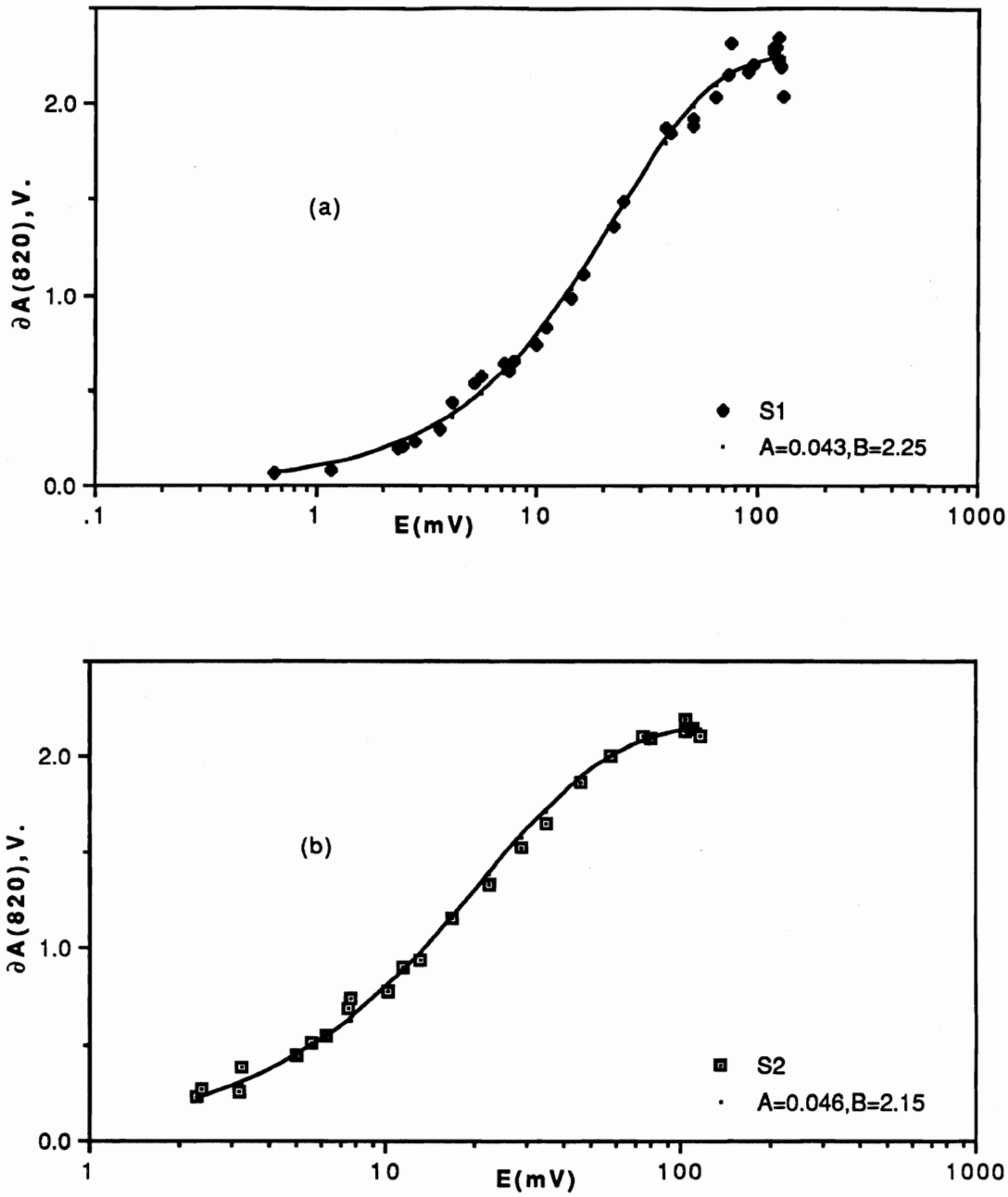

Fig.(41) The fit of PS1 saturation curves in state1 and state2 to Poisson equations. (668nm, p241)

(a) State1. A single component curve with A=0.043±0.002, B=2.25±0.02, rΣsq=0.1507.

(b) State2. S single component curve with A=0.046±0.001, B=2.15±0.02, rΣsq=0.0465.

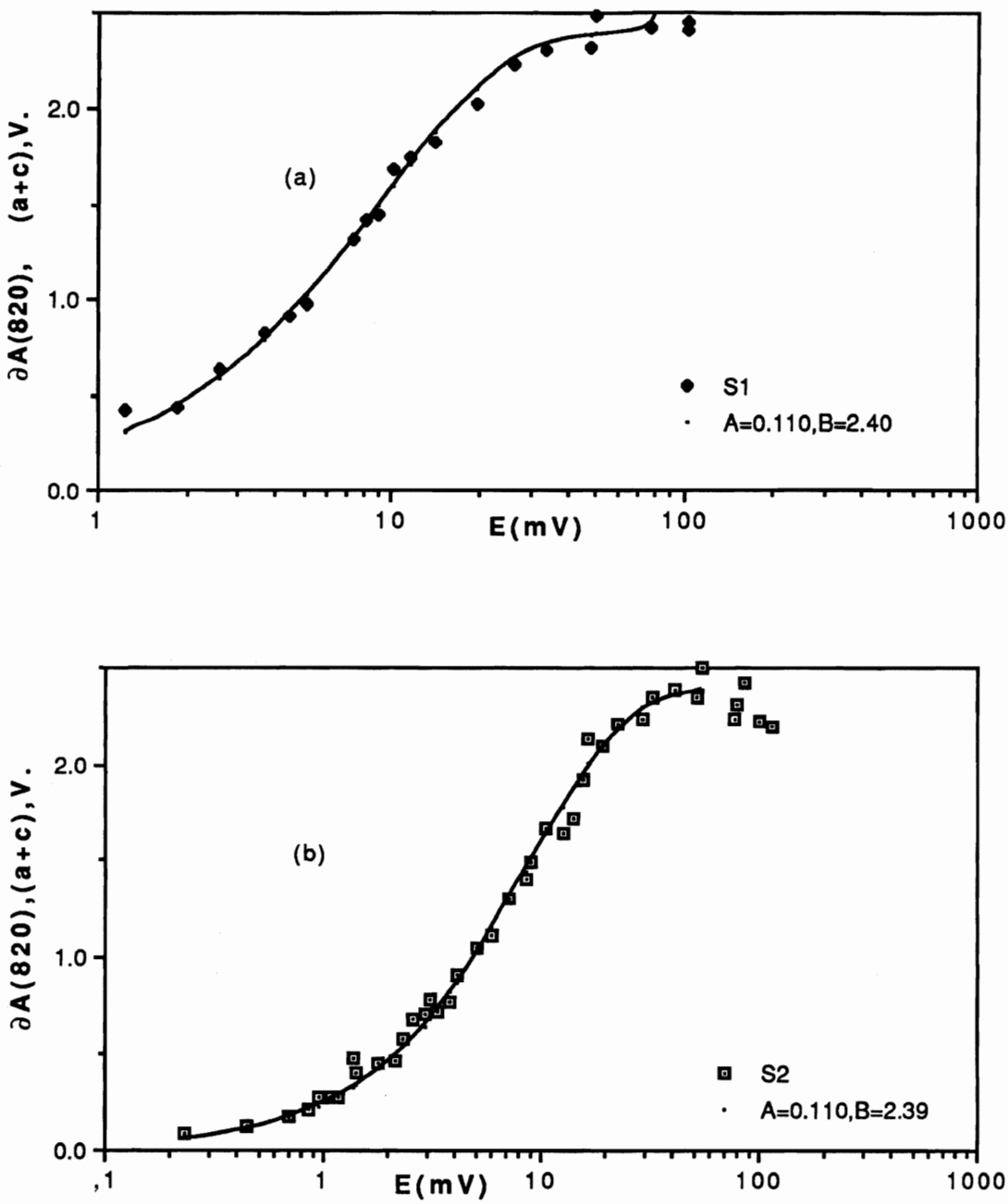

Fig.(42) The fit of PS1 saturation curves in state1 and state2 to Poisson equations. (668nm, p251)

(a) State1. A single component curve, A=0.110±0.003, B=2.40±0.02, rΣsq=0.0582.

(b) State2. A single component curve, A=0.110±0.004, B=2.39±0.03, rΣsq=0.1493.

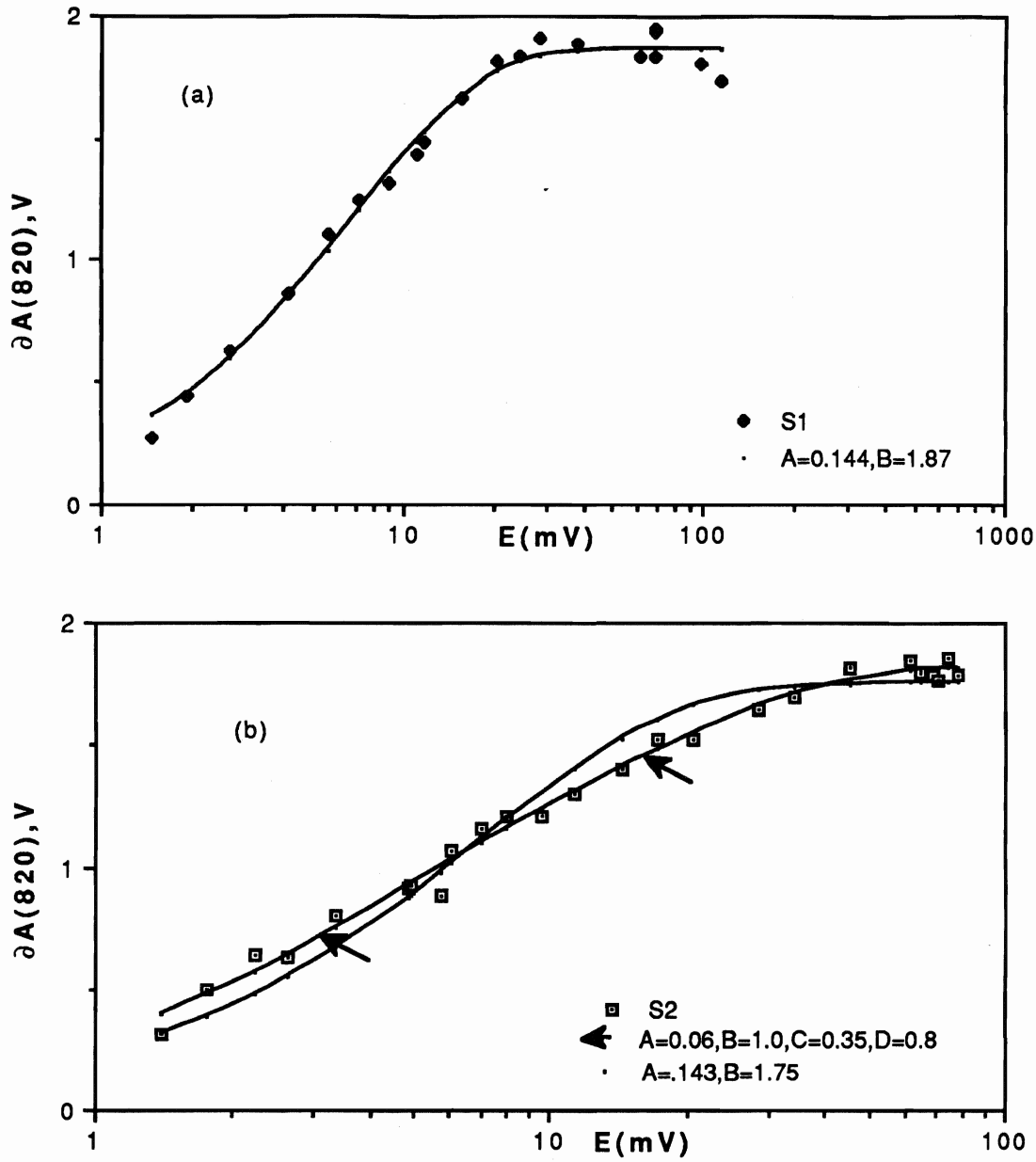

Fig.(43) The fit of PS1 saturation curves in state1 and state2 to Poisson equations. (668nm, p263)

(a) State1 A single component curve, A=0.144±0.006, B=1.87±0.02, rΣsq=0.0658.

(b) State2. A double component curve, A=0.06±0.01, B=1.0±0.2, C=0.35±0.08, D=0.8±0.2, rΣsq=0.0530. The double component curve is indicated by arrows.

State2. A single component curve, A=0.143±0.008, B=1.75±0.03, rΣsq=0.1816.

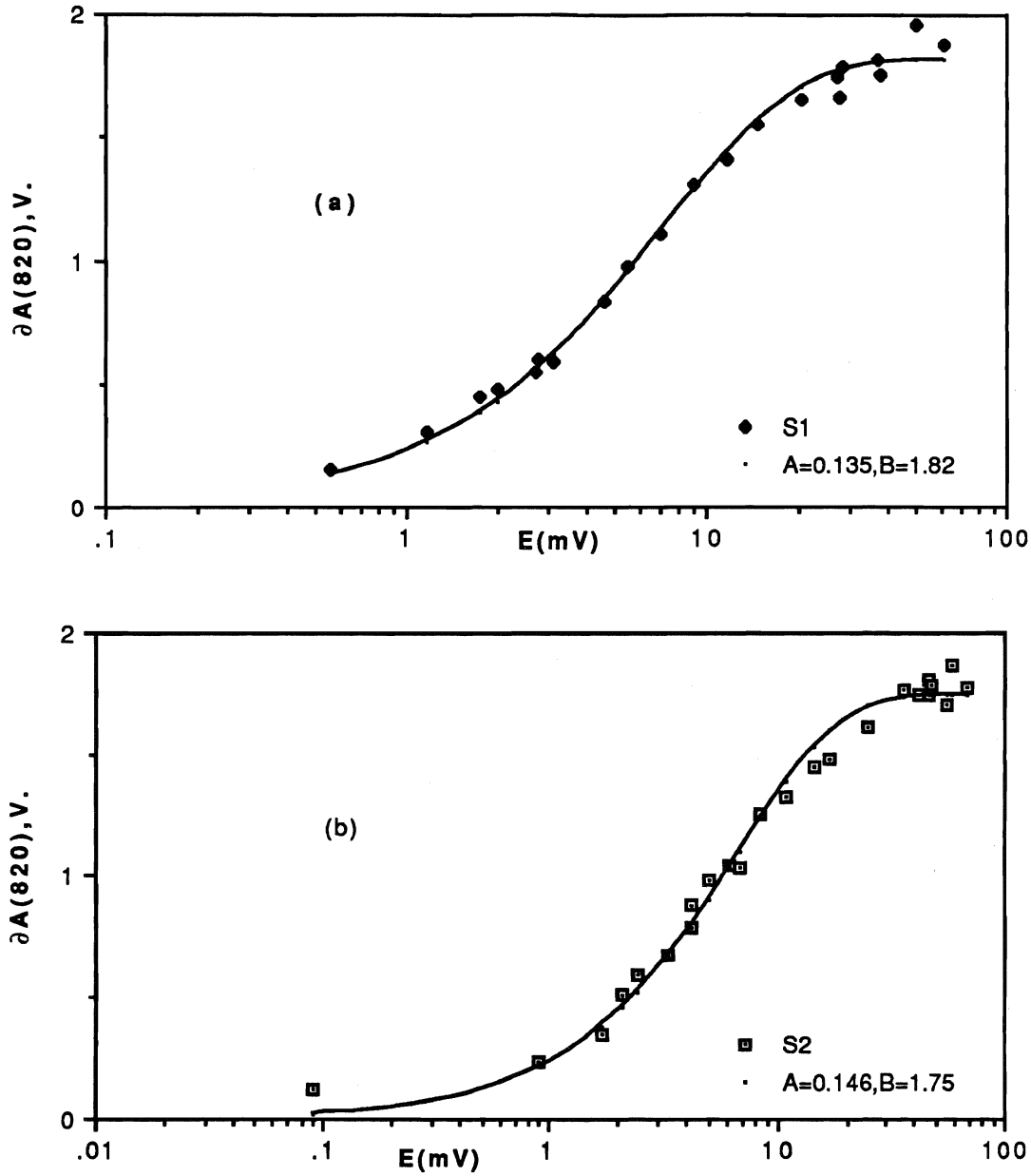

Fig.(44). The fit of PS1 saturation curves in state 1 and state 2 to Poisson equations. (668nm,p271)

(a) State 1. A single component curve, A=0.135±0.005, B=1.82±0.02, rΣsq=0.0546.

(b) State 2. A single component curve, A=0.146±0.006, B=1.75±0.02, rΣsq=0.0942.

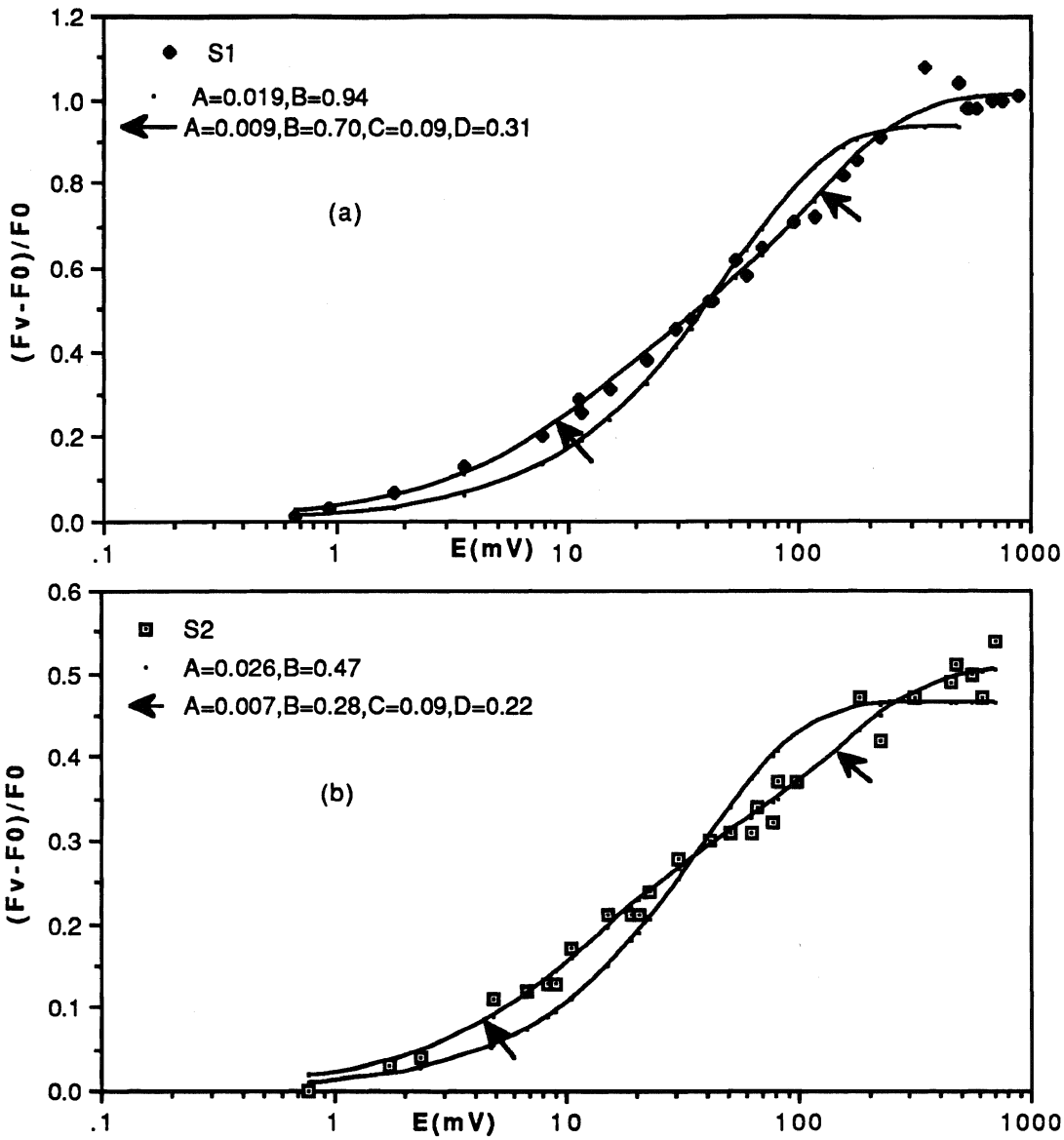

Fig.(45) The fit of PS2 saturation curves in state1 and state2 to Poisson equations (574nm,p292).

(a). State1. A single component curve: A=0.019±0.002, B=0.94±0.03, rΣsq=0.1023.

A double component curve: A=0.009±0.001, B=0.70±0.04, C=0.09±0.02, D=0.31±0.04, rΣsq=0.0204.

(b) State2. A single component curve: A=0.026±0.003, B=0.47±0.01, rΣsq=0.0481.

A double component curve A=0.007±0.002, B=0.28±0.02, C=0.09±0.02,D=0.22±0.03, rΣsq=0.0085.

The double component curves are indicated by arrows.

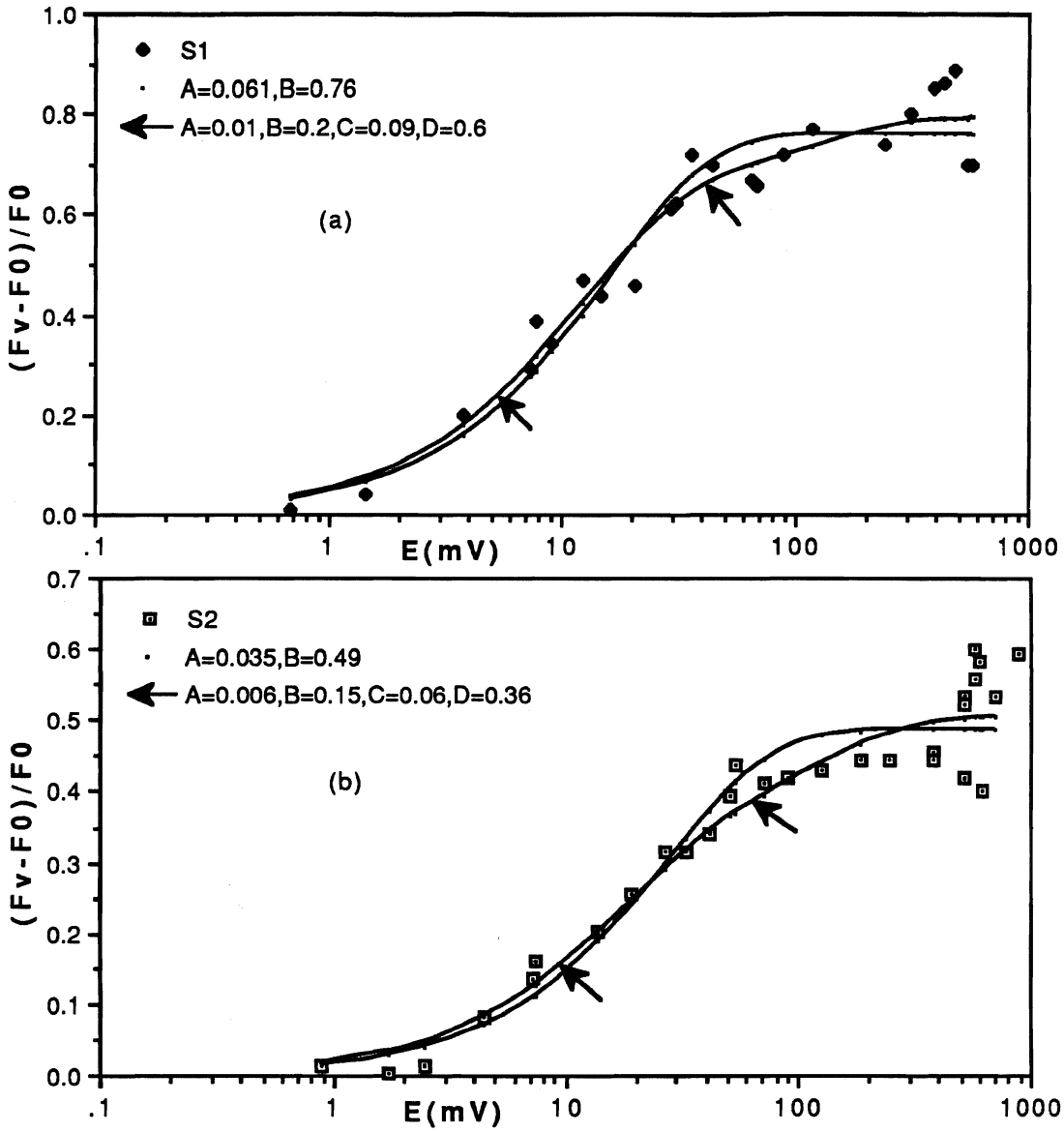

Fig.(46). The fit of PS2 saturation curves in state1 and state2 to Poisson equations. (574nm,p303)

(a) State1. A single component curve: A=0.061±0.006, B=0.76±0.02, rΣsq=0.0878.

A double component curve: A=0.01±0.01, B=0.2±0.1, C=0.09±0.02, D=0.6±0.1, rΣsq=0.0654.

(b) State2. A single component curve: A=0.035±0.004, B=0.49±0.01, rΣsq=0.0621.

A double component curve: A=0.006±0.006, B=0.15±0.06, C=0.06±0.02, D=0.36±0.08, rΣsq=0.0478.

The double component curves are indicated by arrows.

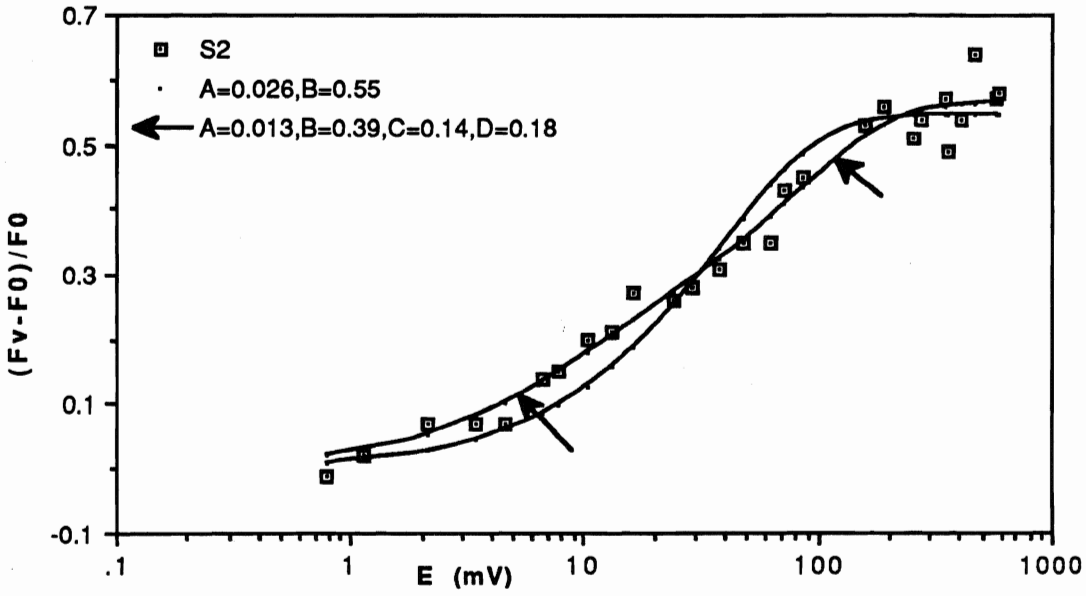

Fig.(47). The fit of PS2 saturation curve in state2 to Poisson equations. (574nm, p306). (State 1 was not completed.)

The single component curve A=0.026±0.002, B=0.55±0.01, rΣsq=0.0511. The double component curve, distinguished by arrows, A=0.013±0.003, B=0.39±0.05, C=0.14±0.06, D=0.18±0.05, rΣsq=0.0222.

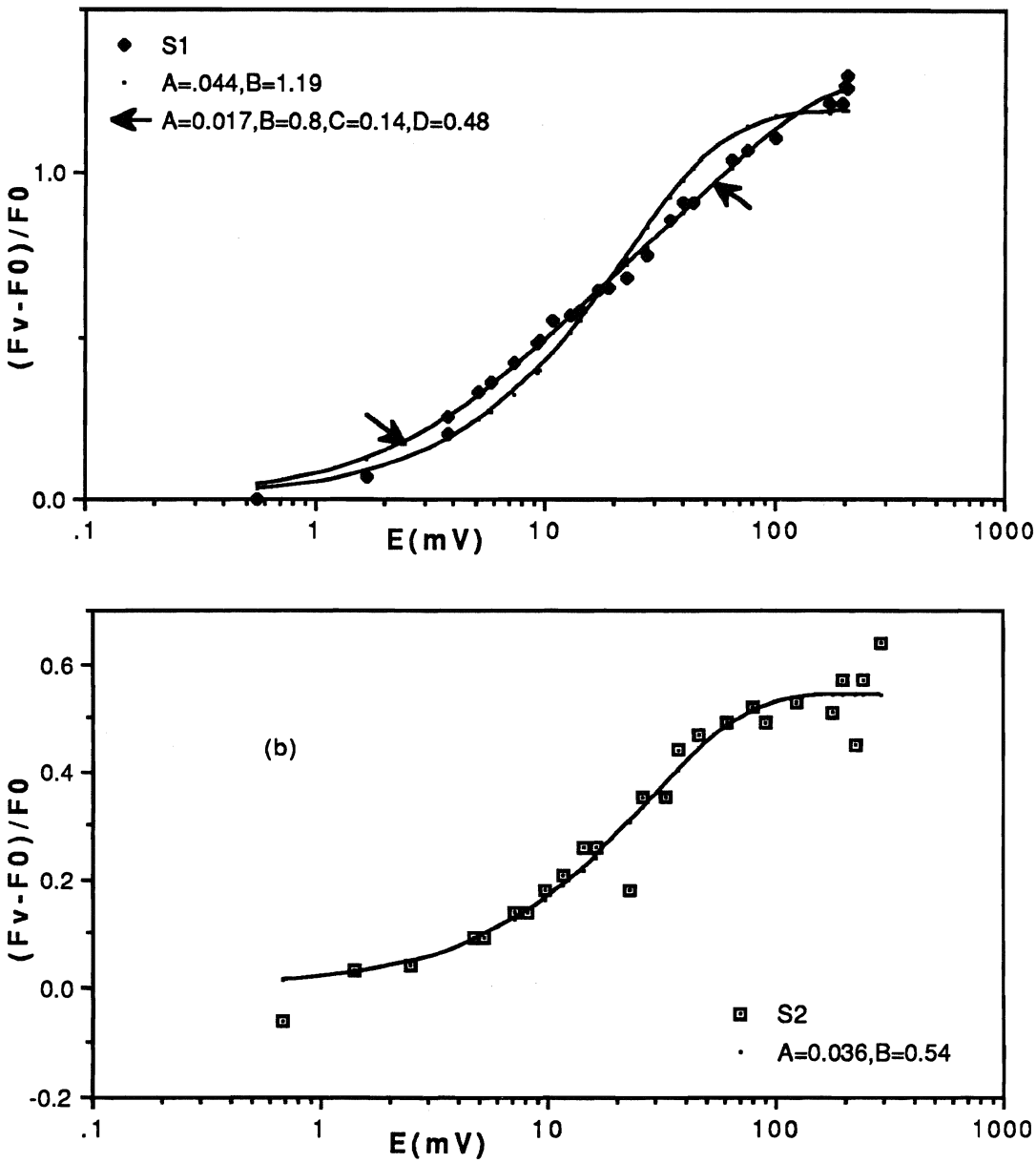

Fig.(48).The fit of PS2 saturation curves in state1 and state2 to Poisson equations. (627nm p268)

(a) State1 . A single component curve: A=0.044±0.003, B=1.19±0.03, rΣsq=0.1354.

A double component curve: A=0.017±0.003, B=0.80±0.06, C=0.14±0.02, D=0.48±0.07, rΣsq=0.0186. The double component curve is distinguished by arrows.

(b) State2. A single component curve: A=0.036±0.004, B=0.54±0.02, rΣsq=0.0487.

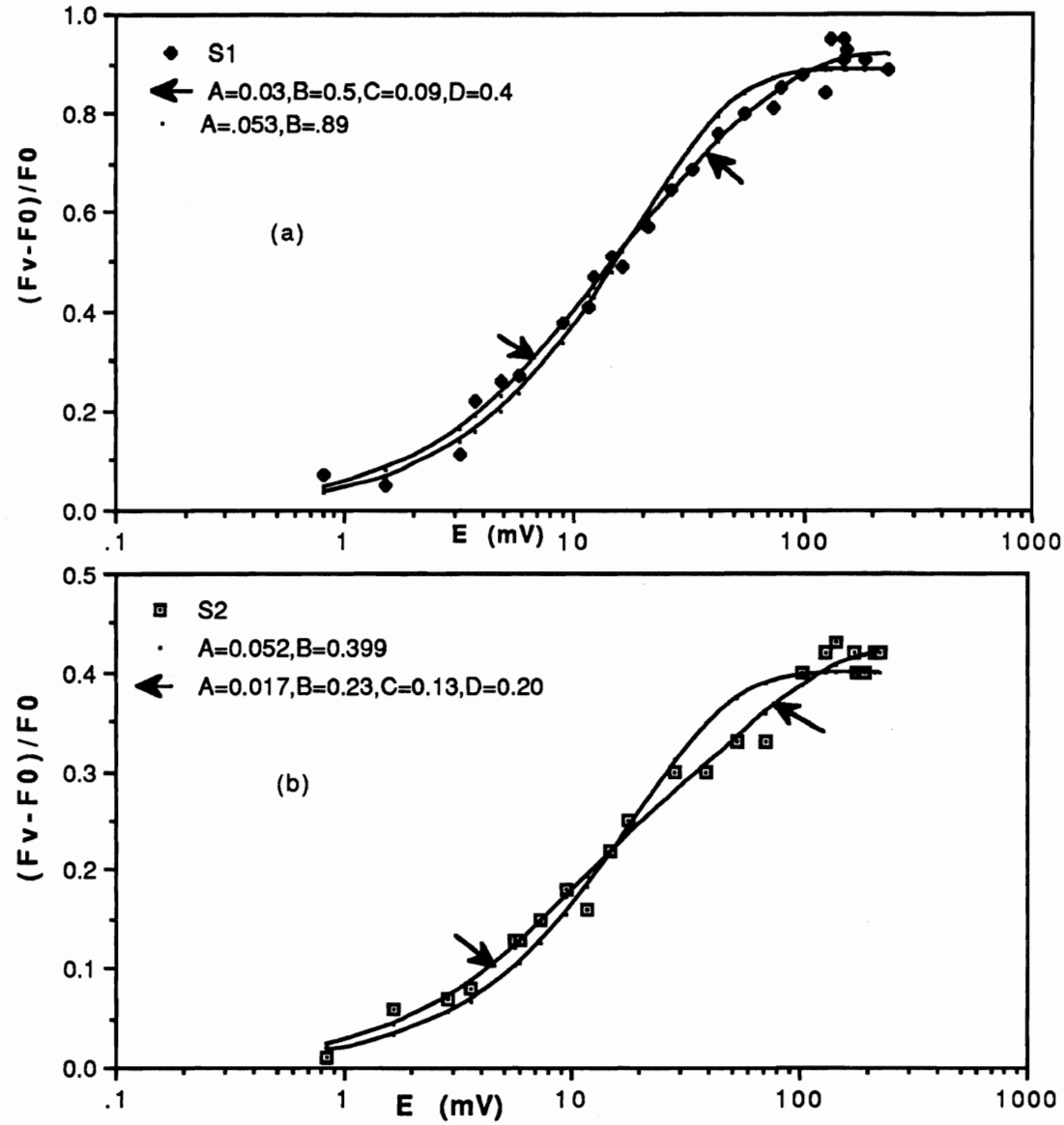

Fig.(49). The fit of PS2 saturation curves in state1 and state2 to Poisson equations. (668nm,p279)

(a) A single component, A=0.053±0.003, B=0.89±0.01, rΣsq=0.0238.

A double component, A=0.03±0.01, B=0.5±0.3, C=0.09±0.05, D=0.4±0.3, rΣsq=0.0158

(b) A single component, A=0.052±0.004, B=0.399±0.009, rΣsq=0.0149.

A double component, A=0.017±0.006, B=0.23±0.04, C=0.13±0.04, D=0.20±0.05, rΣsq=0.0048.

The double component curves are distinguished by arrows.

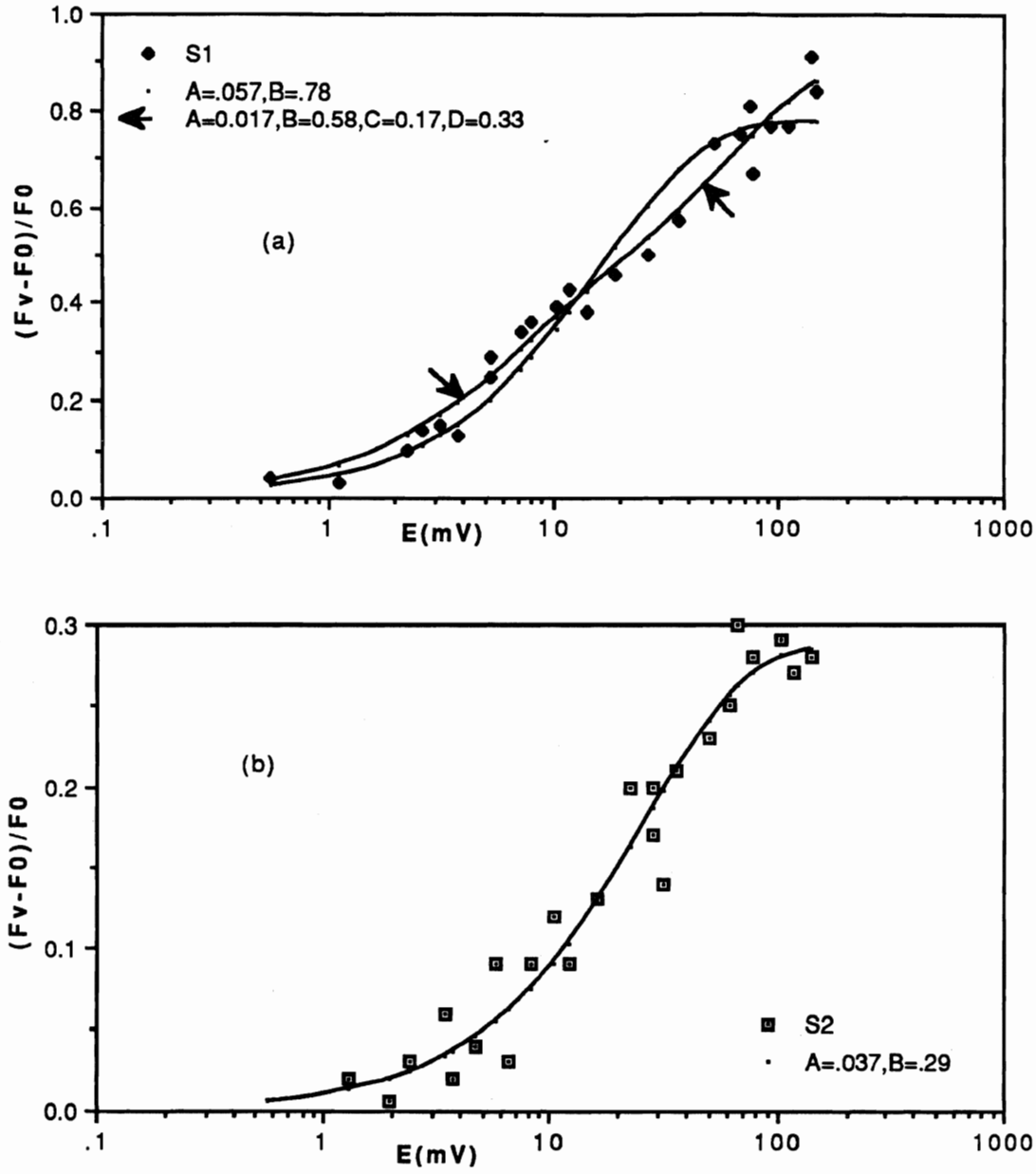

Fig.(50) The fit of PS2 saturation curves in state1 and state2 to Poisson equations. (668nm,p285)

(a) S1 : A single component curve, A=0.057±0.006, B=0.78±0.02, rΣsq=0.0887. A double component curve, A=0.017±0.007, B=0.58±0.07, C=0.17±0.06, D=0.33±0.09, rΣsq=0.0383. The double component curve is distinguished by arrows.

(b) S2: A single component curve,A=0.037±0.004, B=0.29±0.01, rΣsq=0.0126.

COMPARISON OF STATE1 AND STATE2 AVERAGE X-SECTIONS in order to answer:

Is there energy transfer from PS2 to PS1 as S1->S2, evidenced by changes in average X-section of PS1 and PS2, an increase in that of PS1 and a decrease in that of PS2?

Does the energy come from PBS, PS2, or both? That is, do the changes in average X-section occur with PBS-absorbed light (574nm), or chla-absorbed light (668nm) or both?

Experiments in which PS1 and PS2 saturation curves were obtained at the same time were done with 574nm excitation (p292, p303), and with 627nm excitation (p268). It was not possible to obtain both curves simultaneously at 668nm. The density of cells required for a good PS1 saturation curve was too large to obtain saturation of PS2 at this wavelength. Values of the X-section as obtained from fits to the saturation curves were used for comparison. When both saturation curves were well fitted to a single component equation, comparison of the X-sections could be done immediately. Use of the double component curves could make a big difference to the estimated X-section:

e.g. fig.(43),668nm, p263, PS1, S2: single component, X-section=0.143±0.006,
double component, Av. X-section=0.19±0.02.

so comparison of S1 and S2 results may result in a conclusion of a change in X-section if one curve is analysed with a single component equation and the other with a double component equation. For comparison of the S1 and S2 average X-sections, only when two conditions were met was the two-component equation used: $r\Sigma sq$ as shown in fig(36) to (50) for the double component fit should be at most half that of the single component fit and the double component curve should appear, visually, to be a significantly better fit to the experimental points. The average X-section was obtained as described in "materials and methods". In no case was an average X-section obtained from a double component fit compared to one obtained from a single component fit. Qualitative comparisons obtained by visual inspection of the saturation curves were aided by the calculated curves of the appendix. There the three possible ways of increasing the average X-section of a two-component system are

considered, and the resulting saturation curves compared to that of the unchanged system, and to those of single component systems with X-sections equal to the average X-section of the mixed systems. The results of the X-section measurements are listed in table (2).

Table (2) Absorption X-sections of PS1 and PS2 of *Porphyridium cruentum* in state 1 (S1), and state 2 (S2), in relative units, with incident light of wavelengths, 574nm, 627nm, and 668nm The X-sections were obtained from the best fit using the A of the single component equation, Yield=B(1-exp(-AE), or an average X-section (*) of two-components, Yield=B(1-exp(-AE))+D(1-exp(-CE)), obtained as described in "materials and methods". For visual comparison, some PS1 curves were normalised; all PS2 saturation curves were first normalised.

Wavelength	Experiment		S1	S2	X-section change, S1->S2 visual comparison of sat--uration curves.
574nm	PS1	p.231	0.036±0.002	0.043±0.002	increase
	PS1	p.303	0.055±0.010*	0.07±0.01*	increase
	PS2	p.303	0.061±0.006	0.035±0.004	decrease
627nm	PS1	p.245	0.056±0.002	0.061±0.003	no change
	PS1	p268	0.073±0.004	0.085±0.004	no change
	PS2	p268	0.044±0.003	0.036±0.004	heterogeneity in S1, close association, estimation difficult.
668nm	PS1	p241	0.043±0.002	0.046±0.001	no change
	PS1	p251	0.110±0.003	0.110±0.004	no change
	PS1	p263	0.144±0.006	0.143±0.008	heterogeneity in S2, estimation difficult
	PS1	p271	0.135±0.005	0.146±0.006	no change
	PS2	p279	0.053±0.003	0.052±0.004	no change
	PS2	p285	0.057±0.006	0.037±0.004	wide experimental scatter

574nm PS1. Fitting of p231 with single component equations, fig.(36), shows that the X-section increases (~20%), as the state changes S1->S2. Experiment p303, using the double component fits, fig.(38), shows that the average X-section increases (~27%)but the error is large, typical of the double component analyses, which includes the estimated sizes. Visual comparison of the two experimental saturation curves indicates that, for p231, fig.(20), PS1 exists as a two-component system, and as S1->S2 there is an increase in the size of the large component, see fig.(63) of the appendix. In p303, fig.(22), the curves appear to coincide at the low intensity end but they do not contradict the proposition that the average X-section of S2 is greater than that of S1.

PS2. Measurement of p303 indicates a decrease of the average X-section as S1->S2 (~40%). Visual comparison of the normalised S1 and S2 saturation curves at the low intensity end, fig.(32), shows that the average X-section decreases as S1->S2. Visual comparison for PS2 depends largely on the normalisation factors used. More emphasis has to be placed, therefore, on the analysis of the individual S1, S2, curves.

In p303, both PS1 and PS2 X-sections were determined under the same experimental conditions. If, between S1 and S2,there is no change in the total amount of absorbing material connected to the photosystems, any change in the average X-section of one photosystem must be accompanied by a complementary change in the other photosystem; this argument assumes that there is no change in energy loss from fluorescence or heat. Experiment p303 is therefore especially important: saturation curves for both PS1 and PS2 were done simultaneously and the results are consistent in that the average X-section of PS1 increases and that of PS2 decreases as S1->S2.

For 574nm radiation both PS1saturation curves showed that the X-section increased, an average of about 30%, in the transition S1->S2; the expected concomitant decrease in the PS2 X-section is shown by p303.

627nm PS1. Calculated fits for p 245, Fig.(39), show no change outside the experimental error; calculations for p268, fig.(40), show an increase, S1-> S2, which is only just outside the experimental error. Visual comparison of the experimental curves of both p245 and p268 shows that the S1 and S2 curves coincide except at the high intensity end where S2 lies above S1, fig.(23) and fig.(24). A possible aggregation in p268,S1 may account for the deviation of this curve from the single component curve. fig.(40) (this effect is discussed in a later section); the fits for p245 are both single component fits. fig.(39), and separation at the high intensity end cannot be explained by a change in size of the single component. One can only conclude that there is no significant evidence of a change in average X-section.

PS2. Direct comparison of the PS2 saturation curves of the one experiment, p268, shows a distinct separation between S1 and S2, fig.(33); S1 can be fitted with a two-component equation, indicating that any difference in X-section is probably due to the two-components of S1 and the single component of S2. The two-component fit may be due to possible aggregation of the sample in S1. The low intensity end is not sufficiently well defined to demonstrate a difference in average x-section. If the value of the X-section of S1 is obtained from the less well fitting single component equation the calculated change in x-section is a decrease, but within the experimental error.

With 627nm radiation there is no significant change in the average X-section of either PS1 or PS2 in the transition S1->S2.

668nm PS1. In all of the four experiments, calculations of fits show no change in X-section as S1->S2, figs.(41-44). Visual comparison, figs.(25,26,28), indicates no change in X-section; p263, fig.(27), shows separation between the curves at the high intensity end, which is due to the apparent heterogeneity of S2, fig.(43).

PS2. Fits to experiment p279, fig.(49), show no change in X-section.Visual examination of the normalised saturation curves, fig.(34), shows that the average X-sections given by the low intensity region are approximately the same; there is some

separation between the curves at the high intensity end indicating a difference between the small components. Single component fits to experiment p285, fig.(50), show a decrease as S1-> S2. Visual examination of the normalised saturation curves, fig.(35) demonstrates a wide experimental scatter, indicating that the decrease may not be significant.

There appears to be no certain change in X-section with 668nm radiation, of either PS1 or PS2, as S1->S2.

In conclusion, the only consistent changes in X-section due to the transition change, S1->S2, occur as a result of incidence of 574nm radiation, absorbed by PBS. These experiments demonstrate that energy is transferred from PS2 to PS1 in S2 and the path appears to be PBS->PS1 and not PBS->PS2chla->PS1

THE SIGNIFICANCE OF THE TWO COMPONENTS.

It is possible that the two-component data may give some insight into the transition process and this part of the experiments will now be pursued.

According to Mauzerall (1981), a saturation curve can have a bimodal (two-component) shape in any one of three situations. The incident laser pulse is non uniform over the horizontal plane through which the 820nm absorbance light passes, and from which the fluorescence is gathered, there is too great absorption and scattering from an optically dense specimen, or there is, indeed, true heterogeneity of the absorbing species. If the flash is non-uniform over the measured plane the yield comes from a range of effective intensities, resulting in broadening of the light-saturation curve. Ley and Mauzerall (1982), found that as the cell concentration was increased the shape of the curve was similar to that obtained from a bimodal distribution with a minor component of smaller X-section.

In these experiments care was taken to ensure that the laser pulse was uniform, and in only one experiment was it suspected that the cells of the sample had become non uniform, (p268,S1of PS1 and PS2). The samples were indeed optically dense: the density had to be

increased to an optimum which gave a good 820nm absorbance change, and although the density was halved for the measurement of fluorescence under 668nm radiation, at both this wavelength and 574nm there is large absorbance. The use of both these wavelengths and of whole cells with the accompanying heterogeneity and scatter was necessary to the experiment. The samples may, therefore, have had too great an absorbance and scattering. The PS2 measurements had a further disadvantage in that the fluorescence was probably collected from parts of the sample outside the defined 820nm plane, fig.(15), and although the flash intensity at the 820nm plane was uniform, and appeared so for the PS1 measurements, the observed intensity for the PS2 measurements may have had a broad, rather than a narrow range of values. Examination of the information given by the two-component interpretations should not be deterred by the possibility that the two-component interpretations may be artefacts, but the results of such an examination should be accepted with caution. With that in mind the two-component interpretations will be regarded as due to real, photosystem, heterogeneity.

Analysis of experiment p303, 574nm, PS1 and PS2.

The most important experiment at 574nm is that of p.303; both PS1 and PS2 average X-sections were determined and the changes were consistent. It is now the aim to see if overall fits to the saturation curves can be obtained each with a range of the small component X-section (A), big component X-section (C), and the fraction (**B**) of the small component, and if these values have any significance. These overall fits are now obtained in a rather more rigorous, and lengthy, way than that used in the last section to determine a range of average X-sections. As in the estimation of the average X-section of the last section, the fraction of the small component was fixed and values of the individual big and small X-sections and $r\Sigma sq$ (an estimation of how good the calculated fit is) were calculated by Multifit. This was done for a large range of values of the fraction, **B**. The results are in tables 3,4.

Table (3). p303, PS1, S1 and S2. A, C and rΣsq calculations obtained by varying B. A and C are the X-sections of the small and large components, B is the fraction of A. Solutions outside (Limit) are those which vary noticeably from the experimental saturation curves. Values marked with (s) are the single component solutions. Examples of limits and an unacceptable solution are illustrated in fig.(51) and fig.(52).

p.303		Small X-section A)	Fraction of small (B)	Big component X-section (C)	rΣsq	
PS1	S1	0.035±0.001	0.9	0.4±0.3	0.0239	(Limit)
		0.032±0.001	0.85	0.3±0.1	0.0205	
		0.030±0.001	0.8	0.20±0.05	0.0190	
		0.028±0.001	0.75	0.16±0.03	0.0186	
		0.027±0.001	0.7	0.13±0.02	0.0185	"best fit"
		0.025±0.002	0.65	0.11±0.01	0.0186	
		0.024±0.002	0.6	0.10±0.01	0.0189	
		0.021±0.002	0.5	0.085±0.008	0.0197	
		0.018±0.002	0.4	0.073±0.006	0.0210	
		0.015±0.002	0.3	0.064±0.005	0.0227	
		0.011±0.003	0.2	0.056±0.004	0.0253	
		0.006±0.004	0.1	0.049±0.003	0.0299	(Limit)
		—	—	0.046±0.002(s)	0.0355	
	S2	0.027±0.001	0.95	0.9±1	0.0264	
		0.025±0.001	0.9	0.6±0.3	0.0151	(Limit)
		0.023±0.001	0.85	0.4±0.1	0.0104	
		0.021±0.001	0.8	0.24±0.05	0.0091	"best fit"
		0.020±0.001	0.75	0.19±0.03	0.0095	
		0.018±0.001	0.7	0.15±0.02	0.0111	
		0.016±0.001	0.6	0.10±0.01	0.0155	
		0.014±0.001	0.5	0.073±0.009	0.0201	
		0.012±0.001	0.4	0.058±0.007	0.0241	
		0.010±0.002	0.3	0.049±0.005	0.0278	(Limit)
		0.007±0.003	0.2	0.042±0.004	0.0315	
		0.003±0.003	0.1	0.036±0.003	0.0362	
		—	—	0.035±0.003(s)	0.0385	

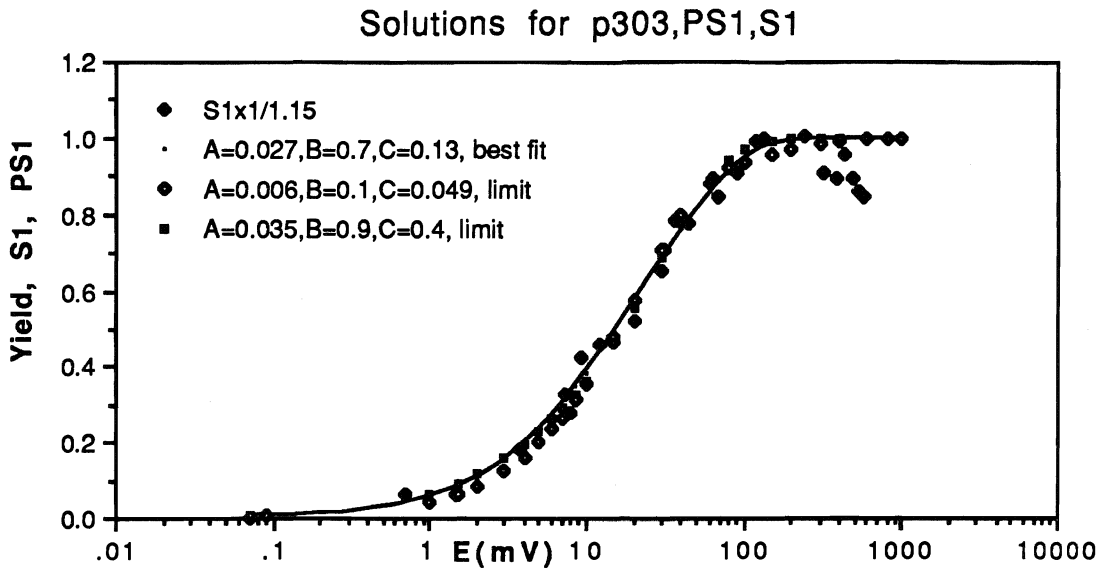

Fig.(51). Calculated solutions that are acceptable for p303,PS1,S1. The limits established in this way led to 'solution 1'.

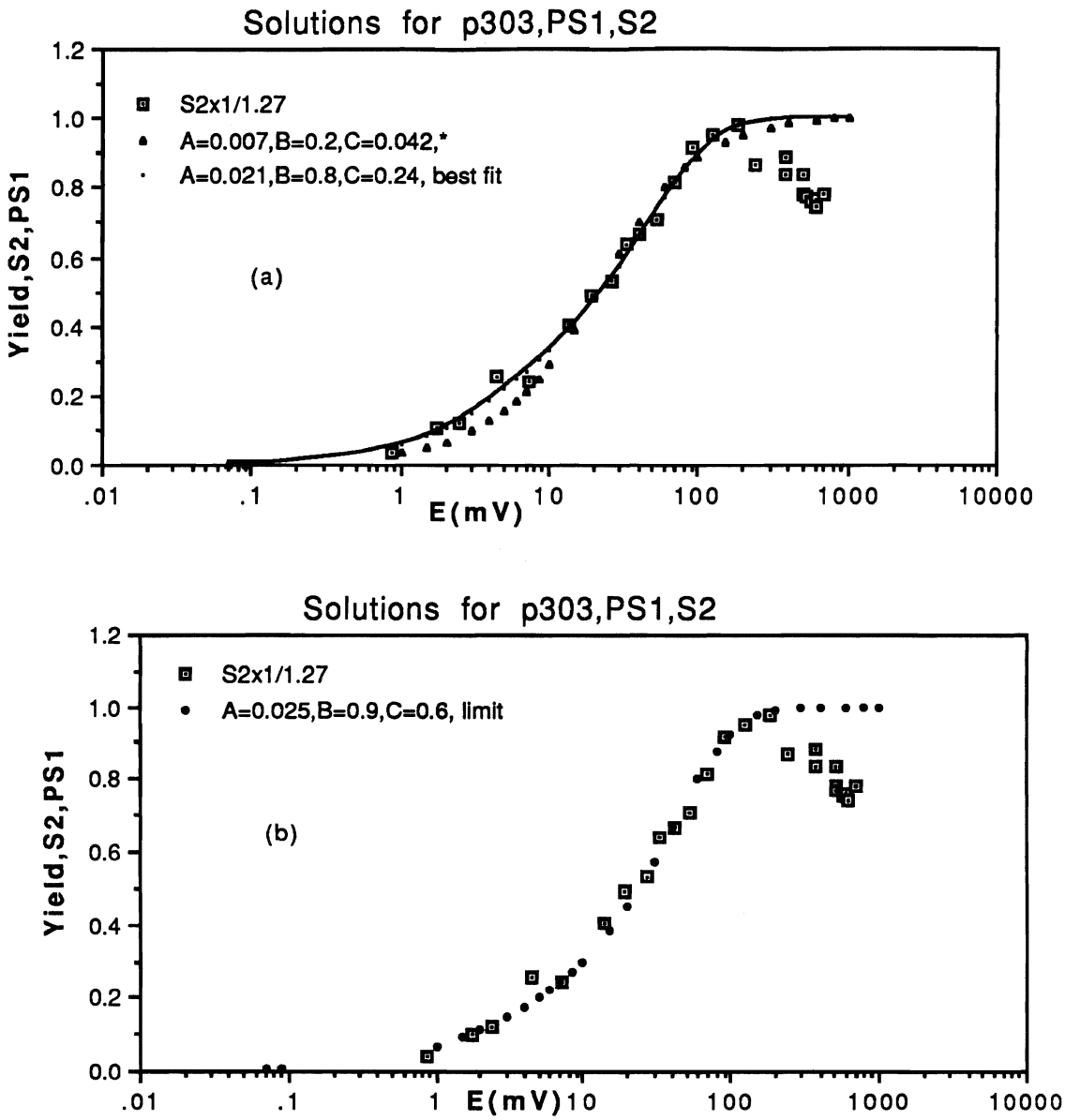

Fig.(52) Calculated solutions for p303,PS1,S2.

(a) shows a solution marked with an asterisk,*, which was unacceptable.

(b)shows that a "limit" solution which was acceptable.

The limits established in this way led to 'solution 1'

Table (4). p303 PS2, S1and S2. A, B, C and rΣsq calculations obtained by varying B. A and C are the X-sections of the small and large components, B is the fraction of A. Solutions outside (Limit) are those which vary noticeably from the experimental saturation curves. Values marked with (s) are the single component solutions. Examples of limits and an unacceptable solution are illustrated in fig.(53) and fig.(54).

		Small X-section (A)	Fraction of small (B)	Big X-section (C)	rΣsq	
PS2	S1	0.004±0.003	0.1	0.070±0.006	0.1155	(Limit)
		0.008±0.003	0.2	0.084±0.008	0.1031	
		0.010±0.003	0.25	0.09±0.01	0.1025	"best fit"
		0.013±0.003	0.3	0.10±0.01	0.1031	
		0.019±0.003	0.4	0.11±0.02	0.1061	
		0.024±0.004	0.5	0.14±0.03	0.1100	(Limit)
		0.029±0.004	0.6	0.17±0.04	0.1143	
		0.034±0.004	0.7	0.21±0.08	0.1193	
		0.040±0.004	0.8	0.3±0.2	0.1275	
		0.063±0.006(s)	0.95	—	0.1368	
	S2	0.003±0.002	0.1	0.041±0.005	0.2141	(Limit)
		0.005±0.002	0.2	0.050±0.006	0.1967	
		0.006±0.002	0.25	0.055±0.008	0.1953	"best fit"
		0.007±0.002	0.3	0.061±0.01	0.1977	
		0.008±0.002	0.35	0.07±0.01	0.2022	
		0.010±0.003	0.4	0.07±0.01	0.2074	
		0.013±0.003	0.5	0.08±0.02	0.2166	
		0.017±0.003	0.6	0.09±0.03	0.2226	(Limit)
		0.024±0.003	0.8	0.13±0.09	0.2350	
		0.035±0.004(s)	0.97	—	0.2483	

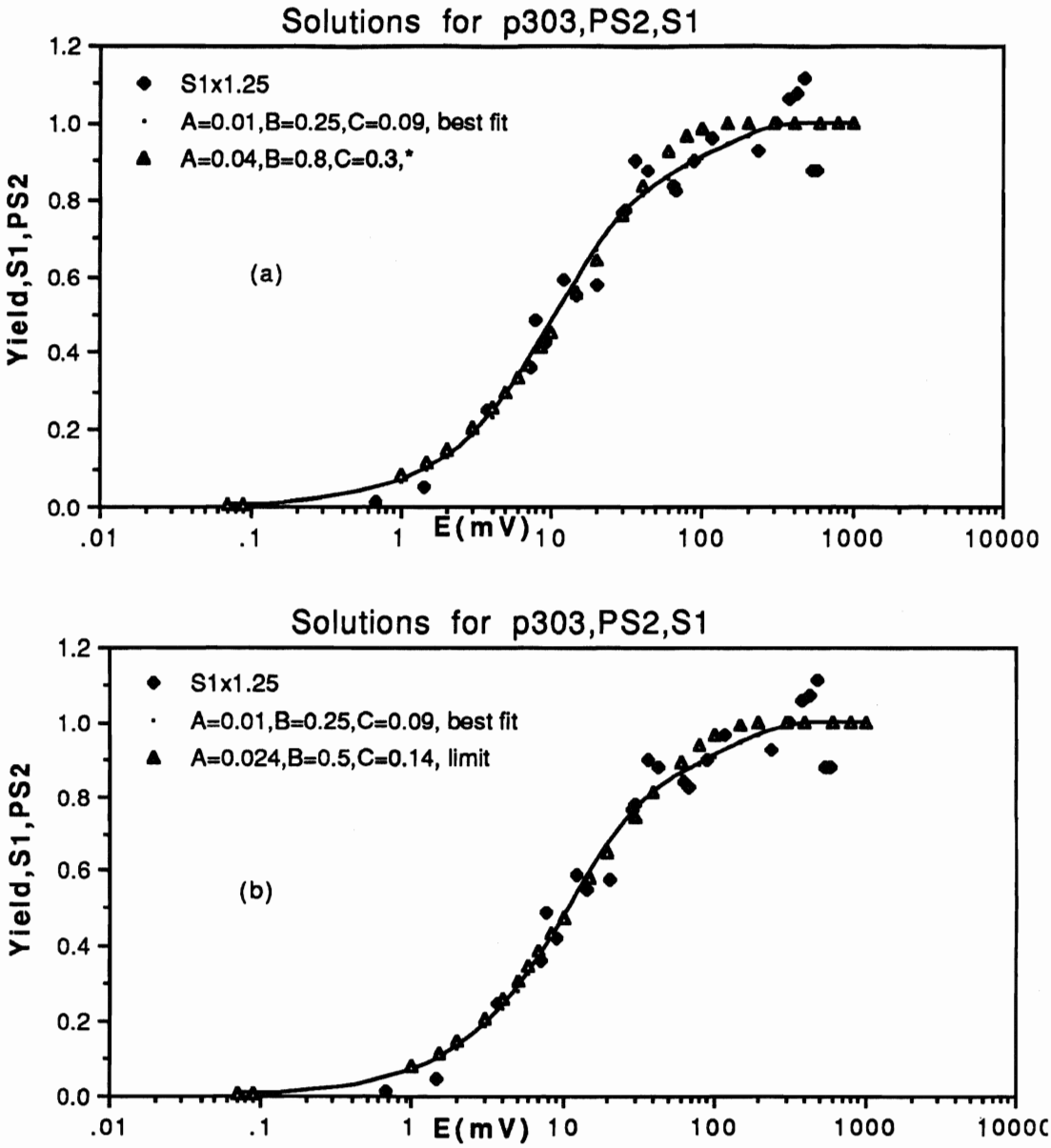

Fig.(53).Calculated solutions for p303, PS2, S1.

(a) shows a solution marked with an asterisk,*, which was unacceptable.

(b)shows that a "limit" solution which was acceptable.

The limits established in this way led to 'solution 1'

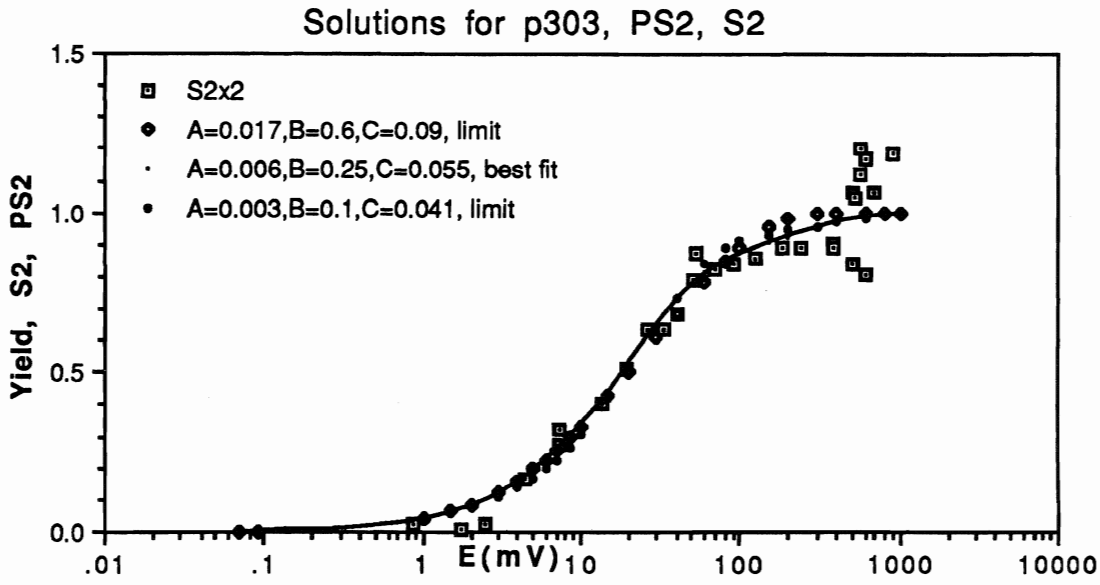

Fig.(54). Calculated solutions that are acceptable for p303, PS2,S2. The limits established in this way led to 'solution 1'.

Experiment p303 has flash energy of 574nm which is energy primarily absorbed by PBS. It is generally accepted that PS2 is coupled to PBS, and two-component curves at this wavelength indicate the existence of two PS2 populations associated with PBS. This may be due to an unequal distribution of photosystems among the PBS, but the big component is about nine times the size of the small component, and it is unlikely that the distribution would be that uneven. One would have to propose that some PBS be connected to PS2 in a one-to-one and others in a one-to-nine ratio. For this reason it is proposed that the two populations of PS2 are due to PS2 either attached to, or disassociated from, PBS. In addition, all the PS1 curves at 574nm, except p292, S2, can be better fitted with two-component curves. It is possible to infer from these experiments that, not only is there a population of PS2 disassociated from PBS but there is a population of PS1 communicating with PBS. For both photosystems the small component, of area A, is the photosystem unassociated with PBS; the big component, of area C, is the photosystem associated with PBS. The fraction, B, is the fraction of the smaller component, that is, the fraction disassociated from PBS. PS1 may be directly connected to PBS, like PS2, or may be communicating via an attached PS2 (spillover). From tables 3,4 it can be seen that the "best" small value of PS1 in both S1 and S2 is two to three times the "best" small value of PS2. As PS1 contains two to three times the amount of absorbing pigment (i.e. chla), this agrees with the proposal that the small X-section, A, is that of the unattached photosystem. Again from the "best fit" values of tables 3,4, the fraction of the small component is larger for PS1 than for PS2, about 0.8 compared to 0.2. If the big component is the combination of photosystem and PBS then the majority of PS2 ,about 80%, is attached to PBS, but there is 20% of PS1 attached to PBS.

The size of the small component, A, from the "best" values for PS1 and PS2, different for the two photosystems, appears to remain constant with 574nm light during the state transition. That A of both PS1 and PS2 remains constant in the transition S1->S2 can be verified visually from saturation curves. Coincidence of the S1 and S2 curves at the near saturation portion indicates that the small component is the same. (See appendix on calculated curves). Of the five experiments only in p292, which is suspect from its fluorescence spectrum, does this not occur. From both the above calculations (which apply only to p303) and the curves of most of the other experiments at this wavelength there is evidence, therefore, that the size of the small component of both PS1 and PS2 does not change in the transition S1->S2. It is assumed, therefore, that there is no observable change in the X-section of the small components.This would imply that with 574nm light there is no change in energy distribution to the unattached photosystems.

For this analysis of p303, the limits of an overall solution were obtained in a very practical way, and here the method differs from that used in determining the average X-section of the last section. An individual solution in the tables above was included unless it showed a distinct difference from the experimental saturation curve.(See fig(51) to fig.(54)for the limits of the solutions.) It is now assumed that for both PS1 and PS2, the small component X-section remains constant as S1->S2, and that the small component X-section of PS1 is about three times as large as the small component X-section of PS2.

With these assumptions the last two tables can be condensed to a solution (1):

p303, 574nm:

		small	fraction of small	big	
PS1	S1	0.010< A< 0.025	0.2< B<0.65	0.06< C< 0.11	
	S2	0.010< A< 0.025	0.3< B< 0.9	0.05< C< 0.6	**Solution1**
PS2	S1	0.003< A< 0.012	0.1< B< 0.3	0.07< C< 0.10	
	S2	0.003< A< 0.012	0.1< B< 0.5	0.04< C< 0.08	

The big component of PS1 in S1 appears to be the same size as that of the big component of PS2, the common range being 0.07-> 0.10, indicating that either PS1 and PS2 occupy similar positions directly connected to PBS, or PS1 is connected via PS2 . The term, spillover, has been used to describe this kind of relative position of PBS, PS2, and PS1 in S2, where it is one of the models of the state transition mechanism. The description of the arrangement of the photosynthetic components in S1, not transition mechanisms, is considered below. The spillover situation is shown is fig.(55,a), where, in S1, the PS2 common to both PBS and PS1 transfers the energy it would normally receive from PBS to PS1 and becomes a small PS2 component similar to an uncoupled PS2, shown in (b). The situation (c) must also be added , since there is nothing in p303 to indicate that this does not exist. With 574nm light, situations (a), (b), and (c) cannot be distinguished; all will have big and small components.

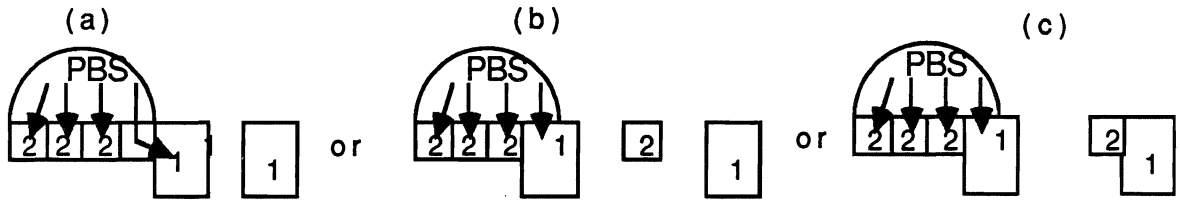

Fig.(55) The possible arrangements of PBS, PS1 and PS2 in state1, compatible with P303 results.

(a) PS1 obtains energy from PBS via PS2, spillover.

(b) PS1 is directly connected to PBS, equivalent to a mobile antenna situation together with PS1 and PS2 not connected to PBS, and not connected to each other.

(c) PS1 is directly connected to PBS, together with PS1 and PS2 not connected to PBS but connected to each other, the equivalent of the combination, mobile antenna and spillover, situation.

The path of 574nm light energy is shown.

From solution 1 the big component of PS2 decreases as S1->S2 ; it is unclear what happens to the size of the big component of PS1 as the range of size in S2 includes the size of the big component in S1 and extends beyond it. It cannot be determined, from solution 1, for either PS1 or PS2, if the fraction of the small component, **B**, changes as S1->S2. It might be profitable to make another assumption and take the analysis further.

If a value for the small component is selected from the possible range of solution 1 can it be determined if **B** changes in the transition S1->S2? If A=0.018, a reasonable value, then, as before, if the fraction of the small component is fixed, a value of the big component can be found which minimises rΣsq. There exist several possible solutions, shown below.

Table (5). p303, PS1, S1 and S2. B, C, and rΣsq calculations with A constant at 0.018. Solutions outside (Limit) are those which vary noticeably from the experimental saturation curves, and were determined as in figs.(51)-(54).

	Small X-section (A)	Fraction of small (B)	Big X-section (C)	rΣsq	
PS1	0.018	0.1	0.045±0.002	0.0384	
S1	0.018	0.2	0.051±0.003	0.0316	(Limit)
	0.018	0.3	0.059±0.003	0.0251	
	0.018	0.4	0.073±0.006	0.0210	
	0.018	0.5	0.093±0.007	0.0232	(Limit)
	0.018	0.6	0.13±0.02	0.040	
PS1	0.018	0.5	0.057±0.006	0.0281	
S2	0.018	0.6	0.08±0.01	0.0189	(Limit)
	0.018	0.7	0.15±0.02	0.0111	
	0.018	0.8	0.3±0.09	0.0244	(limit)

The limits were established in the same way as before. The overall solution, for this single value of the small component of PS1 is:

	small	fraction of small	big	
PS1,S1	A=0.018	0.2< **B**< 0.5	0.048< C< 0.10	**Solution 2**
PS1,S2	A=0.018	0.6< **B**< 0.8	0.07< C< 0.4	

Assume that A(PS2)=0.006, that is the size of the small PS2 component is one third the size of the small PS1 component. The following solutions are possible.

Table (6). p303,PS2, S1 and S2. B, C, and rΣsq calculations keeping A constant at 0.006. Solutions outside (Limit) are those which vary noticeably from the experimental saturation curves. The limits were obtained as before.

	Small X-section (A)	Fraction of small (B)	Big X-section (C)	rΣsq	
PS2 S1	0.006	0.1	0.067±0.005	0.1179	(Limit)
	0.006	0.2	0.086±0.008	0.1064	
	0.006	0.25	0.10±0.01	0.1189	(Limit)
	0.006	0.3	0.11±0.01	0.1471	
PS2 S2	0.006	0.1	0.039±0.004	0.2241	
	0.006	0.2	0.049±0.006	0.2001	(Limit)
	0.006	0.25	0.054±0.007	0.1957	
	0.006	0.3	0.062±0.009	0.1991	(Limit)
	0.006	0.4	0.08±0.01	0.2366	

The overall solution for this one value of of the small component of PS2 is:

	small	fraction of small	big	
PS2, S1	A=0.006	0.1< **B**< 0.25	0.072< C< 0.11	**Solution 3**
PS2, S2	A=0.006	0.2< **B**< 0.3	0.043< C< 0.071	

Solutions 2 and 3 are subsets of solution1 and have been selected by using added, reasonable, assumptions.

Solution 2 indicates that in S2 PS1 has fewer big components but the big components are bigger. There may be conditions therefore when the average change in X-section may be slight, but a change in shape of the S2 saturation curve might be observed. The fitting of Poisson equations to the saturation curves in addition to visual comparison of the S1 and S2 curves is therefore essential.

Solution 3 indicates that in S2 PS2 has smaller big components and maybe more of them. A change in average X-section of PS2 is more likely to be observed by visual comparison of the saturation curves than is a change in X-section of PS1.

Consideration of two-component curves at all wavelengths.

574nm PS1.The results obtained above for p303 , and values of the two-component fits obtained from the best fits to the saturation curves of the other experiment at 574nm are shown below for PS1, in both relative units and transferred to $Å^2$ (see appendix); the latter introduces a further error of 12% because the absolute intensity of the pulse delivered to the examined plane must be measured.

Table (7). The size of PS1 small and large components at 574nm, in relative units as measured from the experimental saturation curves, and in $Å^2$.

PS1,574nm (Relative units)

	S1		S2		
	small	big	small	big	
p231	0.036±0.002	-	0.034±0.004	0.3±0.2	
p303	0.018±0.008	0.08±0.03	0.018±0.008	0.25±0.15	**Solution 2**
(Transferred to $Å^2$)					
p231	65±10	-	65±15	400±300	
p303	30±15	135±65	30±15	400±300	

It is assumed that when a double component fit cannot be obtained, the size of the single component applies to the most numerous component, the uncoupled PS1. From p231, the small component does not change as S1->S2 i.e. the uncoupled PS1 does not receive any extra energy in S2, confirmation of the assumption used in the previous calculations for p303. Only p303 provides two-component fits in both S1 and S2, for a direct comparison of the two components in both states; the big component increases by a factor of about three as S1->S2. It appears from these dimensions that PS1should show an enormous increase in average X-section in S2. It has already been pointed out that the average X-section depends on the fraction of the components as well as their magnitudes. In S2 the big component gets bigger but the number of them decreases.

PS2. The results obtained previously for p303 are shown in Å^2 and compared to the S2 results of p306.

Table (8). The size of PS2 small and large components at 574nm, in relative units as measured from the experimental saturation curves, and in Å^2.

PS2,574nm (Relative units)

	S1		S2		
	small	big	small	big	
p303	0.006±0.005	0.09±0.02	0.006±0.005	0.05±0.02	**Solution3**
p306	-	-	0.013±0.003	0.14±0.06	
Transferred to Å^2:					
p303	10±10	150±50	10±10	85±45	
p306	-	-	10±3	115±65	

As only the S2 saturation curve was obtained for p306, this experiment does not confirm the S1->S2 changes, but the results in S2 are consistent with those of p303.

627nm is energy that is absorbed to an equally small extent, by both PBS and Chla, but is also absorbed by the base pigment of PBS normally considered as being attached to PS2.

PS1. There are only single component fits for PS1, since p268,S1 must be disregarded because of aggregation in the sample during the S1 curve determination. The association of PS1 with PBS should be the same whether the laser pulse is of wavelength 574nm or 627nm, so it might be expected that two-components should be observed. The X-section of a component is not the same at 627nm as at 574nm; it depends on the absorbance of the component. A component composed of chla, such as uncoupled PS1,will appear larger at 627nm than at 574nm as the absorbance of chla is greater at 627nm than at 574nm. The portion of PBS which contributes to PS1, will appear, at 627nm to be smaller than at 574nm, as, conversely, the absorbance of PBS is smaller at 627nm than at 574nm. The difference between the big and small components therefore becomes smaller at 627nm. It was just possible to observe the two-components at 574nm, when the big component was

five to ten times the small component; at 627nm although still present, the heterogeneity might not be observed. The X-section measured will be that of the larger fraction, the 80% disassociated PS1.

PS1 values obtained from experiments at 627nm are:

Table (9). The size of PS1 small component at 627nm, in relative units as measured from the experimental saturation curves, and in $Å^2$. The average is taken over both S1 and S2.

PS1,627nm (relative units)	S1 small	S2 small
p245	0.056±0.002	0.051±0.003
p268	-	0.085±0.004
(transferred to $Å^2$)		
p245	30±5	32±5
p268	-	50±8
	Average 40±10	

In the last section it was shown that the average X-section at 627nm does not change as S1->S2, so the one component of which the X-section is composed will not change.The average of the single component has been taken over both S1 and S2 values. The X-section difference between experiments may well be due to differences in growth conditions of cells.

PS2. The saturation curve for PS2 in S1 of p268, was fitted with a two-component equation but these data were disregarded because of aggregation in the sample; the curve for S2 was fitted with a single component. The same argument used above for PS1, that at this wavelength the difference in absorption between the PS2 coupled and uncoupled to PBS is small, can be applied to PS2. The X-section measured is that of the most numerous component the PS2 coupled to PBS, the big component. PS2 values obtained from the experiment at 627nm are shown in table (10).

Table (10). The size of PS2 big component at 627nm, in relative units as measured from the experimental saturation curves, and in Å².

PS2,627nm (relative units)	S1 big	S2 big
p268	-	0.036±0.004
Transferring to Å²		
p268	-	21±5

668nm is energy absorbed by chla, and hence by the photosystems, and to only a negligible amount by PBS.

PS1. Of the eight PS1 saturation curves all except one, p263 S2, were fitted with single component equations. There was no reason to discard this one curve, but because all the others were single component curves, its data were ignored for the component sizes. The values obtained for PS1 from all experiments at 668nm are:

Table (11). The size of PS1 small component, disassociated PS1, at 668nm, in relative units as measured directly from the experimental saturation curves, and in Å².

PS1,668nm (Relative units)	S1 small	S2 small
p241	0.043±0.002	0.046±0.001
p251	0.110±0.003	0.110±0.004
p263	0.144±0.006	-
p271	0.135±0.005	0.146±0.006
(Transferred to Å²)		
p241	48±8	51±7
p251	110±15	-
p263	145±25	145±25
p271	105±15	110±20
	Average 100±35	

From p241, p251, and p271 the size at 668nm of PS1 does not change as S1->S2. It is at this wavelength, where PS1 and PS2 absorb at the maximum, that there is the best chance of observing any change in X-section due to the transfer of energy directly from PS2 in S2. It appears that PS1 does not receive any more energy directly from PS2 in S2, the

conclusion reached in the section on change in average X-section. The size determined in p241 is noticeably different, but like experiments p245 and p268, it is probably due to different cell growth conditions. Since there is no observed change in size of PS1, the average determined in table (11) is derived from both S1 and S2 results.

PS2. Three of the four saturation curves of PS2 could be fitted with two-component equations. It has been pointed out by Ley and Mauzerall (1982) that with increase in concentration of cells, resulting in inhomogeneous absorption and scattering, the saturation curve took on the form of a two-component system. Although the concentration of cells was decreased to the minimum that would give a reasonable signal to noise, absorbance at 668nm is near a maximum, which may cause absorption similar to that of Ley and mauzerall. The values obtained for the two-components of PS2 from all experiments at 668nm are:

Table (12). The size of the small and big components of PS2, at 668nm, in relative units as measured directly from the experimental saturation curves, and in $Å^2$.

PS2,668nm (relative units)				
	S1		S2	
	extra	small	extra	small
p279	0.03±0.01	0.09±0.05	0.017±0.006	0.13±0.04
p285	0.017±0.007	0.17±0.06	-	-
Transferring to $Å^2$:				
p279	11±5	30±20	6±3	45±20
p285	7±5	65±30	-	-

PS2 is composed of chla and its X-section, at this wavelength, should be much greater than that of the uncoupled PS2 at 574nm (small, measured as 10±10 $Å^2$) because absorbance of chla at 668nm is much greater than that at 574nm. It should also be about one third that of the uncoupled PS1 at 668nm (measured as 100±35 $Å^2$) since it contains about one third the number of molecules of chla. The X-section of the uncoupled PS2 is that of the larger component here and the very small "extra" component is extraneous, and its origin will be considered later.

DISCUSSION

VERIFICATION OF THE TWO-COMPONENT IDENTITIES.

Comparison of PS1 X-sections, in $Å^2$, at different wavelengths, is done in the table below:

Table (13). PS1 X-sections, in $Å^2$, at 574nm, 627nm, and 668nm.

		S1		S2	
		small	big	small	big
PS1	574nm p303, solution 2	30±15	135±65	30±15	400±300
	627nm, table (9), average S1&S2	40±10			
	668nm, table (11), average S1&S2	100±35			

The relative values of the small X-section at 668nm, 627nm, and 574nm should be the same as the relative values of the uncoupled PS1 absorbances at these wavelengths. Redlinger and Gantt (1983) isolated chlorophyll-protein complexes from *Porphyridium cruentum*. CP1, a chlorophyll-protein complex from PS1 had absorbance such that:

A(678) ≈ 4 A(620)≈7 A(574). i.e. A(678): A(620): A(574)=28:7:4

The small X-sections from table (13) at 668nm, 627nm, and 574nm, selecting values within the error ranges, are in the ratio:

130:40:15 =28:9:3, which is in good agreement with the absorbances of the chlorophyll-protein complex. The small X-sections of PS1 from different wavelengths are therefore consistent with their identification as PS1 unconnected with PBS.

Comparison of PS2 X-sections, in $Å^2$, at different wavelengths is shown below:

Table (14). PS2 X-sections, in $Å^2$, at 574nm, 627nm, and 668nm.

PS2	S1			S2		
	small	big	extra	small	big	extra
574nm, solution 2	10±10	150±50		10±10	85±45	
627nm, p268, table(10)	-	-		-	21±5	
668nm, average, table(12)	45±30		9±7	45±20		6±3

From Redlinger and Gantt (1983), CPIII and CPIV, chlorophyll-protein complexes from PS2 have absorbances at 668nm, 620nm, and 574nm, in the ratio 3:1:1. If the

coupled PS2 of 627nm, the major component, can be considered to have the same X-section as the uncoupled PS2, which has a similar X-section as was argued in the 627nm results, then the X-section of the uncoupled PS2 at 627nm is approximately 21±5 $Å^2$. Selecting values within the error range the uncoupled PS2 has X-sections in the ratio 45:15:15 i.e. 3:1:1 at these wavelengths. At 668nm the uncoupled PS2 should be about one third the size of PS1 at 668nm (i.e. 100±35), and it is. The consistency of both the PS1 and the PS2 areas at different wavelengths and of PS1 with PS2 at 668nm makes it appear that the two-components of the bimodal curves have been identified correctly, with the exception of the "extra" in the measurement of the PS2, 668nm, curves.

If the "extra" is an artefact, the saturation curves of PS2 at 668nm would be due to a single component, and discrimination between the possible arrangements of PBS, PS1 and PS2 in S1 of fig.(55) is possible.The paths of 668nm energy in such arrangements are shown in fig.(56)

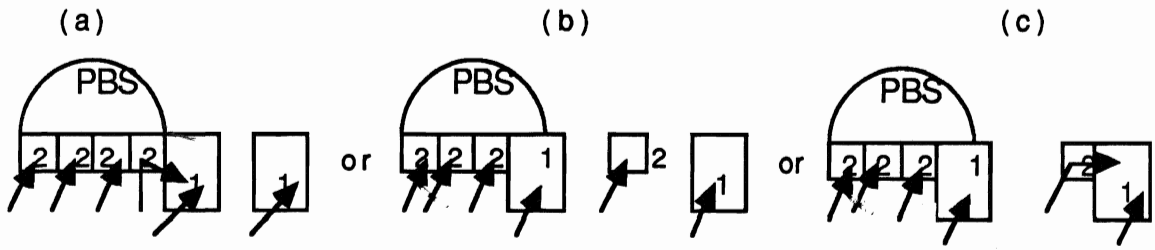

Fig.(56) The possible arrangements of PBS, PS1 and PS2 in state1, compatible with p303 results.

(a) PS1 obtains energy from PBS via PS2, spillover.

(b) PS1 is directly connected to PBS, equivalent to a mobile antenna situation, together with PS1 and PS2 not connected to PBS

(c) PS1 is directly connected to PBS, together with PS1 and PS2 not connected to PBS but connected to each other, the equivalent of the combination, mobile antenna and spillover, situation.

The path of 668nm light energy is shown.

Measurement of the PS1 and PS2 X-sections in S1 should give different results:

		(a)	(b)	(c)
668nm	PS1	2 components	1 component	2 components
	PS2	2 components	1 component	2 components

If the "extra" necessary to describe the PS2 saturation curves at 668nm is an artefact then a single-component equation describes both the PS1 and PS2 saturation curves and arrangement (b) applies. If the "extra' is not an artefact arrangements (a,c) are possible from the PS2 results, and (b) from the PS1 results. This is contradictory, unless the single component of PS1 is actually two components of such similar X-sections that they cannot be distinguished, similar to the situation proposed in the 627nm experiments.

From table (14), if the "extra" component is the PS2 connected to PS1, its size is one fifth that of the PS2 coupled normally to PBS (9 compared to 45). Four fifths of its excitation therefore is transferred to PS1. Suppose that PS2 contains 5n chl*a*, and PS1 contains 15n chl*a*, then in situations (a, c) of fig.(56), the effective X-section of the PS2 connected to PS1 is n, that of the PS2 coupled to PBS is 4n. The X-section of the uncoupled PS1 is 15n, that of the PS1connected to PS2 is 19n. The fitting of a two component curve to PS1 where the sizes of the two components have the ratio 19/15 is far more uncertain than the fitting of a two-component curve to PS2 where the sizes of the two components have the ratio 5/1. It is possible, therefore that in S1 situations (a,c) can apply and not be observed from PS1 X-section measurements.

It can be concluded that in state1 any one of the arrangements (a,b,c) could exist and at this point in the discussion they cannot be distinguished.

STATE TRANSITION MECHANISM.

A model of the transition from S1 to S2 in *Porphyridium cruentum* is more complicated than those postulated in the introduction, fig.(10), not only because several PS2 share a single PBS, but because the existence of two component photosystems makes uncertain the arrangement of PBS, PS1 and PS2 in S1.

X-section changes determined from these experiments. Solution 2 shows, that as S1->S2 the fraction of small component of PS1 increases. That is, some PS1 is released from PBS. If more than one PS1 share the same PBS, the energy which went to the departed PS1 can go to the PS1 still attached to PBS, resulting in an increase in the X-section of the big component of PS1, or it can go to the PS2 attached to PBS, resulting in an increase in the X-section of the big component of PS2.

It is possible to calculate the X-section of the big component of PS1 in S2 if its size is determined only by the number of PS1 sharing PBS, and no assumption is made regarding transfer of energy from PS2. If there is also no change in energy lost by heat or fluorescence the total X-section of PS1 in S1 and S2 remains the same . i. e. A**x**B+C(1-**B**) is a constant. Taking mid-points of solution 2, the fraction of the small component of S1 is 0.35, the X-section of the big component is 0.075, and, in S2, the fraction of the small component is 0.7; the disassociation would lead to a big X-section of 0.14, at the lower end of the range of the calculated size. Anything larger than this, however, can only be caused by changing the distribution of PBS energy, more to PS1 and less to PS2. Solution 3 shows, that as S1->S2, the size of the associated PS2 becomes smaller, even though the number of PS2 associated with PBS possibly decreases but certainly does not increase. This decrease in the size of the big component of PS2 is opposite to that expected by association with PBS alone, and the increase in X-section of the big component of PS1 is greater than that which could be attained by association with PBS alone. The inference is, that some of the energy absorbed by PBS which went to PS2 in S1 is transferred to PS1, making the PS1 still associated with PBS bigger, and that of PS2 associated with PBS smaller.

Do these results fit with any of the models proposed in the introduction (fig.10)? .It is obvious from the preceding paragraph that a simple mobile antenna cannot provide a model. In this situation where several PS2 and a PS1 may share a PBS, the release of PS2, and the capture of PS1 would lead very neatly to an increase in average X-section of PS1 and a decrease in average X-section of PS2. Although the net result is an increase in average X-section of PS1, this model might entail a decrease in the X-section of the big component of PS1 as more PS1 shared the PBS, opposite to results of this experiment. The big component of PS1 would remain the same size if there was direct replacement of PS2 by PS1. There would be no change in the X-section of the coupled PS2, the big component, whereas the results of these experiments show that it decreases. The model cannot explain the decrease in X-section of the big component of PS2.

The spillover model would mean that, in S2, more PS1 would associate with PBS, receiving energy from PBS via attached PS2's. This would result in an increased average PS1 X-section, and a decreased average PS2 X-section. The big X-section of PS1 would remain the same, the small X-section of PS1 would increase, the **B** value for PS1 would decrease, and the **B** value for PS2 would remain the same. Only the last condition agrees with solutions 2,3.

The combination model combines a mobile antenna and spillover between the disassociated PS2 and disassociated PS1. The mobile antenna part has already been dismissed. This kind of spillover would result, with 668nm, as S1->S2, in the small PS2 becoming smaller, the small PS1 becoming bigger, the average X-section of PS1 increasing and that of PS2 decreasing. The 668nm experiments provide evidence for none of these changes.

What model will fit the results of these experiments? None of the models proposed for the PBS-containing cyanobacteria suffices for this red alga.

Consider each one of the fig.(56) situations and see if changes can be proposed which will account for solutions 2,3.

Impediment of the flow of PBS energy to PS2 and its diversion to the coupled PS1 would account for the changes in X-section of the big components of PS1 and PS2. In situation (a) this would result in increased flow through the connecting PS2. If a fixed proportion of the flow through PS2 gets to the RC, the increased flow would result in an increased yield and an increase in the X-section of small PS2, something which, with justification, was assumed not to occur. Situation (a) cannot support the state transition of these experiments. Impediment of the flow of PBS energy to PS2 and its diversion to PS1 could occur in both (b,c) since the arrangement of PBS with PS1 and PS2 is the same. If the "extra" component of PS2,668nm is an artefact then situation (b) applies; if the "extra" component is real then situation (c) applies. In neither of the two last situations does any more energy go from the uncoupled PS2 to the uncoupled PS1 in S2, as there is no change in the average X-section of PS1 or PS2 at 668nm. In both situations, however, an impediment to PBS energy flow to PS2 and its diversion to PS1 must occur to account for solutions 1,2. This is illustrated in fig.(57).

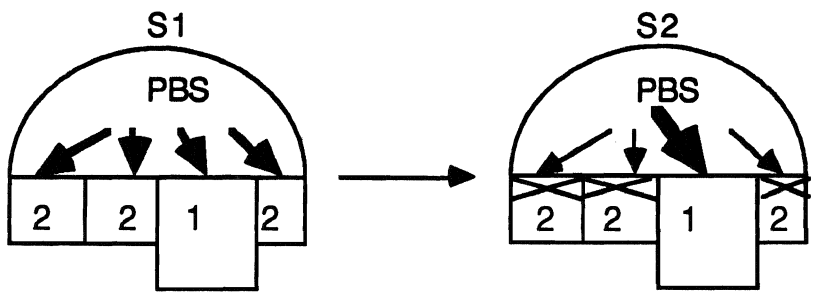

Fig.(57). The energy flow from PBS to the attached PS2 is impeded in S2 and is diverted to the attached PS1.

Criticisms of bimodal interpretation.

Greenbaum and Mauzerall(1991) found that although O_2 saturation curves obtained with energies of low absorption could be fitted with single components, saturation curves obtained with more highly absorbed energies deviated from the Poissonian curve at the part of the curve approaching saturation. It is the opinion of these authors that heterogeneous actinic light absorption in a single cell could cause the addition of a smaller absorption X-section.

The smaller component of PS1 at 574nm , the small component, is that of the uncoupled PS1 the presence of which is accepted; it is the big X-section, the coupled PS1 which is unusual, and this, according to Greenbaum and Mauzerall would not be suspect since it is the larger component. The PS1 saturation curves at both 627nm and 668nm have single component shapes. If the bimodal shape were caused by excess absorption of the sample, such a shape would be expected at 668nm where chla absorbs strongly. That it does not occur is further evidence that for the PS1 experiments, the bimodal shape is not an experimental artefact .

For PS2, however, at 668nm, the second, "extra" component is indeed the smaller one, a reason to suspect that it may be an artefact of high absorption, even though the small size is consistent with models of fig.(56,a,c). The saturation curves at the two highly absorbed wavelengths, 574nm and 668nm, exhibit heterogeneity, whereas that at the less absorbed wavelength, 627nm, is interpreted with a single component, an indication that both 574nm and 668nm results may be suspect, but the 574nm results are consistent with the chla absorbances at 574nm. 627nm, and 668nm as is the larger component at 668nm, table 14. There are double component fits for PS2, with 668nm, done with low cell density samples, which are suspect (p279, p285) but single component fits with PS1 668nm (p241, p251, p271), done with high cell density samples; if cell density is a problem with PS2 it should be a greater problem with the PS1 results. Although the PS2 two-component measurements should be regarded with a certain amount of caution, they can be regarded as

legitimate, until shown otherwise.

With acceptance of the two component result for PS2, situation (c) of fig.(56) exists in S1. That is, some PS1 is directly connected to PBS; some PS1 and PS2 are not connected to PBS, and these free photosystems are closely associated so that the major part of PS2 excitation is transferred to PS1. There is spillover in S1, but there is no evidence that this spillover increases as S1->S2. Spillover exists but not as a mechanism for the state transition.

ARE THESE RESULTS SUPPORTED BY OTHER EXPERIMENTS?

In these experiments the average X-section of PS1 increases, that of PS2 decreases, as S1->S2, with PBS absorbed light, but does not change with chl*a*-absorbed light. A fraction of PS1 is coupled to PBS in both S1 and S2. There is a smaller fraction coupled in S2 than in S1, so PS1 disassociates from PBS in S2. Uncoupled PS1 does not receive any extra energy in S2. There exists some kind of impedance to the energy flow from PBS to PS2 in S2, allowing more energy to go to the PBS-coupled PS1. In addition, results obtained from the PS2 double component data indicate that there is a decrease in the X-section of the coupled PS2 in S2, but it is not decreased to the point that it can be regarded as uncoupled from PBS; the fraction of uncoupled PS2, as measured directly from **B**, indicates an increase which may not be significant.

Ley (1984) measured the PS2 X-section from an O_2 evolution curve and found that *Porphyridium cruentum* in S2 had a single X-section of 160Å^2 at 596nm and a single X-section of 450Å^2 at 546nm. In S1 at 596nm the X-section was 260Å^2. Interpolating between these wavelengths one would expect a X-section of 300Å^2 at 574nm in S2; if a similar increase occurs in S1, one would expect a X-section of 490Å^2 at 574nm in S1, a decrease of 40% as S1->S2. The measured X-sections are 85±45Å^2 and 150±50Å^2, about one third the expected size, with a decrease as S1->S2 of 43%, table 8. The cultures of these

experiments were noticeably red when harvested and sometimes had to be diluted to get the required optical density. It was possible that a good part of their growth occurred in red light as this is the kind of light that penetrated within the culture. Cunningham et al (1990) grew *Porphyridium cruentum* under red, white, and green light. The number of PS2 per PBS was 4.2±0.6 in red-grown cells, and 2.9±0.1 in white-grown cells. If all the PS2 are connected to PBS, whose number according to these authors remains constant, the X-section of the PBS-coupled PS2 can decrease by a factor of 1.7, i.e (4.2+0.6)/(2.9-0.1). With such a decrease, the PS2 X-section of Ley's cells, if grown in red light, would be 290Å^2 in S1 and 175Å^2 in S2. The results of experiments in this thesis, using the maximum error, would be 200Å^2 and 130Å^2 in S1 and S2 respectively, perhaps not too far from Ley's results, especially when the size of the PBS which comprises nearly the whole of the X-section at this wavelength is itself determined by a variety of growth factors. Mullineaux et al (1986) from measurement of fluorescence induction in continuous light deduced that for *Synechococcus 6301* the PS2 X-section was greater in S1 than in S2. Tsinoremas et al (1989) found that as S1->S2 the X-section of PS1 decreased with both chl*a*-absorbed light and PBS-absorbed light, but as the chl*a*-absorbed light was in the near UV (337nm), it may have been less selective for chla than the blue light of Mullineaux (1992), who with *Synechococcus 6301*, determined the X-section of PS1 from yellow and blue-flash induced absorbance changes at 700nm. He found that in S1 the X-section of PS1 with the PBS-absorbed light (yellow) was smaller than that in S2, and there was no significant change with the PS1-absorbed light (blue). Post et al(1991), with *Synechocystis 27170* found an increase in PS2 X-section in S1, with saturation curves of O_2 production from white light flashes.

The proposed model assumes that a fraction of PS1, as well as the major portion of PS2 is coupled to PBS. Mullineaux (1992) At a flash of 630nm (PS2 absorbed) cells in S2 had a X-section only slightly less than that at 680nm (PS1 absorbed). This implies that PBS, which absorb highly at 630nm were transferring energy to PS1, which absorbs very

little at 630nm. He determined that this was not a case of spillover: with light absorbed by chl*a* the X-sections in S1 and S2 did not indicate any significant transfer of energy from PS2 to PS1. The saturation curve with PBS-absorbed light for cells in S2 was bimodal, a confirmation of PS1 heterogeneity, but he did not observe this in S1. The heterogeneity was not seen in chl*a* absorbed light. His results seem to be largely the same as those herein.

The mobile PBS model proposes that some PS2 are decoupled from PS1; these results indicate that PS1 is decoupled. Picosecond measurements (Mullineaux et al,1990) on *Synechococcus 6301* showed that transition to S2 decreased the amplitude of fluorescence decay components associated with PS2 without changing their lifetimes and the state transition had no significant affect on the kinetics of fluorescence decay from the terminal emitter chromophores of the PBS. The authors suggested that PS2 became decoupled from PBS but the decreased amplitude of the components from PS2 could be due to an impedance in energy flow between PBS and PS2, which would operate in this proposed model. Although these results show that there is some disassociation of PS1 from PBS the PS1 may not be coupled to the PBS via a terminal emitter so there would not be any unconnected terminals. The experiments of Mullineaux and Holzwarth (1990) do not agree with the results of this thesis. They used fluorescence induction to determine the extent of PS2 trap closure. *Synecochoccus 6301* was exposed to phycocyanin-absorbed and chl*a*-absorbed light in the presence of DCMU. The number of closed reaction centres in S2 in phycocyanin-absorbed light was less than that closed by chl*a*-absorbed light, leading to the conclusion that, in S2, a fraction of PS2 must be decoupled from PBS.

The uncoupling of PS1 from PBS in S2 could cause an added PBS fluorescence in S2. This does appear to occur in these experiments where F660/F715 is greater in S2 than in S1. These experiments were not designed, however, for precise fluorescence comparisons. Salehian (1992) with a rotating sample of Synechococcus 6301, found that there was no increase in PBS fluorescence in S2. It appears that impedance to PS2 does not cause an increase in the life of the excitation in PBS, but is immediately transferred to PS1. This

kind of argument implies that the PS1 is directly and closely connected to the PBS; it would have been nice to suggest that PS1 was connected via the terminal emitter, but release from that would disagree with the experiment above (Mullineaux et al, 1990)

Laser induced optiacoustic spectroscopy has detected no difference in energy released as heat during S1->S2. (Mullineaux et al, 1991; Bruce and Salehian 1992). These data would support the mobile PBS model with replacement of the uncoupled PS2 by PS1, but also supports the present model, since no energy is lost. The present model was deduced from an experiment which was consistent in that the average X-section of PS1 increased and that of PS2 decreased, so the data used may be biased towards a model which would conserve excitation energy.

The only result of these experiments that is not confirmed by the work of others is the deduction that some PS1 becomes uncoupled from PBS in S2. It is, indeed an unexpected and, apparently contrary, result. It seems to go against common sense for PS1, which is expected to receive energy from the PS2 system in S2, to leave the major antenna of that system.

It is unlikely that cyclic electron transfer in PS2 accounts for the decrease in X-section of the big component of PS2. The decrease was detected by a change in shape of the fluorescence saturation curve and this is not expected to change due to cyclic electron flow. The proposed electron cycle of Falkowski et al (1986) in Chlorella, was QA->QB->PQ->Cytb559->Z, which would cut off the flow of electrons from the water splitting unit, and hence reduce the O_2 production but have no effect on the fluorescence.

Post et al(1991) with Synechocystis 27170, found a greater discrepancy between O_2 evolution and fluorescence occurred in S2. These authors suggest, not a cyclic electron flow, but that ($P^{+}_{680}QA$) persists in S2, so that with continuous background S2 light some of the PS2 traps are closed to the donor side of PS2 at flash incidence. As the experiments of this work do not use a continuous background light; at flash impact the PS2 traps have had time to open; the proposed state of Post et al cannot be used as a mechanism of impedance

between PBS and PS2.

It is likely that an impedance as proposed herein, would be caused by some maladjustment between PBS and PS2, or change of orientation, to prevent easy excitation transfer, a maladjustment which does not occur with PS1. Linear dichroism of Synecochoccus 6301 at 77^0K was interpreted by Bruce and Biggins (1985) to mean that PBS remains functionally attached to PS2 in both states. Homer-Dixon (1992) using linear dichroism of Porphyridium cruentum was unable to detect any significant changes in pigment orientation as S1->S2.

ARE THE CHANGES IN X-SECTION SUFFICIENT TO ACCOUNT FOR THE DECREASE IN PS2 FLUORESCENCE AS S1->S2? The decrease in PS2 fluorescence as S1->S2, has been used to identify the state of the organism. These experiments have used the 77^0K emission spectra to verify the state during different stages of the saturation curves. Attempts to account for this decrease have led to the proposal that in S2 energy is diverted from PS2 to PS1. The PS2 saturation curves all show a considerable decrease in maximum yield in S2. This is shown, for 574nm and 668nm light, absorbed by PBS and chla respectively, in table (15).

Table (15). Fluorescence, $(F_v-F_0)/F_0$, measured at saturation for 574nm and 668nm light.

		Maximum yield S1	S2
574nm	p303	0.8	0.5
668nm	p279	0.9	0.41
	p285	0.82	0.29

If the fluorescence is proportional to the amount of excitation reaching PS2, about one half of the excitation reaching PS2 in S1 goes somewhere else in S2. From table (4), with 574nm light, the average X-section of PS1 increases and the average X-section of PS2

decreases as S1->S2; the average X-section of PS1 goes from 90Å^2 to 150Å^2, and the average X-section of PS2 goes from 100Å^2 to 60Å^2, as S1->S2. The decrease in PS2 average X-section corresponds to the decrease in PS2 fluorescence; it is a reasonable inference that, in S2 about 40% of the energy absorbed by PBS is diverted from PS2 to be channelled to PS1. At 668nm, the PS2 fluorescence decreases to the same extent, but there is no consistently observable change in the average PS2 X-section, and there is no change in in the average PS1 X-section, table (4). The path of the energy absorbed by PS2chl*a* is not changed, in that none is diverted to PS1, but the fluorescence is halved in S2.

There are several possibilities:

(1) There is energy transfer with ch*a*-absorbed energy. There is a change of X-section of PS1 and PS2 which is not observed. An argument can be made that the change in PS1 may be too small to be observed and that the change in PS2 may be masked by the large experimental spread. In this case the model proposed in this thesis must be modified.

(2) There is a change, which occurs at the same time as the state transition, which causes fluorescence quenching in S2, for both PBS and chl*a* absorbed light. The energy path changes observed with PBS-absorbed light coincide with this change. In this case it should be expected that the fluorescence change is not adequately accounted for by the energy diversion. With p303 there seems to be good agreement between the fluorescence decrease and the changes in average X-section.

(3) The decrease in PS2 fluorescence at 574nm in S2 is explained by the energy diversion to PS1, and there is no independent fluorescence quenching. With 668nm light in S2 there is no transfer of energy from PS2 to PS1; the decrease in PS2 fluorescence is caused by a quenching process which is dependent on the energy of the light: it occurs with 668nm but not 574nm.

With neither 574nm light nor 668nm light was there evidence of irreversible fluorescence quenching, indicative of photoinhibition.

FUTURE EXPERIMENTS.

The experiments could be modified or repeated to confirm these results. Two elements of the model, PS1 uncoupling and impedance to energy flow from PBS to PS2, have been derived from a single experiment, p303. Confirmation of these results is necessary.

Differences between cells at the same flash wavelength may be due to different proportions of photosynthetic elements. Harvesting was done at different cell densities; self absorbance at high cell density would cause the growth light to become red. A continuously diluted culture at constant optical density may decrease discrepancy between experiments. It would be interesting to see if a similar model is obtained with cells grown under red and green light, which cause maximum differences in the PS1 and PS2 content (Cunningham et al, 1990)

Repeat of experiments with the presence of a continuous background light would preferentially close the large X-section, so the fraction of small component should increase. Background light of high intensity in S2 causes an increase in X-section in S2 (Falkowski et al 1986), but S1 is not so much affected. These experiments would look for a change in **B**, which is not easy to do if the X-section changes as well, as has been shown in the p303 calculations.

Of overriding importance, however, is the determination of the cause of the PS2 fluorescence change as S1->S2, when chl**a** absorbed light is incident. The question which requires an answer is :

What happens to chl**a** absorbed energy ?

CONCLUSIONS.

Interpretation of saturation curves with two-component Poisson equations indicate that a fraction of PS1 is directly connected to PBS. A fraction of PS2 is not connected to PBS.

On the transition from state1 to state2, only with PBS-absorbed energy (574nm) does the average X-section of PS1 increase, 27%, and that of PS2 decrease, 40%. As S1->S2 the fraction of PS1 associated with PBS decreases, from 0.65 to 0.35. The X-section of PS1 connected to PBS shows a threefold increase in X-section, from 135±65 $Å^2$ to 400±300 $Å^2$.The fraction of PS2 connected to PBS, 0.75, does not change significantly, but the X-section decreases from 150±50$Å^2$ to 85±45$Å^2$. The changes in size cannot be explained only by change of association of the photosystem with PBS. It is proposed that small changes in the attachment of PS2 to PBS cause the PBS-absorbed energy to be diverted to the PS1 associated with PBS. It appears that the energy diverted from PBS goes directly to PS1 and not via PS2 (spillover). It is because PS1 is directly associated with PBS that changes in PS2 which impede its energy income from PBS, cause diversion of such energy to PS1. PS1 not associated with PBS does not receive any increase in energy from PS2 in S2.

None of the previously proposed models of state transition mechanism applies wholly to *Porphyridium cruentum*..There are, however, elements of all three models in the mechanism proposed. The "mobile antena" model applies in that a photosystem does leave PBS, but it is PS1. PS2 can be considered as partially detached in S2. The "spillover" model applies to the extent that the photosystems that are free from PBS can associate together leading to energy transfer from PS2 to PS1, but this energy does not increases in S2. The "combination" model applies in that both photosystems are disconected from PBS to some extent in S2, a fraction of PS1 is completely disconnected and PS2 is partially disconnected.

PS2 fluorescence is approximately halved in S2 for both PBS and chla absorbed light. This can be explained by energy transfer from PS2 to PS1 in 574nm light but such transfer is not detected at 668nm. One possibility is that 668nm light causes fluorescence quenching in S2, but 574nm light does not.

REFERENCES

Allen J.F. (1992). Protein phosphorylation in regulation of photosynthesis. Biochim. Biophys. Acta, 1098, 275-335.

Allen J.F., Holmes N.G. (1986). A general model for regulation of photosynthetic function by protein phosphorylation. FEBS Lett. 202, 175-181.

Allen J.F., Melis A. (1988). The rate of P700 photooxidation under continuous illumination is independent of state1-state2 transitions in the green alga *Scenedesmus obliquus*. Biochim. Biophys. Acta, 933, 95-106.

Allen J.F., Sanders C.E., Holmes N.G. (1985) Correlation of membrane protein phosphorylation with excitation energy distribution in the cyanobacterium *Synechococcus* 6301. FEBS Lett. 193, 271-275.

Anderson J.M., Melis A. (1983) Localization of different photosystems in separate regions of chloroplast membranes. Proc. Natl. Acad. Sci. USA. 80, 745-749.

Anderson L.K., Rayner M.C., Sweet R.M., Eiserling F.A.,(1983). Regulation of *Nostoc sp.* phycobilisome structure by light and temperature. J. Bacteriol. 155, 1407-1416.

Andreasson L.E., Vanngard T. (1988). Electron transport in photosystems I and II. Ann. Rev. Plant Mol. Biol. 39, 379-411.

Arnon D.I., Tang G.M.S. (1988). Cytochrome b-559 and proton conductance in oxygenic photosynthesis. Proc. Natl. Acad. Sci. 85, 9524-9528.

Barber J., Pick U., Gounaris K. (1987). Variable and conserved characteristics of PSII of spinach and of the halotolerant green alga *Dunalliela salina.* Progress in Photosynthesis Research, Proceedings of the VIIth.International Congress on Photosynthesis, Providence, Rhode Island, USA, 1986. (Ed. J. Biggins)

Bassi R., Hoyer-Hansen G., Barbato R., Giacometti G.M., Simpson D.J. (1987). Chrophyll-proteins ot the photosystem II antenna system. Jour. Biol. Chem. 262, 13333-13341.

Biggins J. (1983) Mechanism of the light state transition in photosynthesis.I. Analysis of the kinetics of cyt f oxidation in state 1 and state 2 in the red alga, *Porphyridium cruentum*. Biochim. Biophys. Acta 724 ,111-117.

Biggins J., Bruce D. (1985). Mechanism of the light state transition in photosynthesis. III. Kinetics of the state transition in *Porphyridium cruentum*. Biochim. Biophys. Acta, 806,230-236.

Biggins J., Bruce D. (1989). Regulation of excitation energy transfer in organisms containing phycobilins. Photosyn. Res. 20, 1-34.

Biggins J., Campbell C.L., Bruce D. (1984a). Mechanism of the light state transition in photosynthesis. II. Analysis of phosphorylated polypeptides in the red alga, *Porphyridium cruentum*. Biochim. Biophys. Acta, 767, 138-144.

Biggins J., Campbell C.L., Creswell L.L., Wood E.A. (1984b) Mechanism of the light state transition in *Porphyridium cruentum*. Advances in Photosynthesis research (Ed. C. Sybesma), 2, 303-306.

Biggins J., Mathis P. (1988). Functional role of vitamin K1 in photosystem I,of the cyanobacterium *Synechocystis 6803*. Biochem. 27, 1494-1500.

Bonaventura C., Myers J., (1969) Fluorescence and oxygen evolution from *Chlorella Pyrenoidosa*. Biochim. Biophys. Acta 89, 366-383.

Bowes J.M., Horton P. (1982). The effect of redox potential on the kinetics of fluorescence induction in photosystem II particles from *Phormidium laminosum*. Sigmoidicity, energy transfer and the slow phase. Biochim. Biophys. Acta, 680, 127-133.

Bowes J.M., Horton P., Bendall D.S. (1981). Does the acceptor Q2 fulfil an indispensible function in the primary reactions of photosystem II? FEBS. Lett., 135, 261-264.

Bowes J.M., Horton P., Bendall D.S. (1983). Characterization of photosystem II electron acceptors in *Phormidium laminosum*. Arch. Biochem. Biophys.,225, 353-359.

Breton J. (1982), The 695nm fluorescence (F695) of chloroplasts at low temperature is emitted from the primary acceptor of PSII. FEBS. Lett. 147, 16-19.

Briantais J.M., Vernotte C., Krause G.H., Weiss E. (1986). Chlorophyll a fluorescence of higher plants: chloroplasts and leaves. Light Emission by Plants and Bacteria (Ed. Govindjee, J. Amesz, D.C. Fork), Academic Press Inc.

Bricker T.M., Guikema J.A., Pakrasi H.B., Sherman L.A. (1986) Proteins of cyanobacterial thylakoids. Encyclopedia of Plant Physiology, vol.19. Ed. L.A.Staehelin and C.J.Arntzen. Springer-Verlag, New York.

Brimble S., Bruce D., 1989. Pigment orientation and excitation energy transfer in *Porphyridium cruentum* and *Synechococcus sp. PCC 6301* cross linked in light state 1, and light state 2 with glutaraldehyde. Biochim. Biophys. Acta 973, 315-323.

Bruce D., Biggins J. (1985) Mechanism of the light-state transition in photosynthesis. V. 77 K linear dichroism of *Anacystis nidulans* in state 1 and state 2. Biochim. Biophys. Acta, 810, 295-301.

Bruce D., Biggins J., Steiner T., Thewalt M. (1985). Mechanism of the light state transition in photosynthesis. IV. Picosecond fluorescence spectroscopy of *Anacystis nidulans* and *Porphyridium cruentum* in state 1 and state 2 at 77 K. Biochim. Biophys. Acta, 806, 237-246.

Bruce D., Brimble S., Bryant D.A. (1989) State transitions in a phycobilisome-less mutant of the cyanobacterium *Synechococcus sp. PCC 7002*. Biochim. Biophys. Acta, 974, 66-73.

Bruce D., Hanzlik C.A., Hancock L.E., Biggins J., Knox R.S. (1986) Energy distribution in the photochemical apparatus of *Porphyridium cruentum*: picosecond fluorescence spectroscopy of cells in state1 and state 2 at 77 K.Photosyn. Res. 10, 283-290.

Bruce D., Salehian O. (1992). Laser induced optoacoustic calorimetry of cyanobacteria. The efficiency of primary photosynthetic processes in state 1 and state 2. Biochim. et Biophys. Acta, 1100, 242-250.

Bryant D.A.,1981.The photoregulated expression of multiple phycocyanin species. Eur. J. Biochem. 119, 425-429.

Bryant D.A., Cohen-Bazire G. (1981). Effects of chromatic illumination on cyanobacterial phycobilisomes. Eur. J. Biochem. 119, 415-424.

Butler W.L. (1978a). Energy distribution in the photochemical apparatus of photosynthesis. Annu. Rev. Plant Physiol., 29, 345-378.

Butler W.L. (1978b). On the role of cytochrome b559 in oxygen evolution on photosynthesis. FEBS. Lett., 95, 19-25.

Butler W.L., Tredwell C.J., Malkin R.,Barber J. (1979). The relationship between the lifetime and yield of the 735nm fluorescence of chloroplasts at low temperatures. Biochim. Biophys. Acta, 545, 309-315.

Chain R.K., Malkin R. (1991). The chloroplast b6/f complex can exist in monomeric and dimeric states. Photosyn. Res. 28, 59-68.

Chereskin B.M., Clement-Metral J.D., Gantt E. (1985). Characterization of a purified photosystem II-phycobilisome particle from *Porphyridium cruentum*. Plant Physiol. 77, 626-629.

Clement-Metral J.D., Gantt E. (1983). Isolation of oxygen-evolving phycobilisome -photosystemII particles from *Porphyridium cruentum*. FEBS Lett. 156 185-188.

Cramer W.A., Theg S.M., Widger W.R. (1986) Photosynth. Res. 10,393

Cramer W.A., Black M.T.,Widger W.R., Girvin M.E. (1987). Structure and function of photosynthetic cyt b-c, and b6-f complexes. The Light Reactions. Ed. J. Barber.Elsevier Science Publishers B.V., New York.

Cunningham F.X., Dennenberg R.J., Jursinic P.A., Gantt E. (1990). Growth under red light enhances photosystem II relative to photosystem I and phycobilisomes in the red alga *Porphyridium cruentum*. Plant Physiol., 93, 888-895.

Deisenhofer J., Epp O., Miki K., Huber R., Michel H. (1984) X-ray structure analysis of a membrane-protein complex: electron density map at 3 Å resolution and a model of the chromophores of the photosynthetic reaction center from *Rhodopseudomonas viridis*. J. Mol. Biol., 180, 385-398.

Deisenhofer J., Epp O., Miki K., Huber R., Michel H. (1985) Structure of the protein subunits in the photosynthetic reaction centre of *Rhodopseudomonas viridis*. Nature (London), 318, 618-624.

Dominy P.J., Williams W.P. (1987). The role of respiratory electron flow in the control of excitation energy distribution in blue-green algae. Biochim. Biophys. Act, 892, 264-274.

Falkowski P.G.,Fujita Y., Ley A., Mauzerall D. (1986). Evidence for cyclic electron flow around photosystem II in *Chlorella pyrenoidosa*. Plant Physiol. 81, 310-312.

Farchaus J.W., Widger W.R., Cramer W.A., Dilley R.A. (1982) Kinase-induced changes in electron transport rates of spinach chloroplasts. Arch. Biochem. Biophys. 217, 362-367.

Gantt E. (1981).Phycobilisomes. Ann. Rev. Plant Physiol. 32 327-47

Gantt E. (1986).Phycobilisomes.Encyclopedia of Plant Physiology, vol.19. Ed. L.A.Staehelin and C.J.Arntzen. Springer-Verlag, New York.

Gantt E., Lipschultz C.A., Zilinskas B.A. (1976). Phycobilisomes in relation to the thylakoid membranes. Chlorophyll-Proteins, Reaction centers and Photosynthetic membranes, Brookhaven Symposia in Biology: No.28.

Geacintov N.E. (1982). Exciton annihilation and other nonlinear high-intensity excitation effects. Biological Events Probed by Ultrafast Laser Spectroscopy, Ed.R.R. Alfano, Academic Press, N.Y.

Ghanotakis D.F., Demetriou D.M., Yocum C.F. (1987). Isolation and characterization of an oxygen-evolving photosystem II reaction center core preparation and a 28kDa Chl-a-binding protein. Biochem. Biophys. Acta, 891, 15-21.

Giddings T.H., Wasmann C., Staehelin A. (1983). Structure of the thylakoid and envelope membranes of *Cyanophora paradoxa*. Plant Physiol., 71, 409-419.

Glazer A.N. (1984). Phycxobilisome. A macromolecular complex optimized for light energy transfer. Biochim et Biophys. Acta, 768, 29-51.

Golbeck J.H., Bryant D.A. (1991). Photosystem I. Current Topics in Bioenergetics, (Lee,C.P., Ed.) 16, 83-177.

Golbeck J.H., Cornelius J.M. ((1986). Photosystem I charge separation in the absence of centers A and B. I. Optical characterization of center 'A_2' and evidence for its association with a 64-kDa peptide. Biochem. Biophys. Acta, 849, 16-24.

Golbeck J.H., McDermott A. E., Jones W.K., Kurtz D.M. (1987). Evidence for the existence of [2Fe-2S] as well as [4Fe-4S] clusters among FA, FB and FX. Implications for the structure of the photosystem I reaction centre. Biochim. Biophys. Acta, 891, 94-98.

Golbeck J.H., Parett K.G., Mehari T., Jones K.L., Brand J.J. (1988). Isolation of the intact photosystem I reaction center core containing P700 and the iron-sulphur center FX. FEBS Lett., 228, 268-272.

Govindjee (1990) Photosystem II heterogeneity: the acceptor side. Photosyn. Res. 25, 151-160.

Greenbaum N.L., Ley A.C., Mauzerall D.C., (1987). Use of a light-induced respiratory transient to measure the optical cross section of photosystem I in Chlorella. Plant Physiol., 84, 879-882.

Greenbaum N.L., Mauzerall D., (1991) Effect of irradiance level on distribution of chlorophylls between PS II and PSI as determined from optical cross-sections. Biochim. Biophys. Acta, 1057, 195-207.

Hansson O., Wydrzynski T. (1990). Current perceptions of photosystem II. Phot. Res. 23, 131-162.

Harbinson J., Woodward F.I. (1987). The use of light-induced absorbance changes at 820nm to monitor the oxidation state of P-700 in leaves. Plant Cell and Environment, 10, 131-140.

Harrison M.A., Tsinoremas N.F., Allen J.F. (1991). Cyanobacterial thylakoid membrane proteins are reversibly phosphorylated under plastoquinone-reducing conditions in vitro. Febs. Lett., 282, 295-299.

Homer-Dixon J.A., (1992). Pigment orientation changes detected by low temperature linear dichroism spectroscopy: cold hardening in winter rye and the light state transition in phycobilisome containing organisms. M.Sc. Thesis, Brock University, St. Catharines, Ontario, Canada.

Horton P., Croze E. (1979). Characterization of two quenchers of chlorophyll fluorescence with different midpoint oxidation-reduction potentials in chloroplasts. Biochim. Biophys. Acta,545, 188-201.

Hurt E., Hauska G. (1981). A cytochrome f/b6 complex of five polypeptides with plastoquinol-plastocyanine-oxidoreductase activity from spinach chloroplasts. Eur. J. Biochem. 117, 591-599.

Hurt E., Hauska G. (1982). Identification of the polypeptides in the cytochrome b6/f complex from spinach chloroplasts with redox-center-carrying subunits. Jour. Bioenerg. Biomembr. 14, 405-424.

Hurt E., Hauska G. (1983). Cytochrome b6 from isolated cytochrome b6f complexes. Evidence for two spectral forms with different midpoint potentials. FEBS. Lett. 153, 413-418.

Joliot P., Barbieri G., Chabaud R. (1969). Un nouveau modele des centres photochimique du system II. Photochem. Photobiol. 10, 309-329.

Joliot P., Joliot A. (1977). Evidence for a double hit process in photosystem II based on fluorescence studies. Biochem. Biophysic. Acta, 462, 559-574.

Jones R.F.,Spear H.L.,Kury W., 1963. Studies on the growth of the red alga *Porphyridium cruentum*. Physiol. Plant. 16 636-643.

Kirschner J., Senger H. (1986) Thylakoid protein phosphorylation in the red alga *Porphyridium cruentum.* (Ed. G.Akoyunoglou and H.Senger) Regulation of chloroplast differentiation. Plant Biology.2. 339-344.

Knaff D.B., Arnon D.I. (1969). Light-induced oxidation of a chloroplast b-type cytochrome at -189 C. Proc. Natl. Acad. Sci. USA. 63, 956-961.

Kok B., Forbush B., McGloin M. (1970). Co-operation of charges in photosynthetic O2 evolution. I. A linear four step mechanism. Photochem. Photobiol. 11, 457-475.

Kursar T.A., Alberte R.S. (1983). Photosynthetic unit organisation in a red alga. Plant Physiol. 72, 409-414.

Lagoutte B., Mathis P. (1989). The photosystem I reaction centre: structure and photochemistry. Photochem. Photobiol. 49, 833-844.

Lawlor D.W. (1987) Photosynthesis: metabolism, control and physiology. Longman Scientific and Technical, N.Y.

Ley A.C., 1984. Effective Absorption cross-sections in *Porphyridium cruentum.* Plant Physiol. 74, 451-454.

Ley A.C., Butler W.L. 1977. The distribution of excitation energy between Photosytem I and Photosystem II in *Porphyridium cruentum.* Photosynthetic Organelles. Special issue Plant Physiol. 33-46.

Ley A.C., Butler W.L., 1980. Efects of chromatic adaptation on the photochemical apparatus of photosynthesis in *Porphyridium cruentum.* Plant Physiol. 65, 714-722.

Ley A.C., Butler W.L., 1980. Energy distribution in the photochemical apparatus of *Porphyridium cruentum* in state 1 and state II. Biochim. Biophys. Acta 592 349-363.

Ley A.C., Mauzerall D.C., 1986. The extent of energy transfer among Photosystem II reaction centers in *Chlorella.* Biochim. Biophys. Acta,850, 234-248.

Matsuda H., Butler W.L.(1983). Restoration of high-potential cytochrome b-559 in photosystem II particles in lipisomes. Biochim. Biophys. Acta, 725, 320-324.

Mauzerall D., 1972. Light-induced fluorescence changes in *Chlorella,* and the primary photoreactions for the production of oxygen. Proc. Nat. Acad. Sci. USA, 69, 1358-1362.

Mauzerall D., 1978. Multiple excitations and the yield of chlorophyll a fluorescence in photosynthetic systems. Photochem. Photobiol. 28, 991-998.

Mauzerall D., 1981. Analysis of energy utilization via multiple excitations. Photosynthesis I. Photophysical Processes- Membrane Energization. Ed. G. Akoyunoglou. Balaban International Science Services, Philadelphia,Pa.

Mauzerall D. 1982. Statistical theory of the effect of multiple excitation in photosynthetic systems. Biological Events probed by Ultrafast Laser Spectroscopy. Ed. R.R. Alfano. Academic Press Inc., New York.

Mauzerall D., Greenbaum N.,(1989). The absolute size of a photosynthetic unit. Biochim. Biophys. Acta 974 119-140.

Melis A., Duysens L.N.M. (1979) Biphasic energy conversion kinetics and absorbance difference spectra of photosystem II of chloroplasts. Evidence for two different photosystem II reaction centers. Photochem. Photobiol. 29, 373-382.

Melis A., Homann P.H. (1976) Heterogeneity of the photochemical centers in system II of chloroplasts. Photochem. Photobiol. 23, 343-350.

Michel H., Deisenhofer J. (1988). Relevance of the photosynthetic reaction centre from purple bacteria to the structure of photosystem II. Biochem. 27, 1-7.

Morschel, E., Muhlethaler K. (1983). On the linkage of exoplasmic freeze-fracture particles to phycobilisomes. Planta 158,451-457.

Morschel E., Schatz G.H. (1987). Correlation of photosystem-II complexes with exoplasmic freeze-fracture particles of thylakoids of the cyanobacterium *Synechococcus sp.* Planta, 172, 145-154

Morschel E., Schatz G.H. (1988) On the structure of photosystem II-phycobilisome complexes of cyanobacteria. Photosynthetic Light-Harvesting Systems. Organisation and Function Ed. H. Scheer and S.Schneider. Walter de Gruyter,Berlin, N.Y

Mullineaux C.W., (1992). Excitation energy transfer from phycobilisomes to photosystem I in a cyanobacterium. Biochim. Biophys. Acta, 1100, 285-292.

Mullineaux C.W., Allen J.F. (1986). The state 2 transition in the cyanobacterium *Synechococcus 6301* can be driven by respiratory electron flow into the plastoquinone pool. FEBS Lett. 205, 155-160.

Mullineaux C.W., Allen J.F. (1988) Fluorescence induction transients indicate dissociation of photosystem II from the phycobilisome during the state-2 transition in the cyanobacterium *Synechococcus 6301.* Biochim. Biophys. Acta, 934, 96-107.

Mullineaux C.W., Bittersmann E., Allen J.F., Holzwarth A.R. (1990). Picosecond time-resolved fluorescence emission spectra indicate decreased energy transfer from the phycobilisome to photosystem II in light-state 2 in the cyanobacterium *Synechococcus* 6301. Biochim. Biophys. Acta, 1015, 231-242.

Mullineaux C.W., Griebenow S., Braslavsky S.E. (1991). Photosynthetic energy storage in cyanobacterial cells adapted to light-states 1 and 2. A laser-induced optoacoustic study. Biochim. Biophys. Acta, 1060, 315-318.

Mullineaux C.W., Holzwarth A.R. (1990). A proportion of photosystem II core complexes are decoupled from the phycobilisome in light-state 2 in the cyanobacterium *Synechococcus 6301*. FEBS Lett. 260, 245-248.

Murata N. (1969) Control of excitation transfer in photosynthesis. I. Light-induced change of chlorophyll a fluorescence in *Porphyridium cruentum*. Biochim. Biophys. Acta, 172, 242-251.

Myers J., Graham J.R. (1971). The photosynthetic unit in Chlorella measured by repetitive short flashes. Plant Physiol., 48, 282-286.

Nanba O., Satoh K. (1987). Isolation of a photosystem II reaction center consisting of D1 and D2 polypeptides and cytochrome b559. Proc. Natl. Acad. Sci. USA, 84, 109-112.

Nuijs A.M., Shuvalov V.A., Van Gorkum H.J., Plijter J.J., Duysens L.N.M. (1986) Picosecond absorbance difference spectroscopy on the primary reaction and the antenna-excited states in photosystem I particles. Biochim. Biophys. Acta, 850, 310-318.

Ohki K., Gantt E., Lipschultz C.A., Ernst M.C. (1985) Constant phycobilisome size in chromatically adapted cells of the cyanobacterium Tolypothrix tenuis, and variation in *Nostoc sp.* Plant Physiol.,79, 943-948.

O'Malley P., Babcock G.T. (1984) Electron nuclear double resonance evidence supporting a monomeric nature for P700+ in spinach chloroplasts. Proc. Natl. Acad. Sci. USA, 81, 1098-1101.

Ort D.R. (1986). Energy transduction in oxygenic photosynthesis: an overview of structure and mechanism. Encyclopedia of Plant Physiology, vol.19. Ed. L.A.Staehelin and C.J.Arntzen. Springer-Verlag, New York.

Petrouleas V., Brand J.J., Parrett K.G., Golbeck J.H. (1989). A Mossbauer Analysis of the low-potential Iron-Sulphur center in Photosystem I: spectroscopic evidence that FX is a (4Fe-4S) cluster. Biochemistry, 28, 8990-8983.

Post A.F., Mimuro M., Fujita Y. (1991). Light 2 directed changes in the effective absorption cross-section of Photosystem II in Synechocystis 27170 are related to modified action on the donor side of the reaction center. Biochim. Biophys. Acta, 1060, 67-74.

Pullin C.A.,Brown R.G., Evans E.H. (1979).Detection of allophycocyanin in photosystem I preparations from the blue-green alga, *Chlorogloea fritschii*. FEBS Lett. 101, 110-112.

Redlinger T., Gantt E. (1982). A M 95,000 polypeptide in *Porphyridium cruentum* phycobilisomes and thylakoids: Possible function in linkage of phycobilisomes to thylakoids and in energy transfer. Proc. Natl. Acad. Sci. USA. 79, 5542-5546.

Redlinger T., Gantt E. (1983). Photosynthetic membranes of *Porphyridium cruentum*. Plant. Physiol. 73, 36-40.

Rich P.R. (1984). Electron and proton transfers through quinones and cytochrome bc complexes. Biochem. Biophys. Acta, 768, 53-79.

Ried A., Reinhardt B. (1980) Distribution of excitation energy between photosystem I and photosystem II in red algae.III. Quantum requirements of the induction of a state 2-state 1 transition. Biochim. Biophys. Acta, 592, 76-86.

Rusckowski M., Zilinskas B.A. (1980). Chlorophyll-protein complexes of the Cyanophyte, *Nostoc sp.* Plant Physiol. 65, 392-396.

Rusckowski M., Zilinskas B.A. (1982). Allophycocyanin I and the 95 kilodalton polypeptide. Plant Physiol. 70,1055-1059.

Salehian O. (1992). Distribution of excitation energy in photosynthesis: A study of heat loss, photochemical activity and fluorescence emission in intact cells of cyanobacterium *Synechococcus sp. PCC 6301*. M.Sc. Thesis, Brock University, St. Catharines, Ontario, Canada.

Sanders C.E., Holmes N.G., Allen J.F. (1986) Membrane protein phosphorylation in the cyanobacterium *Synechococcus 6301*. Biochem. Soc. Tran. 14, 66-67.

Satoh K., Fork D.C. (1983). The relationship between state II to state I transition and cyclic electron flow around photosystem I. Photosynth. Res. 4, 245-256.

Shuvalov V.A., Nuijs A.M., Van Gorkum H.J., Smit W.J., Duysens L.N.M. (1986). Picosecond absorbance changes upon selective excitation of the primary electron donor P700 in photosystem I. Biochim. Biophys. Acta, 850, 319-323.

Staehelin L.A. (1986). Chloroplast structure and supramolecular organisation of photosynthetic membranes. Photosynthesis III. Ed. L.A. Staehelin and C.J. Arntzen. Springer-Verlag, N.Y.

Staehelin L. A., Arntzen C.J. (1983). Regulation of chloroplast membrane function: protein phosphorylation changes the spatial organization of membrane components. Jour. Cell Biol. 97, 1327-1337.

Telfer A., Bottin H., Barber J., Mathis P., 1984. The effect of magnesium and phosphorylation of light-harvesting chlorophyll a/b protein on the yield of P700 photooxidation in pea chloroplasts. Biochim. Biophys. Acta 764, 324-330.

Thielen A.P.G.M., van Gorkom H.J. (1981) Quantum efficiency and antenna size of photosystems IIα, IIß and I in tobacco chloroplasts. Biochem. Biophys. Acta, 635,111-120.

Thompson L.K., Brudvig G.W. (1988). Cytochrome b-559 may function to protect photosystem II from photoinhibition. Biochem. 27, 6653-6658.

Thornber J.P. (1986). Biochemical characterization and structure of pigment-proteins of photosynthetic organisms. Encyclopedia of Plant Physiology, vol.19. Ed. L.A.Staehelin and C.J.Arntzen. Springer-Verlag, New York.

Tsinoremas N.F., Hubbard J.A.M., Evans M.C.W., Allen J.F. (1989) P700 photooxidation in state 1 and state 2 in cyanobacteria upon flash illumination with phycobilin- and chlorophyll-absorbed light. FEBS. Lett. 256, 106-110.

Turpin D., Bruce D. (1990). regulation of photosynthetic light harvesting by nitrogen assimilation in the green alga *Selenastrum minutum*. FEBS. Lett., 263, 99-103.

Van Best J.A., Mathis P. (1978). Kinetics of reduction of the oxidised primary electron donor of photosystem II in spinach chloroplasts and in *Chlorella* cells in the microsecond and nanosecond time ranges following flash excitation. Biochim. et Biophys. Acta, 503, 178-188.

Van Gorkum H.J., Tamminga J.J., Haveman J., Van der Linden I.K., (1974). Biochim. Biophys. Acta, 347, 417-438.

Van Gorkum H.J. (1985). Electron transfer in PSII. Photosyn. Res. 6, 97-112.

Velthuys B.R. (1987). The photosystem two reaction center. The Light Reactions. Ed. J. Barber. Elsevier Science Publishing Company, Inc. N.Y.

Vierling E., Alberte R. (1983). P-700 chlorophyll-a protein. Purification, characterizarion and antibody preparation. Plant Physiol., 72, 625-633.

Wang R.T., Graham J., Myers J. (1980). On the origins of 718nm fluorescence from *Porphyridium cruentum* at 77 K. Biochem. Biophys. Acta 592, 277-284.

Wang R.T., Stevens C.L.R., Myers J. (1977). Action spectra for photoreactions 1 and II of photosynthesis in the blue-green alga *Anacystis nidulans*. Photochem. Photobiol., 25, 103-108.

Wollman F.A. (1986). Photosystem I proteins. Encyclopedia of Plant Physiology, vol.19. Ed. L.A.Staehelin and C.J.Arntzen. Springer-Verlag, New York.

Yamagishi , Katoh (1983) Arch. Biochem. Biophys. 225, 836-846.

Zhoa J., Li N., Warren P.V., Golbeck J.H., Bryant D.A. (1992). Site directed conversion of a cysteine to aspartate leads to the assembly of a [3Fe-4S] cluster in psaC of Photosystem I. The photoreduction of FA is independent of FB. Biochem., 31, 5093-5099.

Zilinskas B.A. (1982). Isolation and characterisation of the central component of the phycobilisome core of *Nostoc. sp.* Plant Physiol., 70, 1060-1065.

APPENDIX A

Derivation of the single hit Poisson equation.

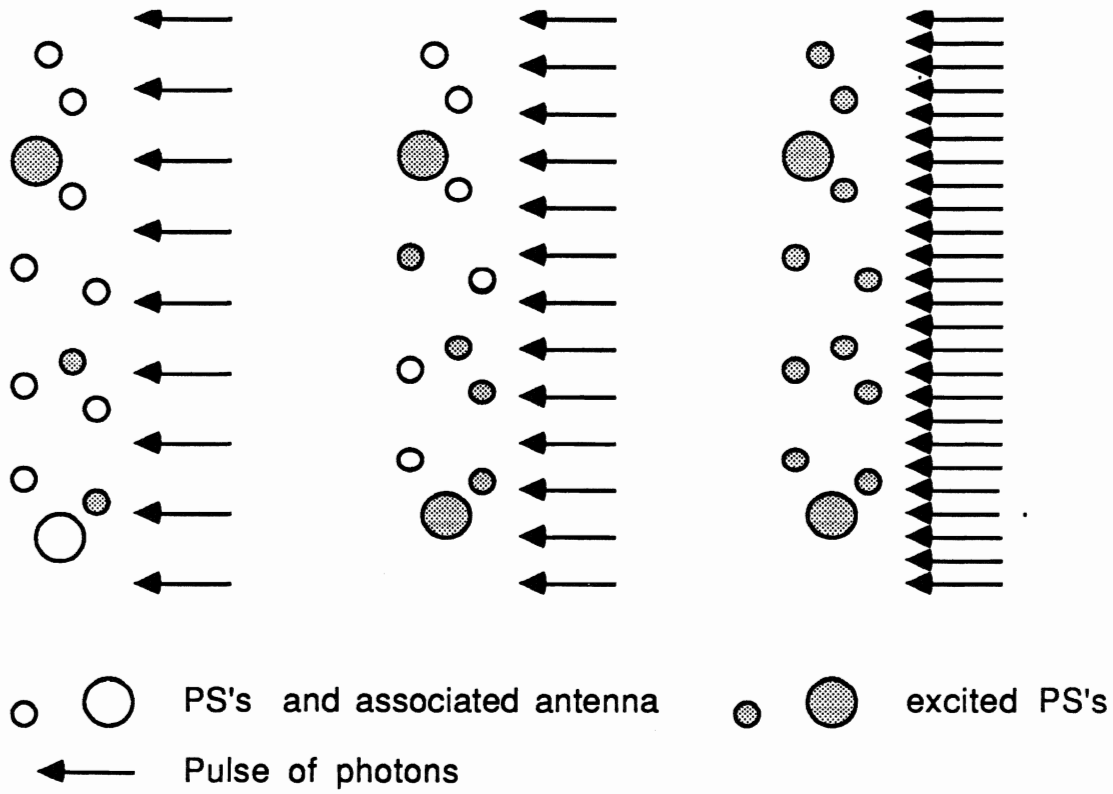

Fig.(58). A thin plane of photosystems impinged upon by a laser pulse of small intensity on the left, to a maximum intensity on the right.

The total flux of the laser pulse is E photons /unit area. Consider a single homogeneous population of photosystems, where σ is the absorption X-section of one photosystem. The average number of hits per photosystem is σE; P_n is the probability of n hits per photosystem. Poisson statistics apply and

$$P_n = (\sigma E)^n e^{-\sigma E} / n!$$

$P_0 = e^{-\sigma E}$, and the probability of a hit of any size is $1-e^{-\sigma E}$. This is also the fraction of photosystems which receives one or more hits.

If Y_0 is the total photosystem yield at saturation , the yield, Y, at intensity E is given by

$$Y = Y_0 (1 - e^{-\sigma E})$$

If both populations of fig.(58) are considered,

$$Y(total) = Y_1(1- \exp(-\sigma_1 E)) + Y_2(1- \exp(-\sigma_2 E))$$ where Y_1 and Y_2 are the maximum yields contributed by the individual populations.

The need for T, the time of the pulse, to be shorter than the turnover time of the photosystem is illustrated below.

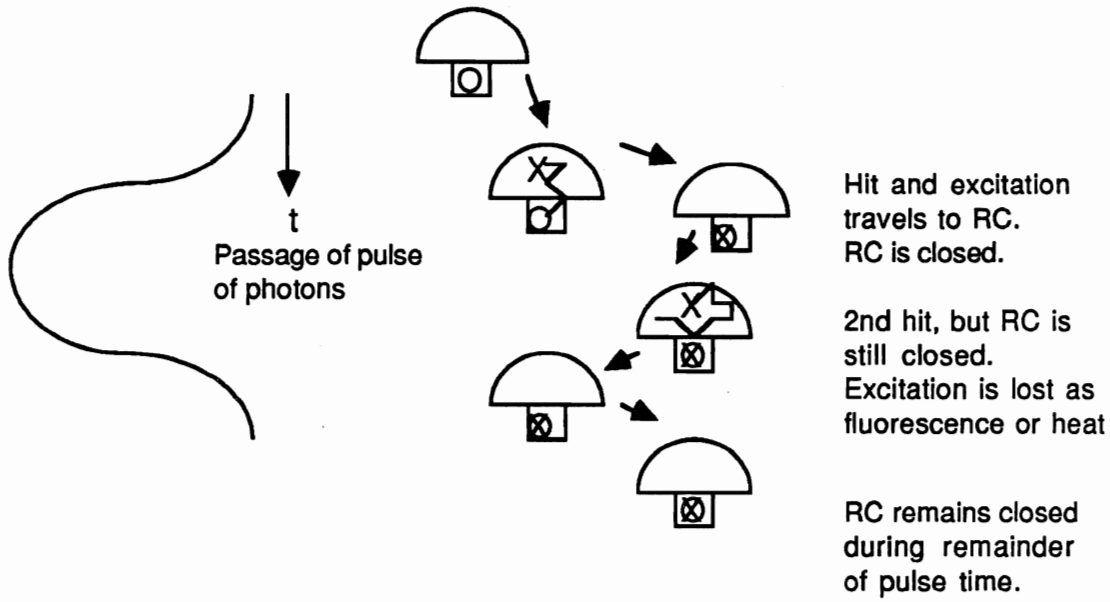

Fig.(59) Passage of pulse through the sample. The duration of the pulse is shorter than the turnover time of the reaction centre, which remains closed during the remainder of the duration of the pulse. There is one trap per antenna.

The derivation of this equation assumes that a second hit to the antenna of a PS causes no more effect than the first. The assumptions are those of semi-annihilation : two excitations react together so that only one survives,

i.e. $P^* + P^*$ (encounter of two excitations) -> P^{**} (a doubly excited state)

decay of excitation from second to first energy level -> $P + P^* + \Delta$ (heat), ...(1)

or another exciton on encountering the trap filled by the first hit exciton, is demolished

i.e. $P^* + T^{+-} \rightarrow P + T^{+-} + \Delta$ (heat), where T^{+-} is the filled trap.....(2)

The latter could be accomplished by escape from the filled trap and then decay by fluorescence. (Mauzerall, 1982)

The method for transferring E, the measurement, in mV, of the laser pulse at the pyrometer, to photons /sq. Å.

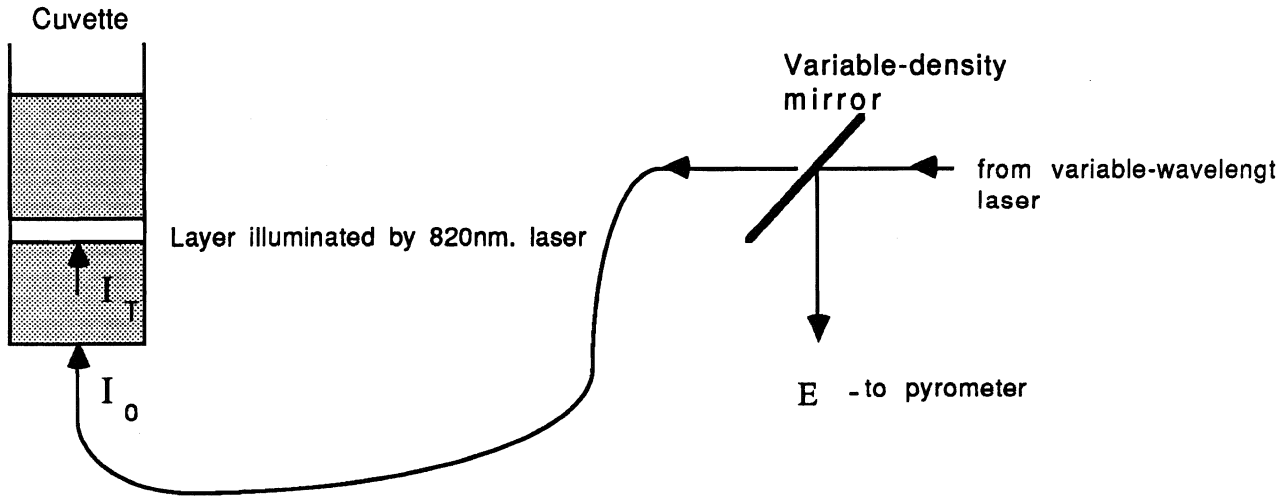

Fig. (60). Diagram showing intensity of pulse measured by pyrometer, E, that delivered to the base of the cuvette, I_0, and that transmitted through the lower portion of the cuvette to the layer illuminated by the 820nm laser, I_T.

A correction was made for absorbance through the distance travelled by the pulse from the base of the cuvette to the 820nmplane to obtain I_T, the intensity of the pulse at the 820nm plane. For all experiments, except where otherwise stated, the distance of the 820nm layer from the base was 8mm. Absorbance, $A(\lambda)$, as determined by the DW2 spectrophotometer, is determined for a path length of 10mm.

$\log(I_o/I_T) = 0.8xA(\lambda)$,

$I_T = I_o x 10^{-0.8A(\lambda)}$

$I_T = Exrx10^{-0.8A(\lambda)}$ $= Exrxt$, where $t = 10^{-0.8A(\lambda)}$

The final transfer to photons per Å^2, is shown below:

For the pyrometer, 2.58V is registered for every mJ energy delivered to the receptor.

Measured diameter of the circular receptor was 5.73mm. ($=0.573x10^8$ Å)

Area of receptor is a square inscribed within the circle

$=0.573x10^8 x\ (0.573/2)x10^8 Å^2$

$=0.164x10^{16} Å^2$

i.e. 1 V is registered by $1/(2.58x0.164x10^{16})$mJ per sq Å, or $2.36x10^{-19}$ J per sq. Å

At 574nm, a photon has energy of $1.986x10^{-16}/574$ J. or $3.5x10^{-19}$ J.

At 574nm, a measurement of 1V at the pyrometer is caused by 2.36/3.5 photons per sq. A°, or 0.67 photons per sq Å.

At 627nm, a photon has energy of 3.16J; a measurement of 1V at the pyrometer is caused by 0.75 photons per sq. Å.

At 668nm, a photon has energy of 3.0J; a measurement of 1V at the pyrometer is caused by 0.79 photons per sq. Å.

Conversion of A, from saturation curves, to σ, the absorption X-section:

$Y = B(1-\exp(-AE))$, with experimental parameters, E is in mV

$A = 1/E\ \ln_e\{B/(B-Y)\}$; { } is a dimensionless quantity.

$Exrxt = I_T$ (mV)

$Exrxtxn/1000 = I$ (photons per sq.Å),where n is the number of photons per sq. Å which cause a 1V potential at the pyrometer, determined above.

σ, the X-section in Å^2 :

$$\sigma = 1/I\ \ln_e\{\ \} = (1000/Exrxtxn)\ln_e\{\ \} = (1000/rxtxn)A$$

Conversion from relative units to Å .

Table (16). The correction factor, rxtxn, for experiments at 574nm, 627nm, 668nm, where σ, the X-section in Å^2, is given by, σ=(A/rxtxn)10^3 and A is the X-section determined by the Poisson equation fits.

	Exp.	r	A(678)	A(λ)	t	rxt	rxtxn
574nm	p.292 (1,2)	3.1	0.82	0.76	0.24	0.7 ±0.1	0.47±0.05
	p.303 (1,2)	3.7	0.81	0.75	0.25	0.9 ±0.1	0.60±0.07
	p.306 (2)*	3.7	0.39	0.36	0.52	1.9 ±0.2	1.2±0.1
	p.231 (1)	3.0	0.81	0.75	0.25	0.8 ±0.1	0.54±0.06
627nm	p245 (1)	6.2	0.83	0.46	0.42	2.6 ±0.3	1.9±0.2
	p268 (1,2)	4.8	0.78	0.43	0.45	2.2 ±0.3	1.7±0.2
668nm	p251 (1)	5.2	0.8	0.75	0.25	1.3 ±0.2	1.0±0.1
	p241 (1)	4.3	0.81	0.73	0.26	1.1 ±0.1	0.9±0.1
	p263 (1,2*)	4.8	0.78	0.70	0.27	1.3 ±0.2	1.0±0.1
	p271 (1,2*)	6.5	0.81	0.73	0.26	1.7 ±0.2	1.3±0.2
	p279 (2)	6	0.32	0.29	0.59	3.5 ±0.4	2.8±0.3
	p285 (2)	5.7	0.33	0.30	0.57	3.3 +0.4	2.6±0.3

(1) PS1 saturation curve.

(2) PS2 saturation curve

(1,2) PS1 and PS2 saturation curves done under same conditions.

* only S2 completed.

r= I_o/E, where E is intensity, in volts, measured by pyrometer, and I_o is intensity, in volts, measured at base of cuvette.

$I_T = Io \times 10^{-0.8\ A(\lambda)}$

I_T= rxtxE, where $t=10^{-0.8\ A(\lambda)}$, and is in volts.

The error in r is approximately 10%, in A(574) approximately 2%, and resultant value of rxt has error of approximately 12%.

n is the number of photons per sq. Å which causes 1V potential at the pyrometer; for 574nm radiation n is 0.67, for 627nm n is 0.75, for 668nm n is 0.79.

What difference between saturation curves can be expected, if the average X-section of a two-component system is doubled?

If a photosystem is heterogeneous and consists of two-components with different absorbance X-sections an increase of the average X-section can be achieved in one of three ways, as illustrated in the figure below.

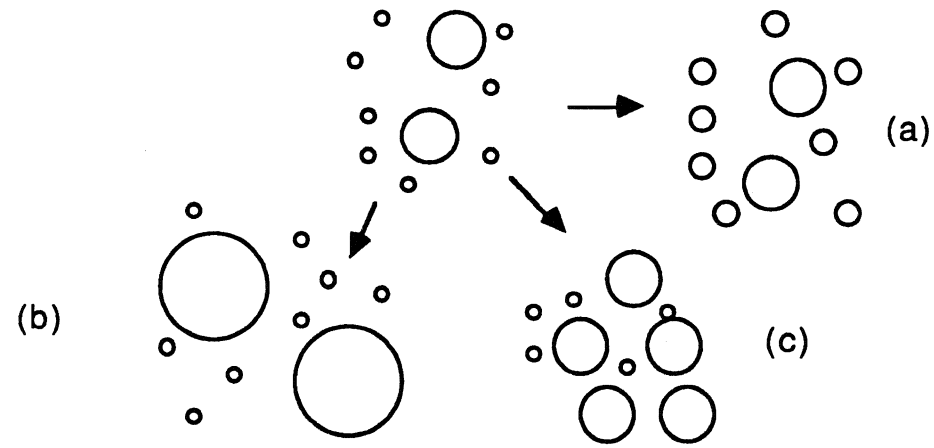

Fig. (61). A change in average X-section in a two-component system obtained in three ways: (a) an increase in the size of the smaller component, (b) an increase in the size of the larger component,and (c) an increase in the % of the larger component.

Suppose that 80% of the system is a small component, area A, and 20% is a large component, area C, A=0.03, B=0.8, C=0.3. The average X-section, given by AxB+C(1-B), is 0.08. The X-section can be doubled in the three ways shown above, and the saturation curves given by such systems can be calculated and compared to that of the unchanged system to demonstrate the difference that might be observed experimentally.

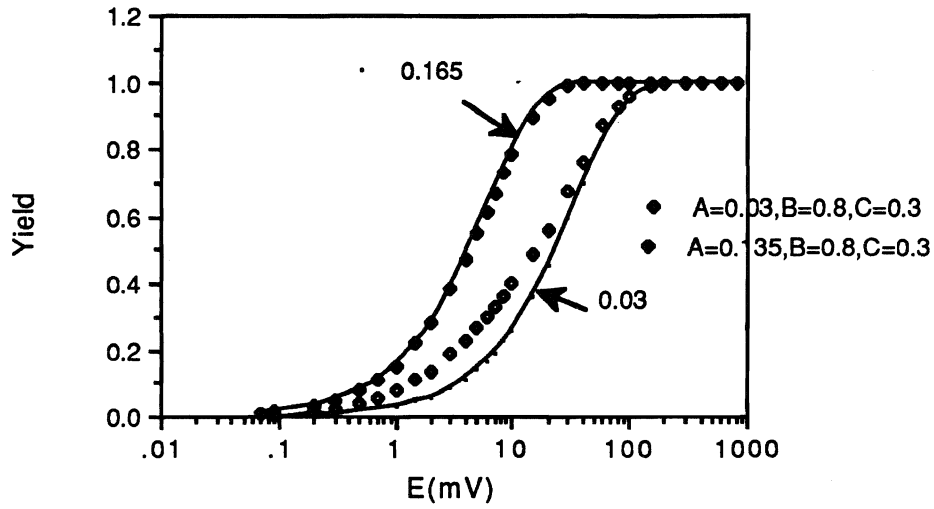

Fig.(62) Comparison of two mixed-system curves; one has an average X-section, as before, of 0.08 (unfilled diamonds); the other has an average X-section of 0.165 (filled diamonds). The former is derived from the latter by changing the area of the small component, from 0.03 to 0.135; the ratio of small to big, 4:1, remains the same. For comparison there are curves from a single component system of X-section 0.03, and from a single component system of X-section 0.165.

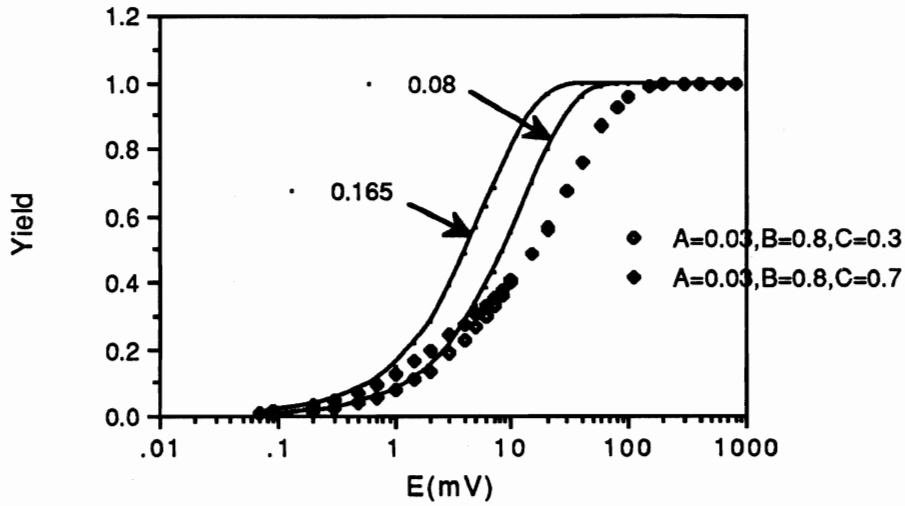

Fig.(63). Comparison of two mixed-system curves; one has an average X-section, as before, of 0.08 (unfilled diamonds); the otherhas an average X-section of 0.165 (filled diamonds). The former is derived from the latter by changing the area of the big component, from 0.3 to 0.7; the ratio of small to big, 4:1, remains the same. For comparison there are curves from a single component system of X-section 0.08, and from a single component system of X-section 0.165.

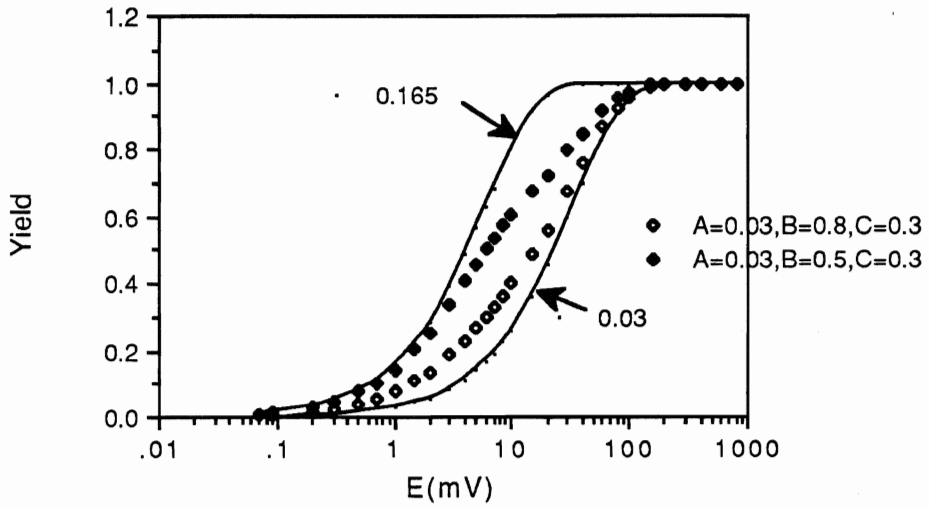

Fig.(64). Comparison of two mixed-system curves; one has an average X-section, as above, of 0.08 (unfilled diamonds);the otherhas an average X-section of 0.165 (filled diamonds). The former is derived from the latter by changing the ratio of the common small and big components (0.03, 0.3), from 4:1 to 1:1.For comparison there are curves from a single component system of X-section 0.03, and from a single component system of X-section 0.165.

If the change ocurs in the small component, either by an increase in its area, fig.(62) or a decrease in its fraction, fig.(64), the difference between the two curves is significant. A change in the area of the large, but minor, component causes only a small difference in the experimental curves, fig.(63). In all cases, however, the saturation curve of the doubled system lies above that of the original, and the shape of the low intensity end approaches that of a single component curve with a X-section equal to the average X-section of the mixed system. It is possible, by varying the composition and the X-sections of both the large and small components to obtain a saturation curve which lies partially above and partially below the saturation curve from a system with half the average X-section. This is shown in the next figure.

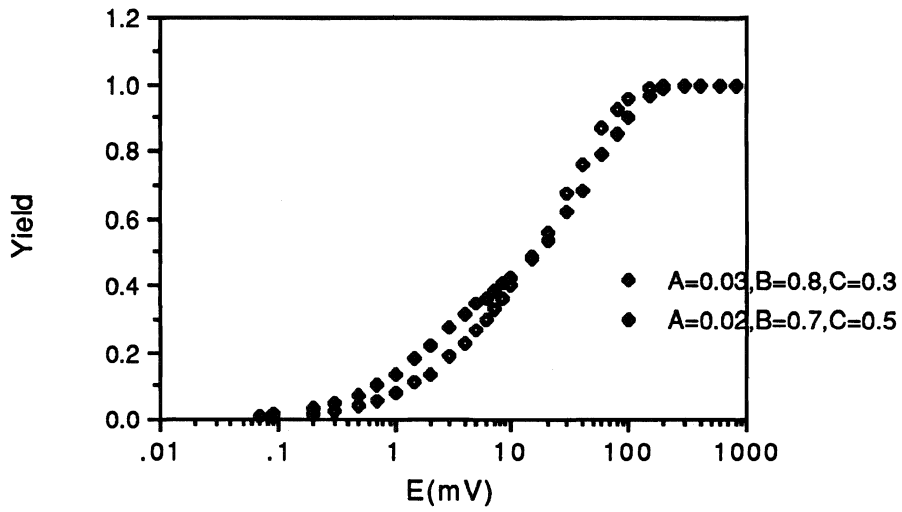

Fig.(65). Two-component curves; one ,filled diamonds, has twice the average X-section of the other, unfilled diamonds, (0.164, 0.08). The ratio of small to big, and the size of both components have been changed.

In some cases, therefore, it may be difficult to observe a difference in average X-section between S1 and S2 directly from the saturation curves. In all the cases considered, however, the difference in average X-section is manifested at the low intensity end, and the high intensity end exhibits a difference in size of the small component.

APPENDIX B

THE DECREASE IN YIELD OF PS1 AT HIGH INTENSITIES

A decrease in yield at high intensities appears in PS1 saturation curves in both S1 and S2, at all flash wavelengths; it starts just before saturation and increases as the intensity increases. There is no difference in decline between S1 and S2. When the cells are subject to a continuous high intensity white light P700 is maximally oxidised, and when the laser flashes under these conditions there is no further absorbance increase at 820nm due to P700+ formation. What is then observed is an absorbance decrease at 820nm. It is likely, therefore, that the decrease in yield is only apparent; at high intensities there is an effect which causes a decrease in absorbance at 820nm. If there is a phenomenon at high intensities which does decrease the amount of P700+ formed, it must be accompanied by a bleaching at 820nm.

The yield of a photosystem depends directly on the number of excitons reaching the RC. At high intensities many of the photosystems capture more than one photon and the effect of multiple excitations in the antenna and of an excitation arriving at a filled trap (a very descriptive word for a RC) must be considered as possible causes of a decrease in yield and/or a change in absorbance at 820nm

Below are listed some experiments in which the decreased yield is observed; the number of excitations present in the antennae at saturation are calculated, for both big and small antennae.

Table (17).The number of photons hitting the PS1 antennae at 574nm, 627nm, 668nm.

		Intensity			# photons received by reaction centres	
					small	big
574nm	p303	150mV	or	0.1photons /Å^2	3±1	14±7 (S1), 40±30 (S2)
627nm	p245	100mV	or	0.06photons /Å^2	1.8±0.3	
668nm	p251	50mV	or	0.04 photons /Å^2	4.4±0.4	

The maximum number of excitations occurring during the laser pulse of 250ns. is forty, in the big antenna of p303, creating an excitation every 6ns. Fluorescence lifetime with an open trap is of the order of a few picoseconds and it probably takes only this long for an excitation to travel to an open trap; Mauzerall (1982) states that exciton transfer to the core of chla to which the RC is coupled occurs in a time of the order of 50ps. Mauzerall (1981) stated that he and Ley have shown that, in Chlorella, at 6500 hits per RC, the lifetime of an exciton was about 30ps. and annihilation could occur in the antenna complex. It is unlikely that in these experiments, excitations in an antenna, even with a filled trap, when the antenna exciton may last longer, would last long enough for two to be present at the same time. Interaction between an exciton and a filled trap seem a possible cause of a decrease in the formation of P700+.

The decrease is in comparison to the cumulative one hit Poissonian determined previously, which assumed that a second hit to the antenna of a PS caused no more effect than the first. The assumptions were those of semi-annihilation (Mauzerall 1981):

An exciton, P*, on encountering the trap filled by the first hit exciton, is demolished

i.e. $P^* + T^{+-} \rightarrow P + T^{+-} + \Delta$ (heat), where T^{+-} is the filled trap.....(1)

In contrast, it can be postulated that a second excitation leads to mutual annihilation of it and the trapped energy:

and $P^* + T^{+-} \rightarrow P + T + 2\Delta$ .....(2)

It appears that the second situation causes a decrease in yield. This is so but it does not produce a maximum followed by a decrease, as in the saturation curves of this experiment. This is because the Poisson distribution decrees that there is a distribution of hits to the individual antenna around the average number.The distribution includes some antenna with an odd number of excitations, and antennae with an even number of excitations, with the result that there is an approximately equal number of antenna with an odd number of excitations and with an even number of excitations; half the antennae will cause a maximum yield and the other half will produce nothing, with the result, that even as

saturation is just reached the total yield will be half that expected from a semi-annihilating system. In addition, Mauzerall (1981) has shown that the assumption of total annihilation leads to equations for the yield which do not differ in form from that of the single component equation. The X-section determined is a multiple of the actual X-section, and the maximum yield is diminished. For example, with a single trap per antenna the yield is given by:

$Y = Y_0/2\ (1-\exp(-2\sigma E))$, where σ is the real X-section, and Y_0 is yield from a semi annihilation system. This experiment cannot distinguish between the two yields. If total annihilation has occurred, however, it would mean that the measured X-sections, shown later to be small compared to the results of Ley (1984) would have to be halved. For this reason it will be assumed that the high intensity effect is not due to annihilation of excitons.

Direct decrease in yield caused by total annihilation in a system of one RC1 per antenna, as above, cannot explain the experimental decrease of the yield after saturation and one must consider other phenomena which may cause a change in 820nm absorbance for PS1, opposite in direction to that caused by P700+, which need not, of themselves, decrease the yield.

There is always the probability of triplet formation; a triplet is an excited state brought about by the change of spin of the excited electron. The more excitations occurring the greater the number of triplets formed. They may also be formed on the encounter of a singlet with the electric field of the filled trap. To return to the singlet state from the triplet requires the addition of a small amount of energy, fig.(3). Because of this, the triplet lasts longer than the singlet state, and is under the influence of neighbouring molecules long enough to take part in chemical reactions. Geacintov (1982) states that the lifetime of a triplet carotenoid, a pigment present in the antennae, is of the order of μs, and for microsecond duration pulses, such as used in these experiments, can take part in singlet-triplet annihilation and lead to a decrease in fluorescence (PS2) yield. Such annihilation is encompassed by one of the processes of the semi or total annihilation of the last paragraph, and will not cause the decrease in yield observed in the saturation curve. The

triplet state itself, of some pigment, may however cause a decrease in absorbance at 820nm to counteract that of P700+, or may react with something else which will cause such a decrease.

It has been proposed that at high intensities there is cyclic flow in PS2 (Falkowski et al, 1986). Cyclic flow in PS2 could affect the rate of reduction of P700+ in PS1, as linear electron flow may be lessened, but it would not cause a decrease in the formation of P700+. The difference between the fluorescence and O_2 yields, which stimulated the proposal of PS2 cyclic flow, was more pronounced in S2. The high intensity effect occurs equally in S1 and S2 and is unlikely to be due to cyclic electron flow around PS2. It is known that PS2 oxidation does cause a change in 820nm absorbance (Van Best and Mathis,1978), but not only is it is too short lived to have an effect at the same time that P700+ is measured, but the change is in the same direction to that caused by P700+.

The decrease in 820nm absorbance which counteracts the increase due to P700+ must be due to something other than, or something which occurs with, an annihilation effect. This something else happens at the beginning of the high intensity pulse and has a recovery time of about 40μs.